Paleontología Mexicana
Volumen 7, núm. 1, 2018, p. 1 – 11

Rusophycus y *Cruziana*, galerías y rastros de trilobites del Terreneuviano (Cámbrico inferior) de la Formación Puerto Blanco, Noroeste de Sonora, México. Implicaciones paleoambientales

Alina Marcela Hernández-Barbosa[a], Francisco Sour-Tovar[a,*]

[a] Museo de Paleontología, Departamento de Biología Evolutiva, Facultad de Ciencias, Universidad Nacional Autónoma de México, Ciudad Universitaria, 04510, Ciudad de México, México.

[*] fcosour@ciencias.unam.mx

Resumen

Se describen cinco galerías asignadas al icnogénero *Rusophycus* y un rastro que se asigna a *Cruziana*. El material se encontró en la unidad 4 de la Formación Puerto Blanco, Cámbrico inferior (Terreneuviano) de la región de Caborca-Pitiquito, en el noroeste de Sonora; entre las galerías se reconoce la presencia de *Rusophycus marginatus*. Se atribuye el origen de los icnofósiles descritos a actividades de descanso y desplazamiento de trilobites. La asociación caracteriza una icnofacies *Cruziana* que se desarrolló en un paleoambiente con cambios de condiciones de meso a infralitorales.

Palabras clave: *Rusophycus*, Icnofacies *Cruziana*, Cámbrico inferior, Sonora, México.

Abstract

Five burrows of the ichnogenus Rusophycus and a Cruziana type trace are described. The material was found at unit 4 of the Lower Cambrian (Terreneuvian), Puerto Blanco Formation from the Caborca-Pitiquito region in northwestern Sonora. The occurrence of Rusophycus marginatus is recognized among the burrows. The origin of these ichnofossils is attributed to resting and locomotion activities of trilobites. The assemblage characterizes a Cruziana ichnofacies which developed in a paleoenvironment with changes from meso to infralitral conditions.

Keywords: Rusophycus, Cruziana Ichnofacies, Lower Cambrian, Sonora, Mexico.

1. Introducción

En la región de Caborca-Pitiquito, al noroeste de Sonora, se han encontrado las rocas fosilíferas más antiguas del territorio mexicano con edades que abarcan del Proterozoico al Cámbrico medio. El primer reporte de las localidades de la región fue realizado por Stoyanow (1942), y posteriormente Cooper y Arellano (1946) describieron y nombraron seis formaciones de edad cámbrica que sobreyacen de manera concordante a la Formación La Ciénega, unidad que contiene rocas ígneas y sedimentarias del Ediacarense (Sour-Tovar *et al*., 2007). De la más antigua a la más reciente, las unidades del Cámbrico inferior son las formaciones Puerto Blanco y Cuarcita Proveedora y del Cámbrico inferior-medio las formaciones Buelna, Cerro Prieto, Arrojos y El Tren. A finales de los años cuarenta y durante la década de los cincuenta del siglo XX, Lochman en 1948, 1952 (en Cooper *et al*., 1952), 1953 y 1956 realizó las primeras descripciones y asignaciones taxonómicas de los trilobites del Cámbrico inferior-medio de la región y una de las primeras correlaciones entre las rocas precámbrico-cámbricas de la región de Caborca y las del suroeste de Estados Unidos. Esta correlación fue apoyada con el trabajo de Damon *et al*. (1962) quienes realizaron fechamientos radiométricos del basamento ígneo presente en Sonora y que resultó ser coetáneo a rocas proterozoicas del suroeste de los Estados Unidos. Entre diversos trabajos posteriores destaca una síntesis de los estudios existentes hasta 1969, sobre las rocas precámbricas (de Cserna, 1970), las descripciones litoestratigráficas de las rocas proterozoicas del estado de Sonora (Anderson y Silver, 1970; Fritz, 1975), la correlación de las rocas de Sonora con rocas del suroeste de Estados Unidos (Palmer y Halley, 1979) y el reporte de una secuencia precámbrica portadora de estromatolitos, asignada informalmente a las "Capas Gamuza" (Gamper y Longoria, 1979), los cuales fueron descritos por Weber y Cevallos-Ferriz (1980). Stewart *et al*. (1984), estudiaron la secuencia sedimentaria de la región de Caborca e identificaron 14 formaciones que abarcan edades neoproterozoicas y cámbricas (Figura 2), 11 reportadas anteriormente (Stoyanow, 1942; Cooper *et al*., 1952; Longoria *et al*., 1978; Longoria y Pérez, 1979; Longoria, 1980, 1981) y proponen como nuevas unidades a las formaciones Clemente y La Cuarcita Tecolote del Neoproterozoico y a la Formación La Ciénega que asignan al Cámbrico inferior. Los mismos autores, de acuerdo a diferencias litológicas y contenido fósil, dividen a la Formación Puerto Blanco en cuatro unidades, hacen referencia a la presencia de trilobites, arqueociátidos, hiolítidos, gasterópodos, braquiópodos e icnofósiles, además realizaron correlaciones con unidades del suroeste de Estados Unidos. Sour-Tovar *et al*. (2007), estudiaron la distribución estratigráfica de los fósiles índice *Cloudina* y *Treptichnus pedum* con la finalidad de determinar la posición del límite Ediacarense-Cámbrico en la región y señalan para la Formación La Ciénega una edad neoproterozoica-cámbrica. Entre los últimos trabajos que se han hecho sobre los afloramientos precámbrico-cámbricos del área están los de Loyd *et al*. (2012, 2013) que señalan la presencia del registro del evento marcado globalmente como la excursión Wonoka-Shuram en estratos de la Formación Clemente, en donde analizan las concentraciones de sulfatos del océano que cubrió la región durante el Neoproterozoico, obteniendo pruebas de fuertes variaciones en la concentración de oxígeno en los océanos y discuten el papel de este fenómeno sobre la evolución de metazoarios.

En este contexto, los estratos que marcan la transición Precámbrico-Cámbrico son ubicados en la parte alta de la Formación La Ciénega y la parte basal de la Formación Puerto Blanco. Tales estratos y su contenido fósil representan el registro de una serie eventos evolutivos relacionados con el origen y diversificación temprana de metazoarios. Los estratos superiores de la Formación La Ciénega contienen restos esqueléticos entre los que se ha identificado a *Cloudina*, fósil índice para la parte terminal del Ediacarense. Estos restos se relacionan al origen de los primeros animales con partes esqueléticas. En la base de la Formación Puerto Blanco, la unidad 1, se encuentra entre otros a *Treptichnus pedum*, icnofósil que se asocia a la colonización del medio infrabentónico. En la parte media-inferior de la Formación Puerto Blanco se registra el hallazgo de fósiles corporales de trilobites y braquiópodos, que representan el registro local de la llamada Explosión Cámbrica. En la parte media y superior de la misma formación, unidades 2 y 3, se encuentran bancos de arqueociátidos, un registro de los arrecifes fanerozoicos más antiguos que se desarrollan en la Tierra, y sobre ellos, en la parte alta de la unidad 3 y en toda la unidad 4 se tiene un registro muy abundante y diverso de icnofósiles. Una síntesis de los icnofósiles que se presentan en las diferentes unidades de la Formación Puerto fue presentada por Sour-Tovar y Hagadorn (2008). Se considera que identificar a los productores de los diferentes icnofósiles establece la presencia de tales organismos en el paleoambiente y que interpretar sus patrones conductuales permite inferir diversas condiciones bajo las que se depositaron los estratos portadores. En este contexto, el presente trabajo se enfoca al análisis de las galerías y rastros de trilobites que se han encontrado en la unidad 4 de la Formación Puerto Blanco.

2. Localidad

La sección tipo de la Formación Puerto Blanco se encuentra en los afloramientos del flanco oeste de los Cerros de la Proveedora, a 11 km al oeste del municipio de Caborca en Sonora, México (Figura 1). Fue descrita originalmente por Cooper *et al*. (1952), con un espesor de 293 m, compuesta de esquisto verde, arenisca y caliza con fósiles de diferentes invertebrados índice del Cámbrico inferior. En esta sección no está expuesta la base de la formación, pero ésta se puede observar en afloramientos que se encuentran en los Cerros Aquituni, Calaveras, Clemente, Rajón, de La Ciénega y en la Sierra del Viejo. El afloramiento en que se colectaron las muestras de estudio se encuentra entre las coordenadas 30°32'37" latitud norte y 111°53'48" longitud oeste, en el flanco noreste del Cerro Rajón localizado al sureste del poblado de Pitiquito, en el noroeste del estado de Sonora (Figura 1). Los icnofósiles que se describen se recolectaron en estratos de la unidad 4 de la Formación Puerto Blanco.

3. Estratigrafía de la Formación Puerto Blanco

Para la Formación Puerto Blanco se ha estimado un espesor de más de 700 metros y fue dividida en cuatro unidades caracterizadas por su litología y contenido fósil (Cooper y Arellano, 1946; Longoria, 1981; Stewart *et al*., 1984) (Figura 2). Para la unidad 1 se ha medido un espesor de alrededor de 285 metros, está compuesta por una alternancia de estratos de diorita, volcaniclastos arenosos y conglomeráticos, dolomita, cuarcita, limolita y dolomita limosa. La unidad 2, con un espesor total de aproximadamente 180 metros, está constituida principalmente por estratos de arenisca y lutita en los que se han encontrado restos de los trilobites *Fallotaspis* y *Nevadella*? que marcan una edad del Montezumano, la base de la Serie 2 del Cámbrico

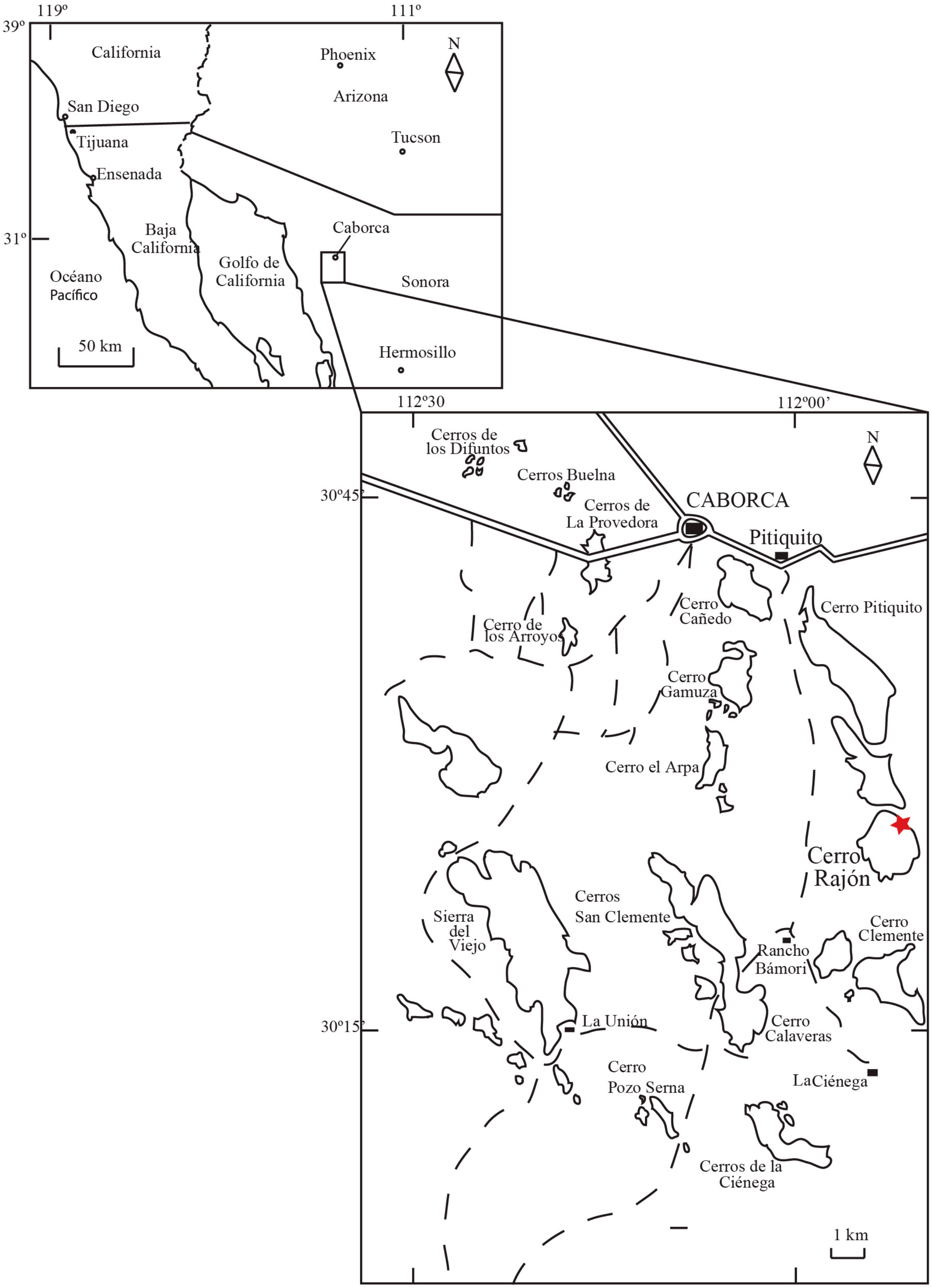

Figura 1. Mapa de ubicación de la localidad “Cerro Rajón”. La estrella señala el flanco noreste de Cerro Rajón donde se recolectó el material que se describe en el presente trabajo (modificado de Stewart *et al*., 1984).

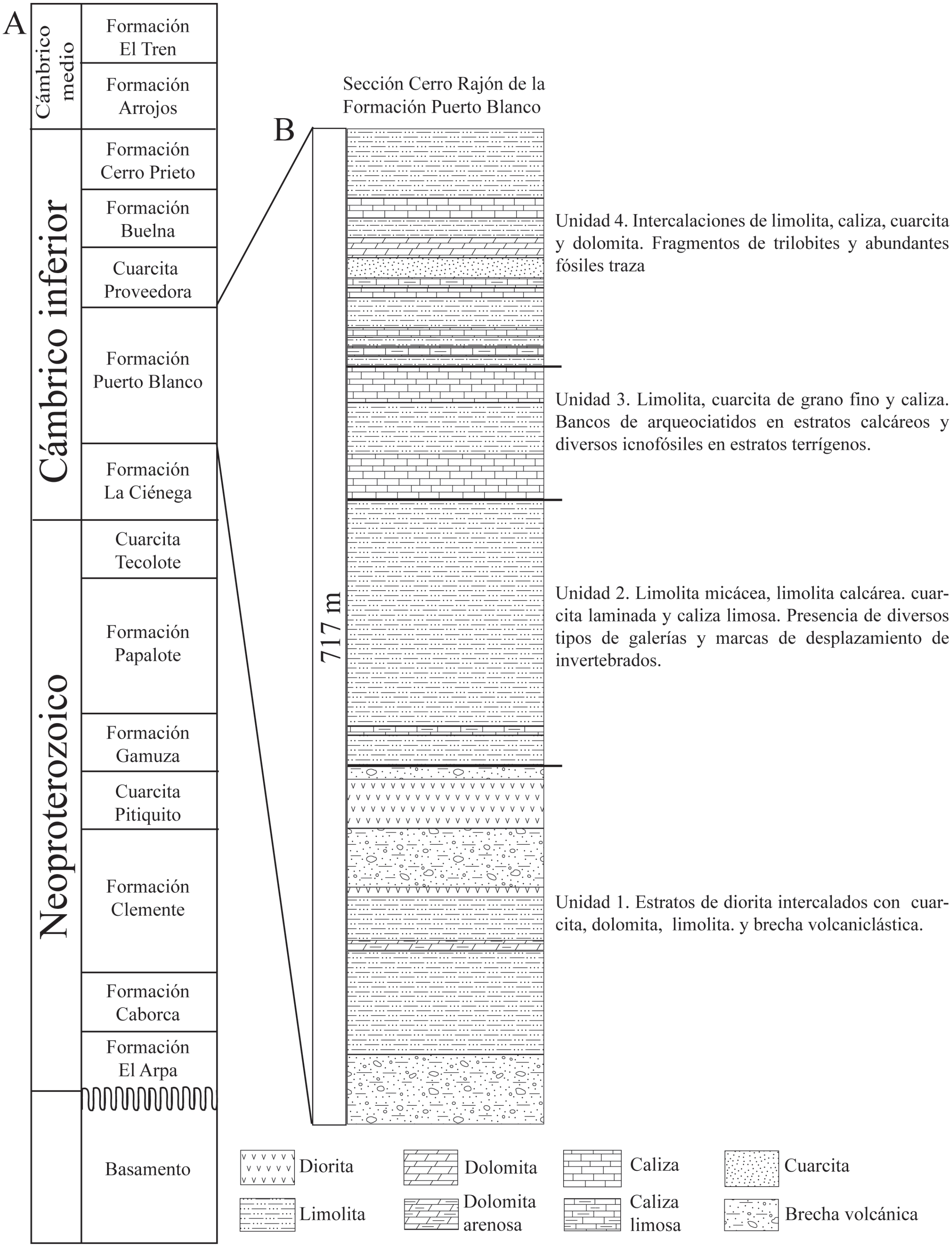

Unidad 4. Intercalaciones de limolita, caliza, cuarcita y dolomita. Fragmentos de trilobites y abundantes fósiles traza

Unidad 3. Limolita, cuarcita de grano fino y caliza. Bancos de arqueociatidos en estratos calcáreos y diversos icnofósiles en estratos terrígenos.

Unidad 2. Limolita micácea, limolita calcárea. cuarcita laminada y caliza limosa. Presencia de diversos tipos de galerías y marcas de desplazamiento de invertebrados.

Unidad 1. Estratos de diorita intercalados con cuarcita, dolomita, limolita. y brecha volcaniclástica.

Figura 2. Derecha (B), Sección estratigráfica de la Formación Puerto Blanco en la localidad de Cerro Rajón y su correlación con la columna general (A) de la secuencia Precámbrico-Cámbrico de la región de Caborca-Pitiquito elaborada por Stewart *et al*. (1984).

(Hollingsworth y Stewart, 2003). La unidad 3 posee un espesor de cerca de 120 metros, presenta principalmente estratos de caliza con algunas intercalaciones de lutita. En esta unidad domina la presencia de bancos arrecifales formados por arqueociátidos con espesores de hasta 6 metros. En la parte alta de esta unidad, en estratos areno-limosos, se encuentran diferentes tipos de icnofósiles, incluyendo a *Rusophycus*, *Scolicia* y *Bergaueria*. La unidad 4, con 140 metros de espesor, se caracteriza por intercalaciones de caliza, dolomita, cuarcita y limolita; en estratos de rocas calcáreas es común la presencia de *Skolithos* y en algunos estratos de dolomita se han encontrado restos de los trilobites *Laudonia* y *Wanneria* que indican una edad del Dyerano, en la Serie 2 del Cámbrico. En la parte alta de esta unidad, en estratos de limolita, se encuentra una asociación con abundantes y diversos tipos de icnofósiles, en su mayoría aún no descritos. Entre ellos, sobresalen los especímenes de *Rusophycus* y *Cruziana* que se describen en el presente trabajo.

La Formación Puerto Blanco sobreyace de manera concordante a la Formación La Ciénega, de edad ediacariana-cámbrica, y subyace a la Formación Proveedora cuya edad se ubica entre los Pisos 2 y 3 del Cámbrico.

4. Icnología Sistemática

Los ejemplares descritos se encuentran depositados en el Museo de Paleontología de la Facultad de Ciencias cuyo acrónimo es FCMP.

Icnogénero *Rusophycus* Hall, 1852

Icnoespecie tipo: *Fucoides biloba* Vanuxem, 1842.

Diagnosis: Galerías cortas, bilobuladas, raramente multilobuladas. Lóbulos con simetría bilateral predominante. Formas convexas (hypichnia) con un surco medio distintivo; formas cóncavas (epichnia) con una cresta media. El contorno varía de ovalado a una forma de grano de café, los rastros presentan rasguños que van de oblicuos a transversales o longitudinales en diferentes arreglos; en algunos casos son lisos (Stachacz, 2012).

Rusophycus marginatus Bersgtröm y Peel, 1988
Figura 3a–3d

Diagnosis: Madriguera (cubichnia) de artrópodo con rasguños de extremidades con forma de peine; ocasionalmente se presentan rasguños transversales acomodados irregularmente; impresión del escudo cefálico con arco anterior; comúnmente presenta forma de *Rusophycus*, pero también puede presentar forma de *Cruziana* [sic] (Bergström y Peel, 1988).

Material: Ejemplares FCMP-1235, FCMP-1236, FCMP-1237, FCMP-1238, FCMP-1239, FCMP-1244, FCMP-1245, FCMP-1248, FCMP-1251, FCMP-1254, FCMP-1255.

Descripción: Madrigueras de descanso (cubichnia) bilobuladas; su longitud varía de 43.45 mm a 103.61 mm, el ancho va desde los 31.05 a los 79.72 mm; la mayoría son madrigueras superficiales sobre el plano de sedimentación, en algunos casos en ligeras depresiones. Las impresiones de los rasguños de las espinas terminales divergen hacia el margen posterior y la mayoría de las veces son interceptadas por impresiones perpendiculares de los endopoditos; la intensidad de los rasguños de las espinas terminales y de las marcas de los endopoditos permiten inferir periodos de enterramiento muy variables. Se observa la impresión del escudo cefálico, asociado a remoción del sustrato, y la unión con los lóbulos; en la parte posterior la separación de los lóbulos es marcadamente mayor.

Discusión: La asignación del material descrito a *R. marginatus* se basa principalmente en la presencia de las impresiones del escudo cefálico con falta de espinas genales. El material se distingue de *Cruziana rugosa* reportada para el Ordovícico de América del Sur (d'Orbigny, 1842), por las impresiones del escudo cefálico; *C. furcifera* (d'Orbigny, 1842), y *C. goldfussi* (Roult, 1850) son icnoespecies similares, sin embargo, carecen de los rasguños de espinas terminales y solo se han reportado para el Tremadociano (Ordovícico Inferior) de América del Sur y Silúrico del Reino Unido. Las madrigueras descritas para Sonora se asocian a eventos de enterramiento durante los cuales el movimiento del cefalón provoca la remoción del sedimento.

Rusophycus isp. A
Figura 4a

Material: Ejemplares FCMP-1241, FCMP -1243, FCMP-1249.

Descripción: Madrigueras de descanso (cubichnia) bilobuladas, su longitud varía entre 24.48 mm y 77.47 mm, el ancho de 26.71 mm a 43.41 mm; y la profundidad entre 12.04 y 33.79 mm. Los lóbulos se encuentran unidos en la parte anterior y divergen hacia la parte posterior en ángulos que van de los 15° a los 36°. En los ejemplares se observan las marcas de endopoditos y en los especímenes FCMP-1241 y FCMP-1243 se encuentran marcas de espinas terminales en posición perpendicular a los endopoditos. No se observa la impresión del escudo cefálico.

Discusión: La morfología es similar a la descrita por Bergström y Peel (1988), para *Rusophycus marginatus* del Cámbrico inferior de Groenlandia, sin embargo, los ejemplares analizados difieren por presentar una mayor profundidad. El hecho de que en sólo dos ejemplares se observen marcas de espinas terminales nos indica que el tiempo de reposo de los trilobites fue diferente para cada madriguera analizada.

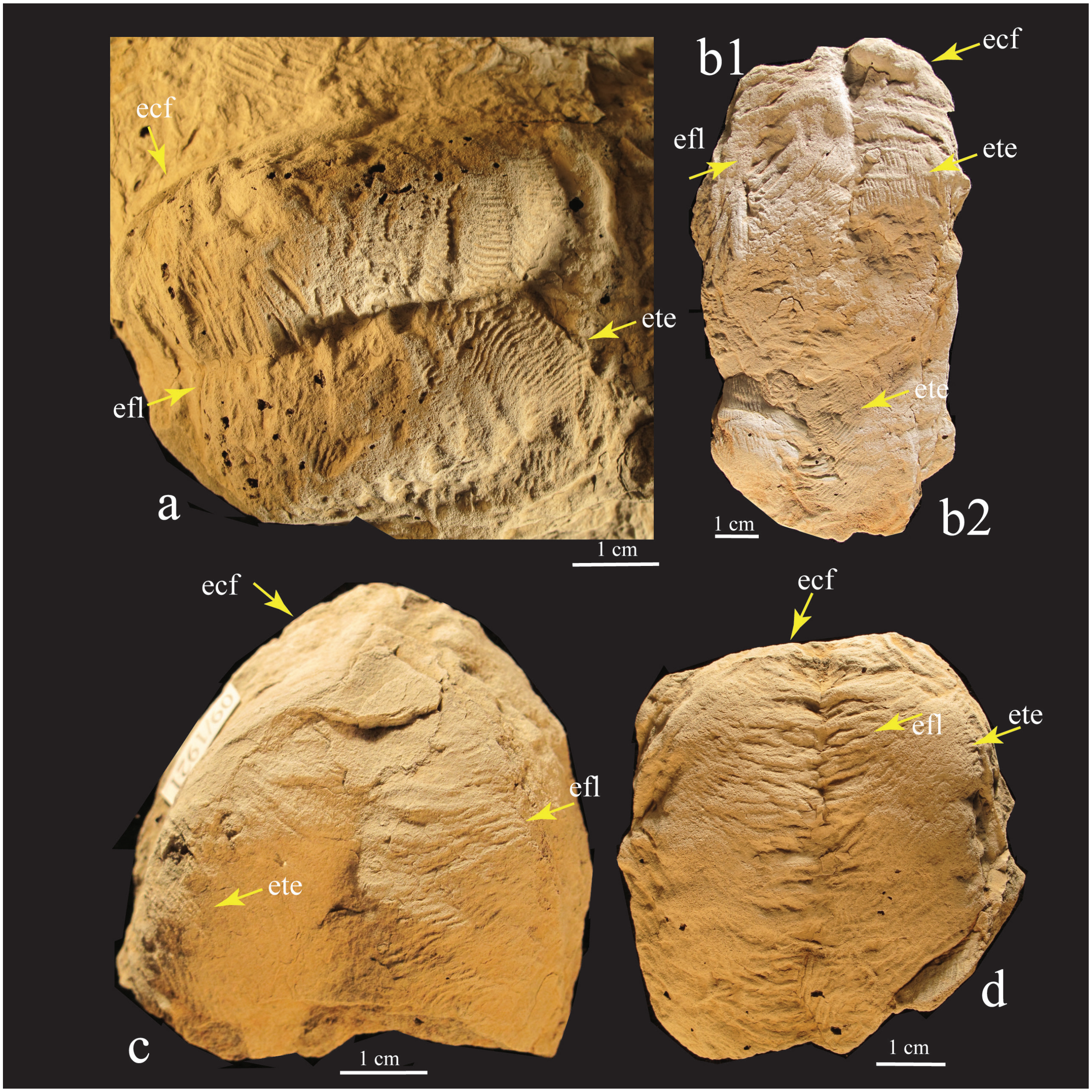

Figura 3. *Rusophycus marginatus*. a. FCMP-1244, b1. FCMP-1245, b2. FCMP-1255, c. FCMP-1238 y d. FMCP-1239. Las cuatro madrigueras muestran bilobulación, las impresiones del escudo cefálico (ecf), de los endopoditos flexionados (efl) y de las espinas terminales de los endopoditos (ete). En b, los ejemplares FCMP-1245 y FCMP-1255 son dos galerías sobrepuestas. Material colectado en la unidad 4 de Formación Puerto Blanco, Sección Cerro Rajón, área de Caborca-Pitiquito, Noroeste de Sonora.

Rusophycus isp. B.

Figura 4e

Material: FCMP-1242.

Descripción: Madriguera de forma bilobulada, con una longitud de 20.05 mm y un ancho de 36.33 mm. Sus lóbulos divergen posteriormente en un ángulo 50° y presentan tres marcas simétricas de los endopoditos en la parte posterior.

Discusión: La morfología que presenta el ejemplar FCMP-1242 es similar a la de *Cruziana salomonis*, del Cámbrico inferior de Turquía y Cámbrico medio de Jordania (Seilacher, 1990), que también presentan rasguños en grupos de tres en la parte posterior; sin embargo *C. salomonis* presenta un ancho y largo mayores a los del ejemplar de Sonora y no presenta una divergencia de los lóbulos en la parte posterior. *Rusophycus* isp. B también presenta una morfología similar a la de *Rusophycus didymus* del Cámbrico inferior de Pakistán (Seilacher, 1955) y de las Montañas White Inyo en California (Alpert, 1976), cuyas dimensiones son menores y presentan rasgos, como las impresiones del escudo cefálico o de las antenas, que no se han preservado con detalle en el ejemplar de Sonora.

Rusophycus isp. C
Figura 4c–d

Material: Ejemplares FCMP-1240, FCMP-1247.

Descripción: Madrigueras bilobuladas con una longitud de 65.24 mm a 97.37 mm, un ancho de 60.02 a 58.81 mm y una profundidad máxima de 22.35 mm. En el ejemplar FCMP-1247 se observan marcas muy finas de espinas terminales; en el ejemplar FCMP-1240 se observan marcas de endopoditos en cada lóbulo; el ejemplar FCMP-1240 presenta la impresión de la parte posterior del escudo cefálico, de las mejillas libres, del hipostóma y de las espinas genales.

Discusión: El material de *Rusophycus* isp. C presenta una morfología similar a la de *Rusophycus dispar*, del Cámbrico inferior de Suecia (Linnarsson, 1859), pero en los ejemplares de Sonora se observa que los rasguños de los endopoditos tienen una dirección anteroposterior, opuesta a la que se observa en *R. dispar*. *Rusophycus* cf. *dispar* del Cámbrico inferior de California (Alpert, 1976), también es parecido, pero se distingue del material de Sonora por la orientación posteroanterior de los rasguños dejados por los endopoditos, por dimensiones menores en la longitud, ancho y profundidad de la galería y por las proporciones entre esas medidas. *Rusophycus marginatus* del Cámbrico inferior de Groenlandia (Bergström y Peel, 1988), se distingue por una anchura y longitud mayores y porque los rasguños se encuentran dispuestos de manera irregular. El ejemplar FCMP-1240 tiene una mayor profundidad de la que se ha observado en ejemplares de *R. marginatus* que se describen en este trabajo y además presenta impresiones de espinas genales. Dado que estas estructuras son muy difíciles de preservar en madrigueras provisionales, el observar las marcas del escudo cefálico, de las mejillas libres, del hipostoma y de las espinas genales, indica que los trilobites productores permanecieron dentro de las madrigueras durante un periodo de tiempo prolongado.

Rusophycus isp. D
Figura 4b

Material: Ejemplar FCMP-1250.

Descripción: Madriguera bilobulada con una longitud de 92.65 mm y un ancho de 60.92 mm. En el lóbulo derecho se observan las impresiones de ocho endopoditos y de siete en el izquierdo. Las marcas de los endopoditos se encuentran flexionadas hacia la parte central del icnofósil, se bifurcan en el extremo en que se presentan las espinas terminales y presentan estrías finas a todo lo largo.

Discusión: El ejemplar presenta similitudes con *Rusophycus avalonensis* del Cámbrico inferior del sureste de Canadá (Crimes y Anderson, 1985), como son la poca profundidad y encontrar rasguños en grupos de 5 o más, sin embargo, el ejemplar descrito tiene un tamaño mayor que el reportado para *R. avalonensis*. El ejemplar también muestra similitudes con *Rusophycus burjensis* del Cámbrico medio de Jordania (Hofmann *et al*., 2012), como lo son un largo y ancho dentro del promedio de la icnoespecie, la parte anterior más ancha que la posterior y grupos de espinas terminales al final de los endopoditos. No se da una asignación icnoespecífica por la carencia de más ejemplares. La fina conservación de las estrías y bifurcación de los endopoditos se ha interpretado como evidencia de un lapso de reposo prolongado posterior al proceso de excavación que realizó el trilobite.

Icnogénero *Cruziana* d'Orbigny, 1842

Icnoespecie tipo: *Cruziana rugosa* d'Orbigny, 1842.

Diagnosis: Madrigueras de interfaz o rastros alargados (relación longitud/ancho 2:1), por lo general en forma de cinta bilobulada (raramente unilobulada) preservados como surcos con cresta media cuando se conserva como epirelieve cóncavo, como senderos bilobulados con surco medio cuando se conservan en hiporelieves convexos o como surcos que están en estrecha proximidad con menos del ancho de un surco de separación. Rastros cubiertos por rasguños en forma de espinas o transversales, con o sin zonas lisas o rasguños longitudinales periféricos a los rasguños internos, con o sin crestas laterales o con marcas difusas si es un hiporelieve (Keighley y Pickerill, 1996).

Cruziana isp. A
Figura 4f

Material: Ejemplares FCMP-1246, FCMP-1252, FCMP-1253.

Descripción: Rastros de desplazamiento (repchnia) con un largo que varía de 17.78 a 75.36 mm y un ancho de 6.01 a 24.11 mm. En general se presenta una mala preservación por lo cual solo se pueden observar impresiones muy tenues de las espinas terminales. El ejemplar FCMP-1253 (Figura 4f), presenta un surco central bien definido con depresiones de 2.41 mm de largo y se intercepta, en un ángulo de 55°, con un rastro de 47.87 mm de largo por 21.03 mm de ancho.

Discusión: La mala preservación de los rastros no permite observar características que permitan asignar el material a alguna icnoespecie de *Cruziana*. Debido a que los rasguños de las espinas terminales se encuentran alargados, se puede inferir que la velocidad del desplazamiento de los organismos que generaron el rastro era moderada. En el ejemplar FCMP-1253 se observa la transición de madriguera a rastro y puede inferirse que se trata del rastro que dejó el trilobite al abandonar la madriguera.

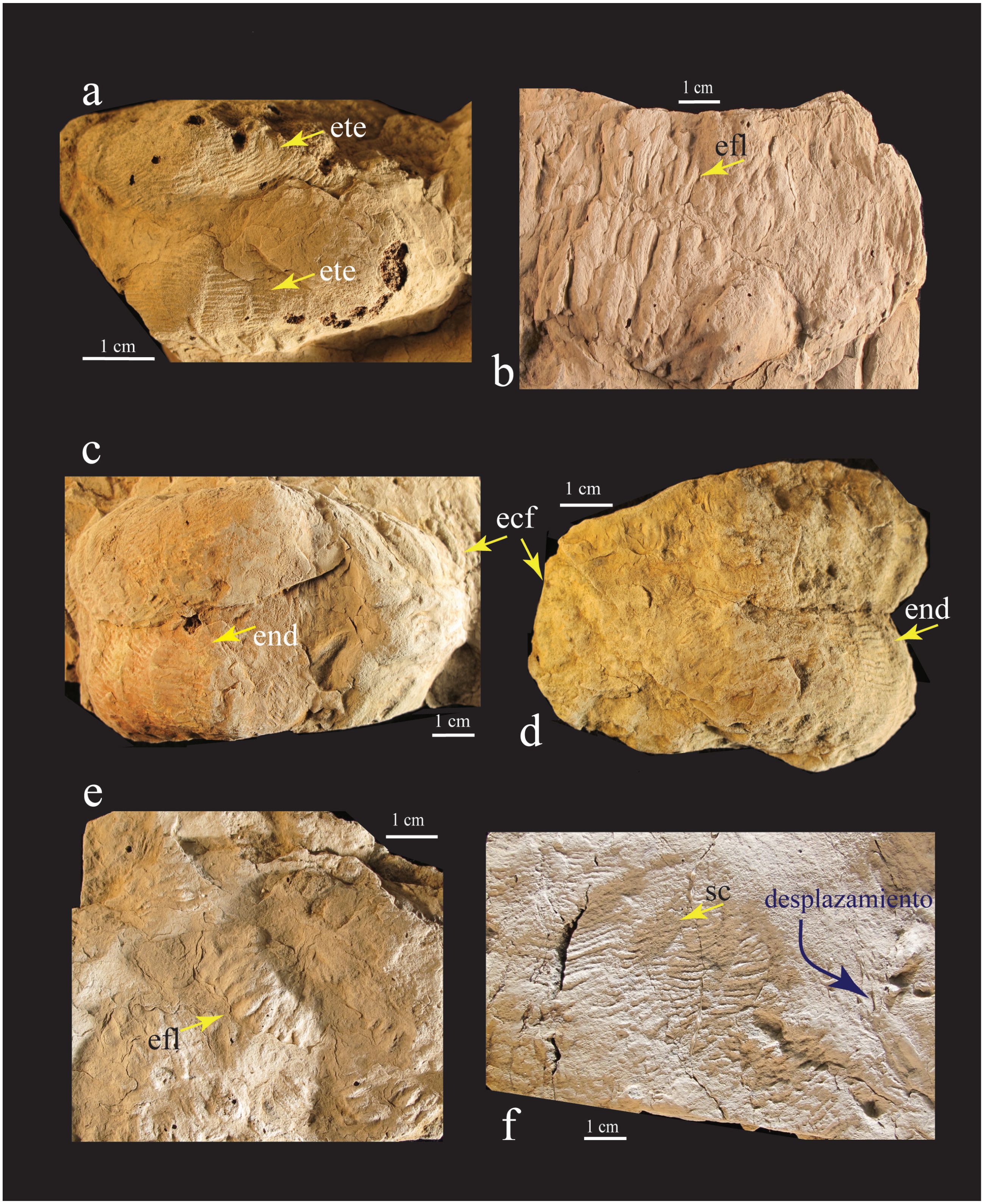

Figura 4. a. *Rusophycus* isp. A, ejemplar FCMP-1243, madriguera bilobulada donde se señalan las marcas de las espinas terminales de los endopoditos (ete); b, *Rusophycus* isp. D, ejemplar FCMP-1250, madriguera bilobulada, se observan las marcas flexionadas de los endopoditos (efl); c y d, *Rusophycus* isp. C, c. ejemplar FCMP-1240, d. ejemplar FCMP-1247, madrigueras bilobuladas que presentan la impresión del escudo cefálico (ecf) y de los endopoditos (end); e, *Rusophycus* isp. B, ejemplar FCMP-1242, madriguera bilobulada con marcas flexionadas de los endopoditos (efl); f, *Cruziana* isp. A, ejemplar FCMP-1253, rastro de desplazamiento que inicia a partir de una galería con surco central (sc) bien definido; la flecha señala la dirección de desplazamiento. Material colectado en la unidad 4 de Formación Puerto Blanco, Sección Cerro Rajón, área de Caborca-Pitiquito, Noroeste de Sonora.

5. Discusión y conclusiones

5.1. Icnotaxonomía

En el presente trabajo se describieron 6 morfotipos de icnofósiles. La presencia de impresiones del escudo cefálico y la ausencia de las de espinas genales permitió que un primer morfotipo se asignara a la icnoespecie *Rusophycus marginatus* (Bergström y Peel, 1988). En cuatro morfotipos la morfología típica de una madriguera bilobulada permite asignarlos al icnogénero *Rusophycus*, sin lograr una asignación específica. Un sexto morfotipo, que se caracteriza como un rastro bilobulado, con un largo de cerca de 7.5 centímetros se asigna al icnogénero *Cruziana*. Los dos icnogéneros determinados tienen una distribución temporal que va desde el Cámbrico inferior hasta el Presente (Osgood, 1970).

5.2. Organismos productores

Rusophycus, *Cruziana* y *Diplichnites* representan los tres tipos de icnofósiles que tradicionalmente se asocian a trilobites como organismos productores, pero también se han asociado a otros artrópodos, como crustáceos y miriápodos (Arbizu *et al*., 2009). Para las formas cámbricas, los trilobites, son los invertebrados bentónicos más abundantes y comunes, y con la morfología correspondiente, son el grupo generalmente considerado como el principal productor de este tipo de trazas. En particular para la Formación Puerto Blanco, cuya edad se ha asignado al Cámbrico inferior (Dyerano, Serie 2 del Cámbrico), se han reportados diversos tipos de trilobites entre los que se encuentra a *Fallotaspis*, presente en la parte media de la unidad 2; *Judomia* y *Nevadia* se encuentran en la unidad 3; *Wanneria* en la unidad 4 (McMenamin, 1987) y *Laudonia* en la parte alta de la unidad 4 (Stewart *et al*., 1984). Todos los géneros mencionados pertenecen al Orden Redlichiida, Suborden Olenellina que son considerados por Lieberman (1998) a partir de análisis filogéneticos, y por Fortey y Owens (1999) por su morfología, como los trilobites más primitivos. El suborden Olenellina se caracteriza por presentar una convexidad dorsoventral moderada, un caparazón con contorno oval, puntas genales, un tórax compuesto por numerosos segmentos, un pigidio pequeño, un cuerpo que se puede arquear considerablemente, ojos grandes y un hipostoma conectado (Rábano, 1999). Los trilobites del género *Laudonia* poseen un cefalón de subcuadrado a subpentagonal en el contorno; espinas genales que se originan opuestas o anteriores al lóbulo 3; espinas procraniales no desarrolladas en adultos; un surco intergenal definido; el área preglabelar no existe o es más corta que el borde, la parte posterior de los lóbulos oculares es opuesta o anterior al lóbulo 1, y el tórax presenta alrededor de 20 segmentos (Palmer y Repina, 1993). Las especies conocidas de *Wanneria* tienen el margen posterior del cefalón recto o curvado hacia la base de la espina genal, carecen de espinas intergenales, el preglabelar está ausente, la parte posterior de los lóbulos oculares es opuesta o anterior al surco occipital y el tórax posee 17 segmentos en los que el quinceavo presenta una espina genal larga. El pigidio es pequeño, subcuadrado con una muesca media prominente. En especímenes bien preservados, el perímetro de los polígonos está marcado por filas de perforaciones en la parte inferior del exoesqueleto (Palmer y Repina, 1993). La morfología de ambos géneros, *Laudonia* y *Wanneria*, es consistente con los rasgos visibles en las galerías de *Rusophycus* que se describen en este trabajo, como su contorno ovalado y las impresiones de las espinas genales, y en las dimensiones de los rastros de *Cruziana* analizados. La presencia de ejemplares, de ambos géneros de trilobites, en la unidad 4 de la Formación Puerto Blanco corrobora su papel de organismos productores.

5.3. Etología

Siguiendo la propuesta de Seilacher (1953) *Rusophycus* y *Cruziana* son estructuras que se clasifican como *Cubichnia* y *Repichnia* respectivamente. El primer tipo son estructuras de descanso que reflejan el tamaño y la morfología latero-ventral del organismo que la produce; el segundo tipo agrupa estructuras superficiales que se asocian a un comportamiento de locomoción. Además de estas interpretaciones, Fortey y Owens (1999) han asociado a *Rusophycus* y *Cruziana* a hábitos depredadores, carroñeros y detritívoros presentados por trilobites olenidos. Por su parte Seilacher y Gishlick (2015) mencionan que algunas madrigueras de *Rusophycus* están asociadas al proceso de muda del exoesqueleto que presentaban los trilobites. Los icnofósiles de *Rusophycus* encontrados en la unidad 4 de la Formación Puerto Blanco, se interpretan principalmente como madrigueras de descanso porque no se observan los nódulos mencionados por Seilacher y Gishlick (2015) que se asocian al proceso de muda del exoesqueleto. Se interpreta que el tiempo que pasaron los trilobites dentro de las madrigueras fue variable, en particular, para los ejemplares FCMP-1240 (*Rusophycus* isp. C) y FCMP-1250 (*Rusophycus* isp. D) (Figura 4b y 4c) se infiere que son madrigueras en donde el trilobite estuvo enterrado por un tiempo prolongado permitiendo la conservación de detalles del hipostoma y la impresión de las espinas terminales de los endopoditos. En el resto de las madrigueras analizadas el tiempo que pasó el trilobite fue menor, rasgo que se interpreta dado que solamente se observan rasguños dejados por los endopoditos. En los ejemplares de *Cruziana* que se han analizado solo se pueden ver marcas alargadas que dejaron los endopoditos, pero la disposición que se observa, en cuanto a la separación corta y homogénea que existe entre cada marca, indica que el trilobite se estaba desplazando a una velocidad moderada. En el ejemplar FCMP-1253 se observa que el trilobite inicia su movimiento a partir de una galería (Figura 4f).

5.4. Icnofacies y Paleoambiente

Además de los icnofósiles *Cruziana* y *Rusophycus*, en la unidad 4 de la Formación Puerto Blanco se han encontrado a los icnogéneros *Bergaueria*, *Paleophycus* y *Skolithos* (Sour-Tovar y Hagadorn, 2008), que en conjunto permiten interpretar la asociación como típica de una icnofacies *Cruziana*. Esta icnofacies es característica de ambientes marinos submareales que presentan una alta diversidad biológica, una salinidad constante, energía moderada y sustratos poco consolidados (MacEachern *et al*., 2007). Se puede observar en costas, frentes deltaicos y bahías donde los recursos alimenticios van a consistir de partículas suspendidas o depositadas por lo cual la mayoría de los organismos van a presentar hábitos detritívoros y suspensívoros, aunque también van a estar presentes organismos carnívoros y carroñeros (MacEachern *et al*., 2007). Los organismos productores de los fósiles traza en esta icnofacies prefieren construir madrigueras horizontales, como es el caso de *Rusophycus*, principalmente por el depósito de gran cantidad de partículas orgánicas; los bajos niveles de energía y los sustratos poco consolidados son factores que también influyen en la construcción de este tipo de madrigueras.

Aunada a la información paleoambiental que aportan las galerías estudiadas, también es de importancia mencionar que la presencia de parches arrecifales de arqueociátidos en la unidad 3 de la Formación Puerto Blanco, permite inferir que en el paleoambiente se desarrollaron facies que representan condiciones de aguas cálidas, con buena oxigenación, poca turbidez, buena iluminación y una profundidad entre los 30 y 40 metros. El hallazgo de galerías del icnogénero *Skolithos*, en los mismos niveles en que se encuentra a *Rusophycus* y *Cruziana*, indica la existencia de organismos con hábitos suspensívoros. *Skolithos*, galería tipicamente vertical y de dimensiones relativamente grandes, es característico de ambientes de alta energía, con un sustrato libre de partículas orgánicas y en donde se van a presentar cambios bruscos en la velocidad de sedimentación, erosión y retrabajo físico de los sedimentos (MacEachern *et al*., 2007). Al encontrar a *Skolithos* en una icnofacies *Cruziana* y asociado a icnofósiles como *Rusophycus* y *Cruziana* podemos inferir que en el depósito de sedimentos de la unidad 4 se presentaban condiciones estacionales con un aumento en la energía y en la erosión de los sedimentos superficiales, condiciones que son comunes en ambientes cercanos a la costa. Estos cambios podrían haberse dado en caso de que se presentaran regresiones y transgresiones del océano o por cambios en la afluencia de una posible desembocadura fluvial. Integrando la información, se puede postular que los sedimentos en que se encuentran los icnofósiles descritos, *Rusophycus* y *Cruziana*, se acumularon en una facies de tipo lagunar que formó parte de un ambiente litoral con zonas arrecifales, registradas por los parches de arqueociátidos, y partes sujetas esporádicamente a exposiciones subáreas o de aumento en el oleaje, marcadas por la presencia de *Skolithos*. La extensión geográfica que abarcaron los diferentes ambientes en que se dio el depósito de la Formación Puerto Blanco es difícil de calcular; sin embargo, la distancia máxima que se tiene entre dos localidades, la de Cerro Rajón y Cerros de la Proveedora es de 20 km. Esta distancia nos da el mínimo que pudo existir entre dos subambientes.

Agradecimientos

A los árbitros R. Guerrero-Arenas y M.A. Torres-Martínez, por la revisión crítica del manuscrito original y sus acertadas observaciones y sugerencias. J.S. Hollingsworth aportó importante ayuda en la determinación taxonómica de los trilobites presentes en la Formación Puerto Blanco. L. Martin-Medrano y D. Navarro-Santillán apoyaron en las actividades curatoriales y al lado de J.W. Hagadorn, E. Smith, K. Castillo-Espinoza e I. de la Mora colaboraron de manera entusiasta durante el trabajo de campo.

Referencias

Alpert, S.P., 1976, Trilobite and star-like trace fossils from the White-Inyo Mountains: California: Journal of Paleontology, 50(2), 226–239. *Disponible en* <http://www.jstor.org/stable/1303490>.

Anderson T.H., Silver L.T., 1970, Reconnaissance survey of Precambrian rocks, northwestern Sonora, Mexico: Geological Society of America Abstracts with Programs, 2(7), 484.

Arbizu, M., Liñan, E., Rábano, I., 2009, Trilobita, *en* Martínez-Chacón, M.L., Rivas, P. (eds.), Paleontología de Invertebrados: Gijón, Sociedad Española de Paleontología, Instituto Geológico y Minero de España, Universidad de Oviedo, Universidad de Granada, 119–153.

Bergström, J., Peel, J.S., 1988, Lower Cambrian trace fossils from northern Greenland: Grønlands Geologiske Undersøgelse Rapport, 137, 43–53.

Cooper, G.A., Arellano, A., 1946, Stratigraphy near Caborca, northwest Sonora, Mexico: American Association of Petroleum Geologists Bulletin, 30(4), 606–611.

Cooper, G.A., Arellano, A.R.V., Johnson, J.H., Okulitch, V.J., Stoyanow, A., Lochman, C., 1952, Cambrian stratigraphy and paleontology near Caborca, northwest Sonora, Mexico: Smithsonian Miscellaneous Collections, 119(1), 184.

Crimes, T.P., Anderson, M.M., 1985, Trace Fossils from Late Precambrian-Early Cambrian Strata of Southeastern Newfoundland (Canada): Temporal and Environmental Implications: Palaeontology, 59(2), 310–343. *Disponible en* <http://www.jstor.org/stable/1305031>.

De Cserna, Z., 1970, The Precambrian of Mexico, *en* Rankam, K. (Ed.), The Precambrian IV: New York, John Willey and Sons, 253–270.

Damon, P.E., Livingston, D.E., Mauger, R.L., Giletti, B.J., Pantoja–Alor, J., 1962, Edad del Precámbrico Anterior y de otras rocas del Zócalo de la región de Caborca–Altar de la parte noroccidental del Estado de Sonora: Boletín del Instituto de Geología, Universidad Nacional Autónoma de México, 64, 11–44.

Fortey, R.A., Owens, R.M., 1999, Feeding habits in trilobites: Palaeontology, 42(3), 429–465. https://doi.wiley.com/10.1111/1475-4983.00080.

Fritz, W.H., 1975, Broad correlations of some Lower and Middle Cambrian strata in the North America Cordillera: Geological Survey of Canada Paper, 75(1), 533–540.

Gamper, M.A., Longoria, J.F., 1979, Sobre la ocurrencia de estromatolitos en la secuencia precámbrica del Cuadrángulo Pitiquito-La Primavera, NW de Sonora: Boletín del Departamento de Geología, Universidad de Sonora, 1, 95–104.

Hollingsworth, J.S., Stewart, J., 2003, Biostratigraphy of the early Cambrian Montezuman stage in western North America: Geological Society of America 55th Annual Meeting, Durango California, Abstracts, Paper 10-1.

Hofmann, R., Mángano, M.G., Elicki, O., Shinaq, R., 2012, Paleoecologic and biostratigraphic significance of trace fossils from shallow-to marginal-marine environments from the Middle Cambrian (Stage 5) of Jordan: Journal of Paleontology, 86(6), 931–955. https://doi.org/10.1666/11-129R1.1.

Keighley, D.G., Pickerill, R.K., 1996, Small *Cruziana*, *Rusophycus*, and related ichnotaxa from eastern Canada: The nomenclatural debate and systematic ichnology: Ichnos, 4(4), 261–285. https://doi.org/10.1080/10420949609380136.

Lieberman, B.S., 1998, Cladistic analysis of the Early Cambrian Olenelloid trilobites: Journal of Paleontology, 72(1), 59–78. https://doi.org/10.1017/S0022336000024021.

Linnarsson, J.G., 1859, On some Fossils found in the Eophyton Sandstone, at Lugnås, in Sweden: Geological Magazine, 6(63), 393–406. https://doi.org/10.1017/S0016756800162910.

Lochman, C., 1948, New Cambrian Trilobite Genera from Northwest Sonora, Mexico: Journal of Paleontology, 22(4), 451–464. *Disponible en* <http://www.jstor.org/stable/1299515>.

Lochman, C., 1953, Corrections to Trilobites in Cambrian Stratigraphy and Paleontology near Caborca, Northwestern Sonora, Mexico: Journal of Paleontology, 27(3), 486–488. *Disponible en* <http://www.jstor.org/stable/1300007>.

Lochman, C., 1956, The Cambrian of the Rocky Mountains and southwest desert of the United States and adjoining Sonora province, Mexico, *en* Rogers, J. (ed.), El Sistema Cámbrico, su paleogeografía y el problema de su base: México, 20th International Geological Congress Book, 529–661.

Longoria, J.F., 1980, Estudios y trabajos geológicos en las áreas del Estado de Sonora, donde afloran las rocas del Precámbrico: Boletín del Departamento de Geología Universidad de Sonora, 158 pp.

Longoria, J.F., 1981, Geologic features of northwest Sonora, *en* Longoria, J.F. (ed.), Regional geology of northwest Sonora: Hermosillo Geological Society of America, Cordilleran Section Annual Meeting Proceedings, 1–48.

Longoria, J.F., González, M.A., Mendoza, J.J., Perez, V.A., 1978, Consideraciones estrucutrales en el cuadrangulo Pitiquito-La Primavera, NW de Sonora: Boletín del Departamento de Geología Universidad de Sonora, 1(1), 19–34.

Longoria, J.F., Pérez, V.A., 1979, Bosquejo geológico de los Cerros Chino y Rajón, cuadrángulo Pitiquito-La Primavera (NW de Sonora): Boletín del Departamento de Geología Universidad de Sonora, 1(2), 119–144.

Loyd, S.J., Marenco, P.J., Hagadorn, J.W., Lyons, T.W., Kaufman, A.J., Sour-Tovar, F., Corsetti, F.A., 2012, Sustained low marine sulfate concentrations from the Neoproterozoic to the Cambrian: Insights from carbonates of northwestern Mexico and eastern California: Earth and Planetary Science Letters, 339–340, 79–94. https://doi.org/10.1016/j.epsl.2012.05.032.

Loyd, S.J., Marenco, P.J., Hagadorn, J.W., Lyons, T.W., Kaufman, A.J., Sour-Tovar, F., Corsetti, F.A., 2013, Local $\delta^{34}S$ variability in 580 Ma carbonates of northwestern Mexico and the Neoproterozoic marine sulfate reservoir: Precambrian Research, 224, 551–569. https://doi.org/10.1016/j.precamres.2012.10.007.

MacEachern, J.A., Pemberton, G.S., Gingras, M.K., Bann, K., 2007, The Ichnofacies Paradigm: A fifty-year retrospective, *en* Miller, W. (ed.), Trace Fossils: Concepts, Problems, Prospects: New York, Elsevier Science & Technology Books, 52–77. https://doi.org/10.1016/B978-044452949-7/50130-3.

McMenamin, M.A.S., 1987, Lower Cambrian trilobites, zonation, and correlation of the Puerto Blanco Formation, Sonora, Mexico: Journal of Paleontology, 61(4), 738–749. *Disponible en* <http://www.jstor.org/stable/1305285>.

Orbigny, A.D.d', 1842, Voyage dans l'Amerique méridionale (le Brésil, la República Argentine, le Patagonia, le República de Chile, le República de Bolivie, le República de Perou) executé pendant les anee 1826, 1827, 1828, 1829, 1830, 1831, 1832 et 1833: Chez P. Bertrand, Paris. 672 pp.

Osgood, R.G., 1970, Trace fossils of the Cincinnati area: Palaeontographica Americana, 41, 301–305.

Palmer, A.R., Halley, R.B., 1979, Physical stratigraphy and trilobite biostratigraphy of the Carrara Formation (Lower and Middle Cambrian) in the southern Great Basin: U.S. Geological Survey Professional Paper, 1047, 1–131.

Palmer, A.R., Repina, L.N., 1993, Through a glass darkly: taxonomy, phylogeny, and biostratigraphy of the *Olenellina*: The University of Kansas Paleontological Contributions, 3, 1–35. https://doi.org/10.17161/PCNS.1808.3760.

Rábano, I., 1999, Historia Evolutiva de los Trilobites, *en* Melic, A., De Haro, J.J., Mendez, M., Ribera, I. (eds.), Evolución y Filogenia de Artrópodos: Boletín de la Sociedad Entomológica Aragonesa, 26, 225–233.

Roult, M., 1850, Note préliminaire sur une nouvelle formation découverte dans le terrain silurien inferior de la Bretagne: Bulletin de la Société Géologique de France, 2(7), 724–744.

Seilacher, A., 1953, Studien zur palichnologie. I. Über die Methoden der Palichnologie: Neues Jahrbuch für Geologie und Paläontologie, 96, 421–452.

Seilacher, A., 1955, Spuren und fazies im Unterkambrium, *en* Schindewolf O.H. und Seilacher, A. (eds.), Beiträge zur Kenntnis des Kambriums in der Salt Range (Pakistan): Akademie der Wissenschaften und der Literatur in Mainz, 373–399.

Seilacher, A., 1990, Paleozoic trace fossils, *en* Said, R. (Ed.), The Geology of Egypt: Rotterdam, Brookfield A.A Balkema, 649–722.

Seilacher, A., Gishlick, A.D., 2015, Trilobites, *en* Press, C. (ed.). Morphodynamics: Londres, CRC Press, 359–379.

Sour-Tovar, F., Hagadorn, J.W., Huitrón-Rubio, T., 2007, Ediacaran and Cambrian index fossils from Sonora, Mexico: Palaeontology, 50(1), 169–175. https://doi.org/10.1111/j.1475-4983.2006.00619.x.

Sour-Tovar F., Hagadorn J.W., 2008, Early Cambrian trace fossils from Sonora, northern Mexico, *en* Uchman, A. (ed.), The Second International Congress on Ichnology: Cracovia, Polish Geological Institute, 118-119.

Stachacz, M., 2012, New finds of *Rusophycus* from the Lower Cambrian Ocieseki Sandstone Formation (Holy Cross Mountains, Poland): Geological Quarterly, 56(2), 237–248. https://doi.org/10.7306/gq.1018.

Stewart, J., McMenamin, M., Morales-Ramirez, J., 1984, Upper Proterozoic and Cambrian rocks in the Caborca region, Sonora, Mexico. Physical stratigraphy, biostratigraphy, paleocurrent studies, and regional relations: United States Geological Survey Professional Paper, 1309, 1–36.

Stoyanow, A., 1942, Paleozoic paleogeography of Arizona: Geological Society of America Bulletin, 53(9), 1255–1282. https://doi.org/10.1130/GSAB-53-1255.

Vanuxem, L., 1842, Geology of New-York Part III. Comprising the survey of the third geological district: New York Geological Survey, 306 pp.

Weber, R., Cevallos-Ferriz, S., 1980, El significado bioestratigráfico de los estromatolitos del Precámbrico sedimentario de la región de Caborca, Sonora: Revista del Instituto de Geología, Universidad Nacional Autónoma de México, 4(2), 104–110.

Manuscrito recibido: Marzo 3, 2018.
Manuscrito corregido recibido: Mayo 18, 2018.
Manuscrito aceptado: Mayo 22, 2018.

Paleontología Mexicana
Volumen 7, núm. 1, 2018, p. 13 – 18

Los holasteroides (Echinoidea: Holasteroida) del Cretácico en México

Alejandra Martínez Melo[a,*], Blanca Estela Buitrón Sánchez[b]

[a] Colección Nacional de Paleontología, Instituto de Geología, Universidad Nacional Autónoma de México. Ciudad Universitaria. C.P. 04510, Ciudad de México, México.
[b] Departamento de Paleontología, Instituto de Geología, Universidad Nacional Autónoma de México, Ciudad Universitaria, CP. 04510, Ciudad de México, México.

[*] a.mtz.melo@gmail.com

Resumen

El Orden Holasteroida actualmente cuenta con tres géneros de morfologías extremas, restringidos a los ambientes de aguas profundas. En el registro fósil se han reportado 49 géneros desde el Cretácico, donde se conocen principalmente en aguas someras. El presente trabajo actualiza la información taxonómica de los holasteroides del Cretácico de México. Para ello se tomaron como base listados previos; los taxa fueron revisados, redeterminados y clasificaron bajo criterios recientemente publicados. Se confirman las especies *Pseudananchys completa*, *Holaster nanus*, *Holaster simplex* para el Cretácico de México; para cada una de las especies reportadas se presenta la información taxonómica disponible, una lámina ilustrando las mismas y un mapa de distribución.

Palabras clave: Echinocorythidae, Holasteridae, *Pseudananchys completa*, *Holaster nanus*, *Holaster simplex*, Formación Aurora, Formación Indidura.

Abstract

Order Holasteroida includes three recent genera kinds of extreme morphologies, restricted to deep-water environments. There are 49 fossil genera reported since the Cretaceous, mainly in shallow waters. This paper updates taxonomic information of the holasteroids from the Cretaceous in Mexico. We based in previous reports; taxa were reviewed, re-determined and classified under current criteria. Species Pseudananchys completa, Holaster nanus, and Holaster simplex are reported for the Upper Cretaceous from Mexico. We present taxonomic information, plates and distribution of the reported species.

Keywords: Echinocorythidae, Holasteridae, Pseudananchys completa, Holaster nanus, Holaster simplex, Aurora Formation, Indidura Formation.

1. Introducción

Los holasteroides pertenecen al superorden Atelostomata, conocido como "erizos acorazonados", y cuentan con formas "inusuales" dentro de la clase Echinoidea; Mooi y David (1996) realizaron un análisis filogenético de las especies recientes de Holasteroides, pertenecientes a los géneros *Urechinus* A. Agassiz, 1879, *Plexechinus* A. Agassiz, 1898 y *Pilematechinus* A. Agassiz, 1904; dicho análisis se basó principalmente en la morfología de la testa y de los apéndices. En dicho trabajo se muestra la parafilia de la familia Urechinidae y se proponen el género *Antrechinus*; sin embargo, los taxa recientes son solo tres de los 52 reportados a la fecha.

Se ha propuesto una hipótesis filogenética del orden Holasteroida (Smith, 2004), basada en caracteres de la estructura atípica del sistema apical presente en el orden, el desarrollo de las placas del plastrón y las fasciolas. En dicha propuesta se datan cuatro migraciones de los holasteroides de aguas someras a mar profundo; tres de ellas en el Cretácico Superior-Terciario y una última posiblemente en el Mioceno superior. Este grupo sufrió gran pérdida de diversidad durante la extinción al final del Cretácico (Eble, 1998); los representantes actuales de holasteroides solo se reportan en aguas marinas profundas (Smith, 2004).

El territorio mexicano estuvo cubierto por mares continentales durante el Cretácico debido a diversos eventos de transgresión y regresión, por lo que hay registros fósiles de equinoideos irregulares de dicho periodo. La fauna de Norteamérica, México y Cuba era muy similar a la de la región del circum-Mediterráneo durante el Cretácico Inferior, pero se volvió muy característica a finales del Cretácico, extendiéndose más tarde hasta Brasil y la costa de Perú (Smith, 1984). Cuando se da el mayor evento de transgresión dentro de Norteamérica y extendiéndose hasta Alberta, la fauna se extendió a estas aguas pero con una menor diversidad a nivel de género (Smith, 1984). En el presente trabajo se revisa la Paleontología de los holasteroides del Cretácico para México, actualizando la información taxonómica y morfológica de las especies, incluyendo imágenes de las mismas.

2. Métodos

Se tomó como base el listado más reciente de equinoideos del Cretácico de México (Nieto y García, 2006); se eliminaron las sinonimias y las especies *affinis*; así mismo, se completó el listado con reportes de literatura especializada y con registros de la Colección Nacional de Paleontología del Instituto de Geología, UNAM y del Museo de Paleontología, Facultad de Ciencias (FC), UNAM, del Museum of Comparative Zoology, Universidad de Harvard (MCZ-IPEC) y del Smithsonian Museum of Natural History (USNM-PAL); los ejemplares se determinaron y clasificaron bajo el criterio de Kroh y Smith (2010). Para cada una de las especies reportadas se presenta la información taxonómica disponible (sinonimias, descripción, reportes para México, alcance estratigráfico). Se registraron tres especies clasificadas en dos géneros y dos familias.

Las especies que fueron confirmadas se enlistan a continuación y se menciona su situación en la discusión.

3. Sistemática Paleontológica

Orden Holasteroida Durham y Melville, 1957

Holasteroida Durham y Melville, 1957, p. 260.

Diagnosis. Petaloides pareados no hundidos. Sistema apical elongado sin placa genital 5. Plastron ligeramente diferenciado; floscele ausente (Akers y Akers, 1987).

Familia Echinocorythidae Wright, 1857

Echinocorythidae Wright, 1857, p. 21.

Diagnosis. Ambulacro impar hinchado con poros iguales a los de los petaloides pareados. Sistema apical de estructura holasteroidea. Plastrón meridosterno con placa esternal casi del mismo tamaño que las placas episternas (Smith y Kroh, 2011).

Género *Pseudananchys* Pomel, 1883

Pseudananchys Pomel, 1883, p. 45. Lamber y Thiéry, 1924, p. 417. Cooke, 1946, p. 233. Mortensen, 1950, p. 71.
Pseudananchis Cotteau y Gauthier, 1895, p. 5.
Holasteropsis Elbert, 1902, p. 115.
Craginaster Lambert, 1903, p. 33.

Diagnosis. Testa alta, con la superficie oral plana y de borde ovalado. Ambulacros petaloides muy abiertos y extendiéndose hasta el ámbito. Poros alargados transversalmente en los ambulacros con el poro externo aún más largo. Periprocto por debajo del ámbito (modificada de Cooke, 1953).

Especie tipo. *Ananchys algiris* (Coquand, 1862) por designación original (Cooke, 1953, p. 25).

Alcance estratigráfico. Albiano superior a Cenomaniano inferior (Smith y Kroh, 2011).

Pseudananchys completa (Cragin, 1893)
Figura 1, a–d; figura 2

Holaster completus Cragin, 1893, p. 155, lám. 24, fig. 10; lám. 25, fig. 14; lám. 27, fig. 6–8.
Pseudananchys completa Lambert y Thiéry, 1924, p. 417. Akers y Akers, 1987, p. 83. Buitrón, 1971, p. 27–28, lám.6, fig. 3, 5, 6, lám.7, fig. 1–3.
Pseudananchytes completa Nieto y García, 2006.

Descripción. Testa subcónica, de gran altura, superficie superior convexa, superficie inferior plana, de contorno ovalado y bordes redondeados, con el área posterior ligeramente prolongada hacia adelante y el área anterior desvanecida suavemente. Las áreas ambulacrales son poco notables, superficiales y no petaloides, con poros de dos formas diferentes, los de la serie interna ovalados y los de la externa en forma de ranuras horizontales; la zona interporífera es más ancha que la porífera. Las placas interambulacrales tienen tubérculos pequeños, perforados, crenulados y aureolados, rodeados por pequeños tubérculos escrobiculares, el resto de la placa presenta numerosas granulaciones. Los tubérculos son más grandes en la superficie oral de la testa. El sistema apical es pequeño, con cuatro placas genitales separadas entre sí por dos placas oculares centrales, las placas oculares posteriores están en contacto. El periprocto es ovalado y está situado en la parte oral, del lado posterior. El peristoma es sub-reniforme y está situado en la parte anterior del lado inferior de la testa (Modificada de Buitrón, 1971).

Reportes previos para México. Albiano superior en Formación Aurora, Río Conchos, Ojinaga, Chihuahua (Buitrón, 1971).

Familia Holasteridae Zittel, 1879

Holasteridae Zittel, 1879, p. 532.

Diagnosis. Surco frontal presente desde el ámbito hasta el peristoma; poros del ambulacro anterior pequeños y diferenciados de esos en ambulacros anteriores pareados. Sistema apical con cuatro gonoporos. Placas del plastron meridosternas, con la placa esternal similar en tamaño a las episternas, que son biseriales; en algunos taxa, las episternas (Smith y Kroh, 2011).

Género *Holaster* Agassiz, 1836

Holaster Agassiz, 1836, p. 183. Cooke, 1946, p. 233. Mortensen, 1950, p. 47.

Holasteropsis Elbert, 1902, p. 115.

Ananchothuria Fossa-Mancini, 1919, p. 3–18.

Diagnosis. Testa cordiforme, con surco anterior poco profundo y sin quilla, extremo posterior trunco y superficie oral plana. Ambulacros pareados subpetaloides; columnas en los ambulacros anteriores mucho más delgados que

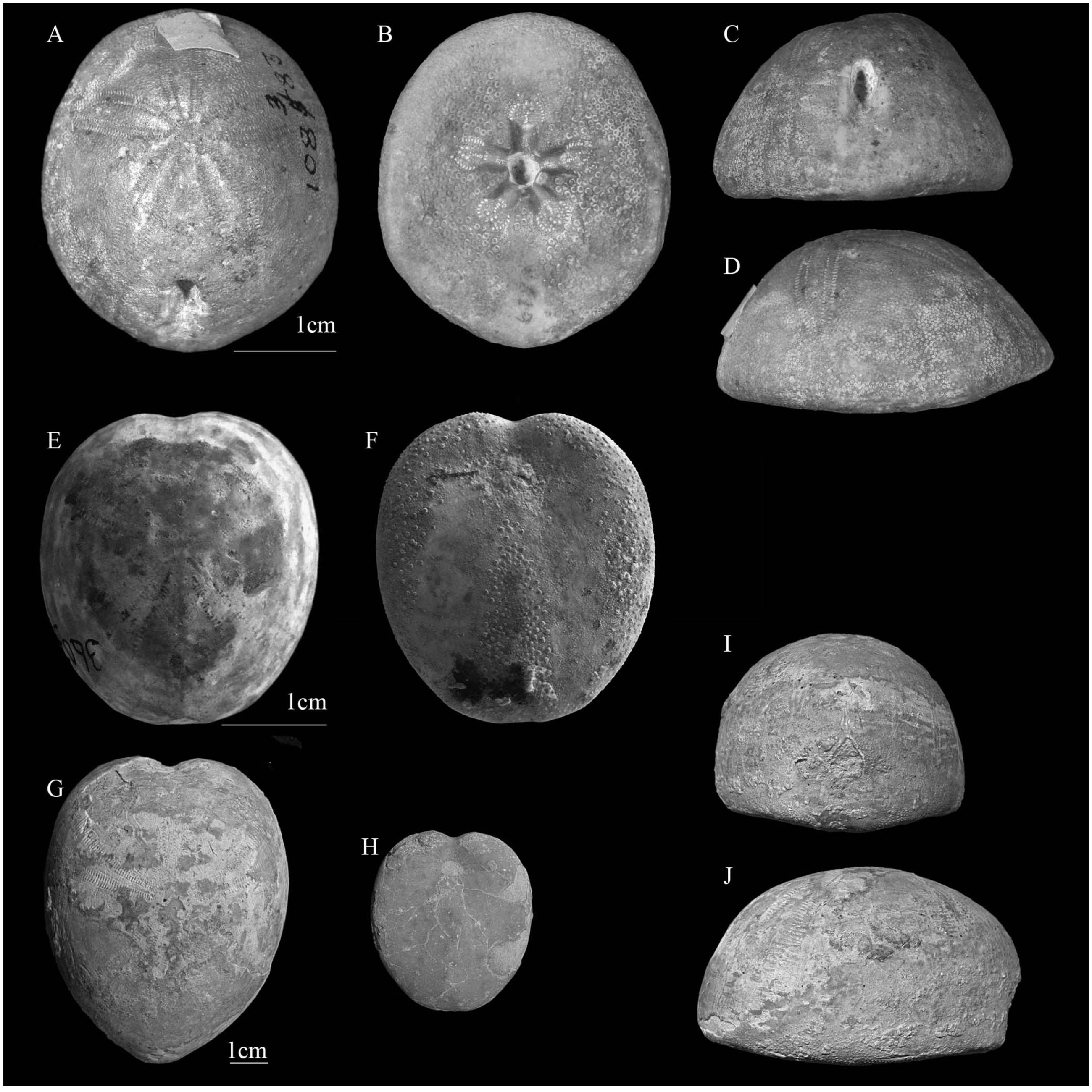

Figura 1. A–D. *Pseudananchys completa* (Cragin, 1893) USNM PAL 103880 (Sin datos). A, vista aboral; B, vista oral; C, vista posterior; D, vista lateral (Fotografías: Ryan Roney). E–F. *Holaster nanus* Cragin, 1983 MCZ-IPEC 3603 (Texas, Formación Weno). E, vista aboral; F, vista oral (Fotografías: Jessica Cundiff). G–J *Holaster simplex* Shumard, 1853. Springer Collection, USNM (Sin datos). G, vista aboral; H, vista oral; I, vista posterior; J, vista lateral.

los de las columnas posteriores. Surco frontal continuo desde el ápice al peristoma. Sin fasciolas. Sistema apical con cuatro gonoporos. Periprocto ubicado en la parte más alta de la superficie posterior de la testa. Peristoma oval transversalmente; plastrón meridosterno (modificada de Smith y Kroh, 2011).

Especie tipo. *Spatangus nodulosus* Goldfuss, 1829 (Cooke, 1953).

Alcance estratigráfico. Hauteriviano a Cenomaniano (Cretácico) (Smith y Kroh, 2011).

Holaster nanus Cragin, 1893
Figura 1, e–f; Figura 2

Holaster nanus Cragin, 1983, p. 156, lám. 24, fig. 14; lám. 25, fig. 11. Jones, 1938, lám. 13, figs. 11–16. Akers y Akers, 1987, p. 68.

Descripción. Testa pequeña, generalmente oval; puede ser alta o baja. Superficie aboral convexa y superficie oral plana. Los poros del ambulacro impar redondos y moderadamente conspicuos. Los pares de poros son oblicuos. Los poros de los ambulacros pareados tienen forma de coma (Akers y Akers, 1987).

Reportes para México. Turoniano (Cretácico) en Formación Indidura, al Norte de Tanque Toribio, Sierra de Santa Ana, Coahuila (Jones, 1938).

Alcance estratigráfico. Albiano (Cretácico).

Holaster simplex Shumard, 1853
Figura 1, g–j; Figura 2

Holaster simplex Shumard, 1853, p. 210. Clark, 1915, p. 85, lám. 34, fig. 3a–b; lám. 38, fig. 1a–j. Cooke, 1955, p. 107, lám. 24, fig. 6–8. Buitrón, 1971, p. 25–27, lám.5 figs. 9–10, lám. 6. figs.1, 2, 4. Akers y Akers, 1987, p. 80.

Holaster nanus Cragin, 1893, p. 156, lám. 24, fig. 14; lám. 25, fig. 11.

Holaster laevis (Brogniart, 1822). Cooke, 1946, p. 234, lám. 34, fig. 1–3. Akers y Akers, 1987, p. 78.

Descripción. Testa de tamaño medio, cordiforme, con la cara apical convexa y la cara oval aplanada, con excepción del plastrón, que es ligeramente saliente y de la concavidad donde se localiza el peristoma. La superficie posterior está truncada, la superficie anterior está suavemente redondeada y desvanecida, está cortada en el centro por un surco superficial que va del aparato apical al peristoma. El ambulacro impar, no petaloide, está alojado en un surco, la zona porífera está constituida por pares de poros dispuestos diagonalmente, redondos, muy pequeños y espaciados. Los ambulacros pares anteriores son subpetaloides, anchos y ligeramente curvados hacia la parte anterior; la zona porífera está formada por pares de poros de forma de ranura, muy

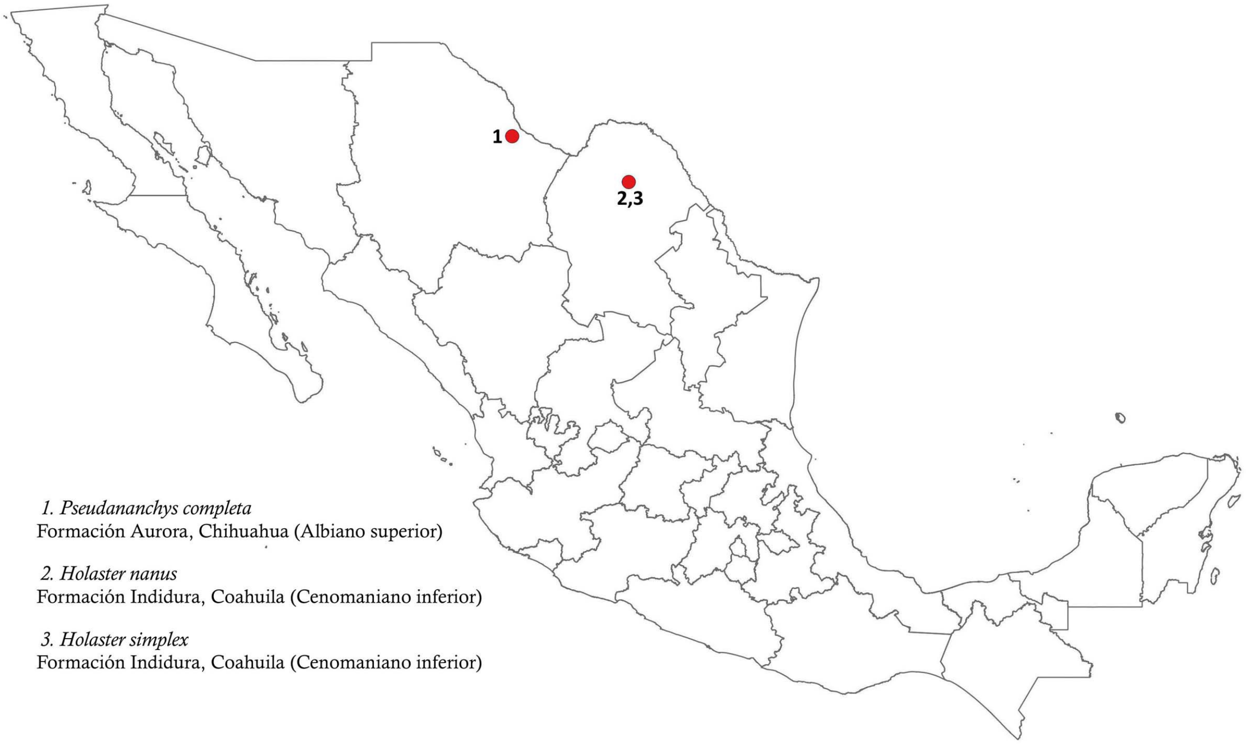

Figura 2. Mapa con registros del orden Holasteroida durante el Cretácico de México.

cercanos entre sí y del siguiente par, la serie anterior es más estrecha que la posterior. Los ambulacros posteriores son subpetaloides, rectos y están constituidos por hileras de poros en forma de ranura, iguales a los de la serie posterior de ambulacros anteriores. El sistema apical es central y alargado, con cuatro placas genitales, separadas de dos en dos por placas oculares, las placas oculares centrales y posteriores se encuentran unidas. El periprocto es ovalado verticalmente, situado en la parte inferior de la pared posterior. El peristoma es de contorno redondeado y está situado en la parte anterior de la base de la testa (tomada de Buitrón, 1971).

Reportes para México. Turoniano (Cretácico) en Formación Indidura, al Norte de Tanque Toribio, Sierra de Santa Ana, Coahuila (Buitrón, 1971).

4. Discusión

El género *Pseudananchys* se cree que es un grupo parafilético por la exclusión del género *Echinocorys*, sinónimo de *Ananchytes* (Smith y Kroh, 2011). Nieto y García (2006) reportan a *Ananchytes striata* y *A. sulcatus* para el Cretácico de México, sin embargo, solo se encontraron reportes de dichas especies en Europa. El género *Holaster* actualmente también se considera parafilético por la exclusión de *Cibaster*, *Offaster* y posiblemente otros géneros (Smith y Kroh, 2011).

Los reportes aquí presentados provienen de ambientes someros, posiblemente previos a las cuatro migraciones a aguas profundas desde el Cretácico Superior (Smith, 2004). *Pseudananchys completa* es reportada para la Formación Aurora, en la que se describen facies de plataforma somera (Servicio Geológico Mexicano, 2014); las especies del género *Holaster* son reportadas para la formación Indidura (Jones, 1938; Buitrón, 1971), que consta de calizas arcillosas y lutitas, previamente datada para el Cenomaniano inferior; sin embargo, Barboza-Gudiño y colaboradores (2004) la ubican para el Turoniano al Coniaciano, describiendo un ambiente medio batial a sublitoral (Cretácico Superior).

Agradecimientos

Martínez Melo agradece al CONACYT la beca de doctorado No. 35167. Agradecemos a los árbitros Francisco Solís Marín y Alfredo Laguarda-Figueras por su revisión crítica y constructiva. Agradecemos a Ryan Roney (Department of Earth and Planetary Sciences, University of Tennessee) y Jessica Cundiff (Museum of Comparative Zoology, University of Harvard) por el apoyo para el registro fotográfico. A Greta Ramírez por su colaboración en el escrito.

Referencias

Akers, R.E., Akers, T.J., 1987, Texas Cretaceous echinoids: Texas Paleontology Series Publication, 3, 1–143.

Barboza-Gudiño, J.R., Hoppe, M., Gómez-Anguiano, M., Martínez-Macías, P.R., 2004, Aportaciones para la interpretación estratigráfica y estructural de la porción noroccidental de la Sierra Catorce, San Luis Potosí, México: Revista Mexicana de Ciencias Geológicas, 21(3), 299–319.

Brogniart, A., 1922, *en* Cuvier, G., Recherches sur les Ossemens Fossiles, (parte 2): Paris, Dufour et E. d'Ocagne, 333–609.

Buitrón, B.E., 1971, Equinoides del Cretácico del Norte de México: Paleontología Mexicana, 31, 1–70.

Clark, W.B., 1915, *en* Clark, W.B., Twitchell, M.W., The Mesozoic and Cenozoic Echinodermata of the United States: Washington D.C., Monographs of the United States Geological Survey, 54, 1–341.

Cooke, C.W., 1946, Comanche echinoids: Journal of Paleontology, 20(3),193–237.

Cooke, C.W., 1953, American Upper Cretaceous Echinoidea. A Shorter Contribution to General Geology: Geological Survey Professional Paper, 254-A, 1–44.

Cooke, C.W., 1955, Some Cretaceous echinoids from the Americas: Geological Survey Professional Paper, 264-E, 87–112.

Coquand, H.,1862, Géologie et paléontologie de la région sud de la province de Constantine: HardPress Publishing, 382pp.

Cragin, F.W., 1893, A contribution to the in vertebrate paleontology of the Texas Cretaceous: Texas Geological Survey Anna. Survey Annual Reports, 4(9), 139–294.

Eble, G.J., 1998, Diversification of disasteroids, holasteroids and spatangoids in the Mesozoic, *en* Mooi y Telford (eds). Echinoderms: San Francisco: Rotterdam, Balkema, 629–638.

Goldfuss, A., 1829, Petrefacta Germaniæ tam ea, quae in Museo Universitatis Regiae Borussicae Fridericiae Wilhelmiae Rhenanae servantur, quam alia quaecunque in Museis Hoeninghusiano Muensteriano aliisque extant, Iconibus et Descriptionibus illustrata. Abbildungen und Beschreibungen der Petrefacten Deutschlands und der angränzenden Länder, unter Mitwirkung des Herrn Grafen Georg zu Münster: Düsseldorf, Arnz & Co, 1(1), 1–76; 1(2), 77–164.

Jones, T.S., 1938, Geology of Sierra de la Peña and Paleontology of The Indidura Formation, Coahuila, México: Bulletin of the Geological Society of America, 49, 69–150.

Kroh, A., Smith A.B., 2010, The phylogeny and classification of post-Paleozoic echinoids: Journal of Systematic Palaeontology, 8(2), 147–212.

Lambert, J., Thiéry, P., 1924, Essai de nomenclature raisonnée des Échinides: Chaumont, Septime Ferriere, Chaumont, 607pp.

Mooi, R., David, B., 1996, Phylogenetic analysis of extreme morphologies: deep-sea holasteroid echinoids: Journal of Natural History, 30, 913–953.

Nieto, I., García, P., 2006, Cretaceous echinoids of México, *en* Vega, F.J., T.G. Nyborg, M.C. Perrilliat, M. Montellano-Ballesteros, S.R.S. Cevallos-Ferriz, Quiroz-Barroso S.A. (eds), Studies on mexican Paleontology: Dordrecht, The Netherlands, Springer, 101–112.

Servicio Geológico Mexicano, 2014, Formación Aurora (en-línea), *en* Léxico Estratigráfico de México, Servicio Geológico Mexicano, *disponible en* <http://mapserver.sgm.gob.mx/lexico/Aurora.pdf>, *consultado* 15 de junio, 2016.

Shumard, B.F., 1853, Description of the species of Carboniferous and Cretaceous Fossils Collected, *en* Marcy, R.B. (ed.), Exploration of the Red River of Louisiana, in the year 1852. 33rd Congress, 1st Session, Senate Executive Document 54, Appendix E.

Smith, A.B., 1984, Echinoid Palaeobiology. Special Topics In Palaeontology: London, George Allen And Unwin, 189 pp.

Smith, A.B., 2004, Phylogeny and systematics of holasteroid echinoids and their migration into deep-sea: Palaeontology, 47(1), 123–150.

Smith, A.B., Kroh, A., 2011, The Echinoid Directory (on line): London, England, Museum of Natural History, *disponible en* <http://www.nhm.ac.uk/our-science/data/echinoid-directory/index.html>, *consultado* 15 de noviembre de 2017.

Manuscrito recibido: Mayo 17, 2018.
Manuscrito corregido recibido: Mayo 22, 2018.
Manuscrito aceptado: Mayo 25, 2018.

Paleontología Mexicana
Volumen 7, núm. 1, 2018, p. 19 – 22

Una macroconcha de ammonoideo enigmática procedente de la Formación La Peña, Sierra del Rosario, estado de Durango, norte de México

Josep A. Moreno-Bedmar[a,*]; Jesús Quiroz-Barragán[b]

[a] Instituto de Geología, Universidad Nacional Autónoma de México, Ciudad Universitaria, Coyoacán, C.P. 04510. Ciudad de México, México.
[b] Museo Paleontológico de la Laguna, Torreón, C.P. 27000, Coahuila, México.

[*] josepamb@geologia.unam.mx

Resumen

En este trabajo se reporta por vez primera para México una macroconcha adulta de un ammonite de difícil asignación taxonómica, colectada en los materiales del Aptiano de la Formación La Peña, procedente del estado de Durango. La descripción y comparación detallada de este ejemplar, con otras macroconchas similares presentes en la literatura, ha permitido asignarla a un acanthohoplítido.

Palabras clave: Ammonite, Acanthohoplítido, Aptiano, Formación La Peña, México.

Abstract

In this work we report, for the first time from Mexico, an adult macroconch of an ammonite of difficult taxonomic assignation collected in the Aptian materials of the La Peña Formation from the Durango state. The detailed description and comparison of this specimen with other similar macroconchs present in the literature has allowed us to assign it to an acanthohoplitid.

Keywords: Ammonite, Acanthohoplitid, Aptian, La Peña Formation, Mexico.

1. Introducción

Este trabajo forma parte de un proyecto de investigación que estudia los ammonites del Aptiano de México con especial atención a aquellos procedentes de la Formación La Peña, como es el caso del ejemplar aquí estudiado. Los ammonites de la Formación La Peña han sido objeto de numerosos trabajos (*e.g.* Burckhardt, 1925; Humphrey, 1949; C.M. Cantú-Chapa, 1976; A. Cantú-Chapa, 1989; Barragán, 2001; Barragán y Szives, 2007; Barragán y Maurrasse, 2008; Moreno-Bedmar *et al.*, 2012; Moreno-Bedmar y Delanoy, 2013; Moreno-Bedmar *et al.*, 2013; Ovando-Figueroa *et al.*, 2015, 2018; Zunun *et al.*, 2015; Barragán *et al.*, 2016; A. Cantú-Chapa y Quiroz-Barragán, 2016; Matamales-Andreu y Quiroz-Barragán, 2017; Mendoza-Maya *et al.*, 2017; Moreno-Bedmar *et al.*, en prensa) pero entre todos estos trabajos son relativamente escasos los reportes de macroconchas. Sin embargo cabe mencionar: macroconchas adultas de ancyloceråtidos (Matamales-Andreu y Quiroz-Barragán, 2017) macroconchas juveniles/subadultas de desmocerátidos (Burckhardt, 1925; Ovando-Figueroa *et al.*, 2015; Moreno-Bedmar *et al.*, en prensa) macroconchas subadultas/adultas de chelonicerátidos (Burckhardt, 1925; Humphrey, 1949; Moreno-Bedmar y Delanoy, 2013; Zunun *et al.*, 2015; A. Cantú-Chapa y Quiroz-Barragán, 2016) y una macroconcha subadulta de un deshayesítido (Ovando-Figueroa *et al.*, 2015). La identificación de macroconchas es complicada debido a que generalmente la mayoría de especies fueron descritas con ejemplares en estadios ontogenéticos juveniles pues son las formas más ornamentadas y que por lo tanto poseen mayor cantidad de caracteres que permiten su determinación. Cuando los ammonites crecen generalmente su ornamentación se simplifica y no sólo la asignación específica se vuelve compleja, en ocasiones puede llegar a ser imposible, sino que incluso la asignación genérica puede tornarse también complicada o inviable. Por lo comentado anteriormente resulta mucho más compleja la identificación de la región adulta de las macroconchas en estado fragmentario y aunque son fósiles relativamente comunes en la Formación La Peña han sido proporcionalmente poco estudiados. En este trabajo se reporta por vez primera un fragmento de macroconcha adulta de difícil asignación taxonómica que parece no ser atribuible a ninguno de los grupos de ammonoideos anteriormente mencionados (ancylocerátidos, desmocerátidos, chelonicerátidos y deshayesítidos). El reporte de este ammonoideo permite ampliar nuestro conocimiento de las macroconchas de ammonoideos de la Formación La Peña y por lo tanto permite disponer de una concepción un poco más completa de los ammonites presentes en esta unidad litoestratigráfica.

2. Paleontología sistemática

2.1. Material

Un molde interno calcáreo de media vuelta de una macroconcha adulta de un ejemplar constituido casi esencialmente por la cámara de habitación (Figura 1). El ejemplar, MPL-103, se conserva en la colección del Museo Paleontológico de la Laguna (= MPL) ubicado en la ciudad de Torreón, estado de Coahuila. Este ammonoideo fue colectado en la Formación La Peña en la localidad de Graceros, Sierra del Rosario, estado de Durango por el director del museo (Q.-B.). El ejemplar fue colectado hacia la parte media de la formación donde se halla la transición entre el Aptiano inferior terminal-Aptiano superior basal, aunque la edad más probable del ejemplar es Aptiano superior basal pues en las salidas de campo realizadas en la localidad de Graceros hemos podido observar que hay un incremento en la abundancia de macroconchas en el Aptiano superior basal.

2.2. Descripción

Media vuelta de un espécimen adulto de 36.5 cm de diámetro máximo. Concha fuertemente evoluta (Figura 1) con flancos planos y paralelos entre sí con una región ventral ligeramente arqueada. La ornamentación está constituida por una alternancia de costillas primarias y secundarias mostrando dos patrones ligeramente diferentes. El primer patrón se halla en el cuarto de vuelta más próximo al fragmocono presentando una mayor densidad de costulación

Figura 1. Vistas laterales y ventral del ejemplar estudiado (MPL-103) un acanthohoplítido colectado en Graceros posiblemente en el Aptiano superior basal, el triángulo gris indica el inicio de la cámara de habitación. Escala gráfica igual a 10 cm.

con costillas relativamente gráciles. Las costillas primarias son ligeramente flexuosas y entre ellas se intercalan las costillas secundarias en una relación muy regular 1:1, una primaria y una secundaria. Las costillas secundarias nacen del tercio inferior del flanco, casi en el borde umbilical. El cuarto de vuelta más próximo a la apertura de la concha muestra el segundo patrón de ornamentación que consiste en una menor densidad de costulación con costillas más robustas, especialmente las primarias. Las costillas primarias son ligeramente flexuosas y entre ellas se intercalan las costillas secundarias en una relación 1:1 aunque algo irregular, pudiéndose también observar dos costillas primarias seguidas o dos secundarias entre las primarias. Las costillas secundarias nacen predominantemente de la parte media del flanco.

3. Discusión

El evidente cambio en el patrón de costulación se interpreta como el tránsito entre el estadio subadulto al estadio adulto tratándose pues de una macroconcha adulta. El ejemplar estudiado es claramente evoluto siendo esto una característica muy destacable. Entre los ammonites de la Formación La Peña son muy pocas las morfologías tan fuertemente evolutas: *Macroscaphites* sp., *Colombiceras mexicanus* (Humphrey, 1949), *Colombiceras spathi* (Humphrey, 1949), *Colombiceras* sp. y *Gargasiceras*? *adkinsi* (Humphrey, 1949). De los taxones anteriormente mencionados los que más similitudes muestran con la macroconcha aquí estudiada sería el género *Colombiceras* y la especie *Gargasiceras*? *adkinsi*. En la literatura es posible observar lo que posiblemente sean macroconchas juveniles de *Colombiceras* y *Acanthohoplites* que suelen poseer unas conchas menos evolutas con costillas primarias que se inician a partir de bullas umbilicales y tanto las costillas primarias como las secundarias se engrosan hacia la región umbilical (*e.g.* Drushchits y Kudriavtsev, 1960, lám. 9, figs. 2a–b y lám. 11, figs. 1a–b; Kotetishvili *et al*., 2005, lám. 104; Bogdanova y Mikhailova, 2016, lám. 14, 1a–c y 2 a–c, lám. 15, 3a–b, lám. 18, 3). Entre los ejemplos de especímenes figurados en la literatura cabe señalar que algunos muestran patrones de costulación muy similares al ejemplar aquí estudiado, como es el caso del ejemplar del género *Acanthohoplites* de Bogdanova y Mikhailova, (2016, lám. 15, 3a–b) que presenta un patrón de costulación similar al estadio subadulto del ejemplar mexicano, aunque difiere claramente del ejemplar caucásico por poseer una concha claramente más evoluta y no tener bullas. Otro ejemplo de gran similitud es el ammonite ilustrado por Ropolo *et al.* (2008, lám. 23, fig. 3). El ejemplar francés identificado como *Acanthohoplites* sp. es una macroconcha adulta que muestra los dos mismos estadios ontogenéticos, subadulto y adulto, que se asemejan en gran medida al ejemplar mexicano. En este caso, la concha es también fuertemente evoluta, pero difiere en que el estadio subadulto en el ejemplar francés presenta claramente bullas. Entre los Acanthohoplítidos no son raros los ejemplos de conchas fuertemente evolutas como por ejemplo el espécimen colombiano del género *Protacanthoplites* ilustrado por Sharikadze *et al*. (2004, lám. 81, fig. 3 a–c), o el ejemplar caucásico del género *Acanthohoplites* ilustrado por Anthula (1900, lám 11, fig. 1). Estas similitudes entre los ammonites de los géneros *Colombiceras*, *Acanthohoplites* y *Protacanthoplites* con el ejemplar mexicano ponen de manifiesto que el ejemplar Mexicano debe ser atribuido a una macroconcha de un acanthohoplítido pero no es asignable a ninguno de los géneros mencionados. Respecto a los taxones presentes en la Formación La Peña que muestran mayores similitudes con la macroconcha aquí estudiada falta mencionar la especie *Gargasiceras*? *adkinsi* pues posee grandes afinidades en su forma general de la concha fuertemente evoluta pero difiere en que las costillas primarias son muy robustas entre la región umbilical y la parte media del flanco. Ovando-Figueroa *et al*. (2015) ilustran el ejemplar más grande conocido de este taxón. Este ejemplar (Ovando-Figueroa *et al*., 2015, fig. 3A) si bien muestra todas las características típicas de *Gargasiceras*? *adkinsi* no posee la robustez típica de las costillas primarias. Por eso creemos que la macroconcha adulta aquí estudiada posee grandes similitudes con la especie descrita por Humphrey *Gargasiceras*? *adkinsi* pero la gran diferencia de tamaño entre el ejemplar de Ovando-Figueroa *et al*. (2015) de 8.9 cm y el ejemplar aquí estudiado de 36.5 cm no permiten una comparación precisa.

4. Conclusiones

La macroconcha adulta estudiada en este trabajo se atribuye a un acanthohoplítido cuya edad más probable es Aptiano superior basal.

Agradecimientos

Esta investigación ha sido financiada por el proyecto PAPIIT IA102717 perteneciente a la DGAPA, Universidad Nacional Autónoma de México. Los autores quieren agradecer las correcciones y sugerencias realizadas por los revisores, Rafel Matamales Andreu y Emmanuel Robert, que ayudaron a mejorar el trabajo.

Referencias

Anthula, D.J., 1900, Über die Kreidefossilien des Kaukasus mit einem allgemeinen Ueberblick über die Entwicklung der Sedimentärbildungen des Kaukasus: Beiträge zur Paläeontologie und Geologie Öesterreich-Ungarns und des Orients, 12(1899), 55–159 (1–106).

Barragán, R., 2001, Sedimentological and paleoecological aspects of the Aptian transgressive event of Sierra del Rosario, Durango, northeast Mexico: Journal of South American Earth Sciences, 14, 189–202.

Barragán, R., Szives, O., 2007, New records of *Mathoceras* Casey (Deshayesitidae, Ammonoidea) from the Aptian (Lower Cretaceous) of Mexico and Hungary: Biostratigraphic and paleobiogeographic implications: Geobios, 40, 21–30.

Barragán, R., Maurrasse, F.J-M.R., 2008, Lower Aptian (Lower Cretaceous) ammonites from the basal strata of the La Peña Formation of Nuevo León State, northeast Mexico: biochronostratigraphic implications: Revista Mexicana de Ciencias Geológicas, 25(1), 145–157.

Barragán, R., Moreno-Bedmar, J.A., González-Arreola, C., 2016, Aptian ammonites from Mazapil, Zacatecas State (north-central Mexico) studied by Burckhardt in 1906: A revision: Carnets de Géologie [Notebooks on Geology], 16, 355–367.

Bogdanova, T.N., Mikhailova, I.A., 2016, Middle Aptian Biostratigraphy and Ammonoids of the Northern Caucasus and Transcaspia: Paleontological Journal, 50(8), 725–933.

Burckhardt, C., 1925, Faunas del Aptiano de Nazas (Durango): Boletín del Instituto Geológico de México, 45, 1–71.

Cantú-Chapa, A., 1989, La Peña Formation (Aptian): a condensed limestone-shale sequence from the subsurface of NE Mexico: Journal of Petroleum Geology, 12(1), 69–84.

Cantú-Chapa, A., Quiroz-Barragán, J., 2016, A bizarre ammonite of the Aptian (Cretaceous) from state of Durango, north Mexico: PetroQuiMex, 80, 65–69.

Cantú-Chapa, C.M., 1976, Estratigrafía de la Formación La Peña (Aptiano Sup.) en el área de Monterrey, N.L.: Revista del Instituto Mexicano del Petróleo, 8(4), 7–16.

Drushchits, V.V., Kudriavtsev, M.P. (eds), 1960, Atlas of the Lower Cretaceous fauna of the northern Caucasus and the Crimea: Vsesoiuznyi Nauchno-Issledovatel´skii Institut Prirodnykh. Gasov. Moscow, Gostoptekhizdat, 701 pp. (en Ruso).

Humphrey, W.E., 1949, Geology of Sierra de Los Muertos area, Mexico (with descriptions of Aptian cephalopods from the La Peña Formation): Bulletin of the Geological Society of America, 60, 89–176.

Kotetishvili, E.V., Kvantaliani, I.V., Kakabadze, M.V., Tsirekidzé, L.R. (eds.), 2005, Atlas of Early Cretaceous fauna of Georgia. Proceedings of the Georgian Academy of Sciences, A. Janelidze Geological Institute Tbilissi, New series, 120, 788 pp. (en Ruso).

Matamales-Andreu, R., Quiroz-Barragán, J., 2017, Algunos ammonites heteromorfos de la Formación La Peña, Aptiano del estado de Durango, Norte de México, resguardados en el Museo Paleontológico de la Laguna: Paleontología Mexicana, 6(2), 67–71.

Mendoza-Maya, A.K., Moreno-Bedmar, J.A., Chávez-Cabello, G., 2017, Amonites del Aptiano superior de la Formación La Peña de la sección de Los Chorros, Coahuila, noreste de México: Paleontología Mexicana, 6(1), 43–49.

Moreno-Bedmar, J.A., Bover-Arnal, T., Barragán, R., Salas, R., 2012, Uppermost Lower Aptian transgressive records in Mexico and Spain: chronostratigraphic implications for the Tethyan sequences: Terra Nova, 24, 333–338.

Moreno-Bedmar, J.A., Barragán Manzo, R., Company Sempere, M., Bulot, L.G., 2013, Aptian (lower Cretaceous) ammonite biostratigraphy of the Francisco Zarco Dam stratigraphic section (Durango State, northeast Mexico): Journal of South American Earth Sciences, 42, 150–158.

Moreno-Bedmar, J.A., Delanoy, G., 2013, About the generic attribution of *Megatyloceras casei* Humphrey, 1949 (Ammonoidea, Ancyloceratina), from the Aptian of Mexico: Carnets de Géologie [Notebooks on Geology], Letter 2013/06 (CG2013_L06), 315–323.

Moreno-Bedmar, J.A., Casados-Monroy, A., Frau, C., Pictet, A., Chávez-Cabello, G., Esquivel-Macías, C., Ammonite biostratigraphy of the Sierra del Patrón section (Durango State, Mexico) and its bearing on the lower/upper Aptian boundary of the Central Atlantic Province: Cretaceous Research (en prensa), doi: 10.1016/j.cretres.2017.10.015.

Ovando-Figueroa, J.R., Moreno-Bedmar, J.A., Chávez-Cabello, G., Minor, K.P., 2015, Lower Aptian ammonites of the Sierra de Parras, Coahuila State, northern Mexico: Carnets de Géologie [Notebooks on Geology], 15(1), 1–11.

Ovando-Figueroa, J.R., Moreno-Bedmar, J.A., Minor, K.P., Franco-Rubio, M., Oviedo, A., Patarroyo, P., Robert, E., 2018, Ammonite taxonomy and biostratigraphy for the upper Aptian-lower Albian (Lower Cretaceous) of Cerro Chino, Chihuahua State, northeast Mexico: Cretaceous Research, 82, 109–137.

Ropolo, P., Conte, G., Moullade, M., Tronchetti, G., Gonnet, R., 2008, The Douvilleiceratidae (Ammonoidea) of the Lower Aptian historical stratotype area at Cassis-La Bédoule (SE France): Carnets de Géologie [Notebooks on Geology], Memoir 2008/03 (CG2008_M03), 1–60.

Sharikadze, M.Z., Kakabadze, M.V., Hoedemaeker, Ph.J., 2004, Aptian and Early Albian Douvilleiceratidae, Acanthohoplitidae and Parahoplitidae of Colombia: Scripta Geologica, 128, 313–514.

Zunun, N.O., Moreno-Bedmar, J.A., Quiroz-Barragán, J., Matamales Andreu, R., 2015, Un amonite con un traumatismo en la concha del Aptiano (Cretácico inferior) del estado de Durango, norte de México: Paleontología Mexicana, 4(2), 7–12.

Manuscrito recibido: Mayo 6, 2018.
Manuscrito corregido recibido: Mayo 21, 2018.
Manuscrito aceptado: Mayo 23, 2018.

Paleontología Mexicana
Volumen 7, núm. 1, 2018, p. 23 – 56

Cambrian oncolites from San José de Gracia, Sonora, Mexico

Hugo Beraldi-Campesi[a,*], Francisco Cuen-Romero[b], Blanca E. Buitrón-Sánchez[c]

[a] Sociedad Mexicana de Astrobiologia-SOMA. Ciudad Universitaria, Coyoacán, C.P. 04510, Ciudad de México, México.
[b] Universidad de Sonora, División de Ciencias Exactas y Naturales, Departamento de Geología. Blvd. Luis Encinas y Rosales, C.P. 83000, Hermosillo, Sonora.
[c] Instituto de Geología, Universidad Nacional Autónoma de México. Ciudad Universitaria, Coyoacán, C.P. 04510, Ciudad de México, México.

[*] hberaldi@gmail.com

Abstract

Recently discovered oncolites from a Lower Cambrian locality in San José de Gracia (SJG), Sonora (Mexico), illustrate the wide geographic distribution that they had in this part of Laurentia some 515–510 Ma ago. They are exceptionally large (~44 mm) in comparison to other marine forms of the North American Cambrian Carbonate Bank, but similar in their overall morphology and depositional environment. Their association with abundant biomorphs, especially indigenous filamentous structures with the curvature and spatial arrangement that fit the minimum criteria for biogenicity, supports their biological origin. Key morphological features include laminated growth in at least a portion of the oncolite, subspherical shape with internal porosity, and a nucleated habit on skeletal debris (mollusk shells) and mud concretions. The similarity of SJG oncolites with others from Cambrian outcrops separated today by hundreds of kilometers, suggests that massive microbially-driven, shallow marine ecosystems existed in western Laurentia during this time. This speaks of the impact that microbes had in shaping marine sediments, and the global primary productivity and carbon cycle during early stages of the Phanerozoic.

Keywords: oncolites, Paleoecology, Geobiology, microbialites, sedimentary biostructures.

Resumen

Oncolitos descubiertos recientemente en una localidad del Cámbrico Temprano en San José de Gracia (SJG), Sonora (México), ilustran la amplia distribución que éstos tuvieron en esta parte de Laurentia hace unos 515–510 Ma. Son excepcionalmente grandes (~44 mm) en comparación con otras formas marinas del Banco de Carbonato del Cámbrico de Norte América, pero similares en morfología y ambiente de depósito. Su asociación con abundantes biomorfos, especialmente estructuras filamentosas con la curvatura y arreglo espacial que demuestran su biogenicidad, apoyan su origen biológico. Características morfológicas clave incluyen su crecimiento laminado al menos en alguna porción del oncolito, su forma sub-esférica con porosidad interna, y que están nucleados por fragmentos esqueletales (conchas de molusco) y concreciones pelíticas. La similitud de los oncolitos de SJG con otros de localidades que hoy se encuentran a cientos de kilómetros de distancia, sugiere que en esta parte de Laurentia existieron ecosistemas microbianos masivos en aguas someras en ese tiempo. Eso habla del impacto que tuvieron los microbios en la estructuración de los sedimentos, así como en la productividad primaria global y el ciclo del Carbono durante el Fanerozoico Temprano.

Palabras clave: oncolites, Paleoecología, Paleobiología, microbialitas, bioestructuras sedimentarias.

1. Introduction

1.1. A note on paleontological terminology

Although the terms 'oncolite' and 'oncoid' have been used interchangeably, they have different meanings. 'Oncolite' implies biogenicity while 'oncoid' refers to semispherical and layered sedimentary structures, regardless of origin (Flügel, 2004, p 123). In this contribution we use 'oncolite' to refer to microbially-mediated, individual, chemical sedimentary structures that are subspherical, concentrically laminated (at least to some degree), and unattached to the substrate. This usage is consistent with the use of the term 'stromatolite', a widely recognized type of microbialite. Likewise, we may refer to 'oncolitic limestone', 'oncolitic pavement', 'oncolitic conglomerate' as rocks bearing oncolites or simply 'oncolites' as a group of oncolites.

Oncolites have been mistakenly called 'calcareous algae', 'algal balls' or 'algal biscuits', or referred to the genus '*Girvanella*' in the literature. The term 'calcareous algae' refers to eukaryotic algae that precipitate carbonate on their surfaces (teguments), that is not necessarily microbially-driven nor concentrically laminated. 'Algal balls' can be regarded as rhodoliths, which are produced by eukaryotic red algae and where tegumentary features can be seen. *Girvanella* refers to tubular microfossils usually related to cyanobacteria (Riding, 1975) and not sedimentary structures. Lastly, 'algal biscuit' is a local term coined before 1960 to refer to oncolites. Other oncolites can even be built by foraminifers and metazoans (Rider and Enrico, 1979; Balson and Taylor 1982; Hillmer *et al*., 1996; Scholz, 2000). Therefore, in the strict sense of the term 'microbialite' (chemical sedimentary structure mediated by microbes), oncolites built by animals and centimetric algae must be differentiated from those built mainly by bacteria. If microbial oncolites are 'microbialites', eukaryotic types could be termed 'macrobialites'.

In coastal and fluvial environments, mid- to high-energy currents overturn millimeter-sized particles that gradually grow encrusted by mineral precipitates (typically calcium carbonate; Peryt, 1981), to finally form a bigger semi-spherical structure that results in an oncolite that is > 5 mm to several cm in diameter. Similar, but smaller structures (< 2 mm) are called 'ooids' and are prevalent since the Archean (Reimer, 1975). Note that much of the shape of oncolites is due to the shape of their nuclear materials. In a crater lake in Mexico one of the authors (HBC) has studied oncolites that range from 5 mm to meter-long 'tree' trunks that have been encrusted with carbonates the same way, and where a green layer of microbes can be seen ~1 mm below the surface. In fact, significantly larger oncolites could occur in fluvial and lacustrine environments (Winsborough *et al*., 1994; Wade and Garcia-Pichel, 2003; Pickford *et al*., 2009) in comparison to those of marine environments.

1.2. Oncolites in Mexico

Fossil oncolites have been poorly studied in Mexico, although examples are known from Cambrian (Cooper *et al*., 1952) and upper Paleozoic (Buitrón-Sánchez *et al*., 2012) strata, and also the Holocene (Winsborough *et al*., 1994; Wade and Garcia-Pichel, 2003). These investigations have approached the study of oncolites and other microbialites from a variety of different perspectives including paleontology, stratigraphy, ecology, and DNA surveys, and have increased our knowledge about their occurrence, morphology, ecology, and environmental requirements for development.

The oldest reported oncolites from Mexico come from Lower Cambrian rocks of the Caborca region in Sonora (Cooper *et al*., 1952; Nardin *et al*., 2009). Recently discovered Lower Cambrian oncolites in San José de Gracia (SJG), near the city of Hermosillo (Figure 1), widen the extension of those from northern Caborca and represent important repositories of the history of microbialites in Mexico. They are also useful paleoenvironmental indicators whenever associated with index fossils and lithological successions. Moreover, this type of oncolites could be useful markers to correlate distant Cambrian outcrops, which is the case for Sonora and western North America. However, this is only true when index fossils and the overall lithology are also considered.

2. Cambrian strata in Sonora

Cambrian outcrops in Mexico typically display igneous and metamorphic rocks, while sedimentary rocks are rare (Figure1A). Sedimentary units of Cambrian age are known only from Sonora. King (1940) studied Cambrian to Ordovician rocks in the Cobachi region, while Cooper *et al*. (1952) worked on the stratigraphy and fossil content of marine deposits of the Caborca region, providing the first descriptions of archaeocyathids, brachiopods, trilobites, and oncolites (then referred to *Girvanella*). Baldis and Bordonaro (1981) discussed the correlation between Cambrian trilobites from Sonora with those from the Precordillera in Argentina, giving the first hints of biostratigraphic correlations at the continental scale for Cambrian rocks in Mexico. Stewart *et al*. (1984, 2002) further correlated Cambrian units of Sonora and Western USA, and compiled a stratigraphic and paleontological report, where they mention the presence of oncolites in the Buelna, Cerro Prieto, and Arrojos formations, some of which have been found in SJG (Cuen *et al*., 2016). McMenamin (1985, 1987) contributed to the biostratigraphy of Cambrian trilobites in the region of Puerto Blanco (Sonora), which helped to refine ages based on index fossils of the *Nevadella*, *Olenellus*, and *Bonnia* types. Rivera-Carranco (1988a, b) defined the paleoenvironmental onditions of various Cambrian sedimentary units of Sonora, and Almazán-

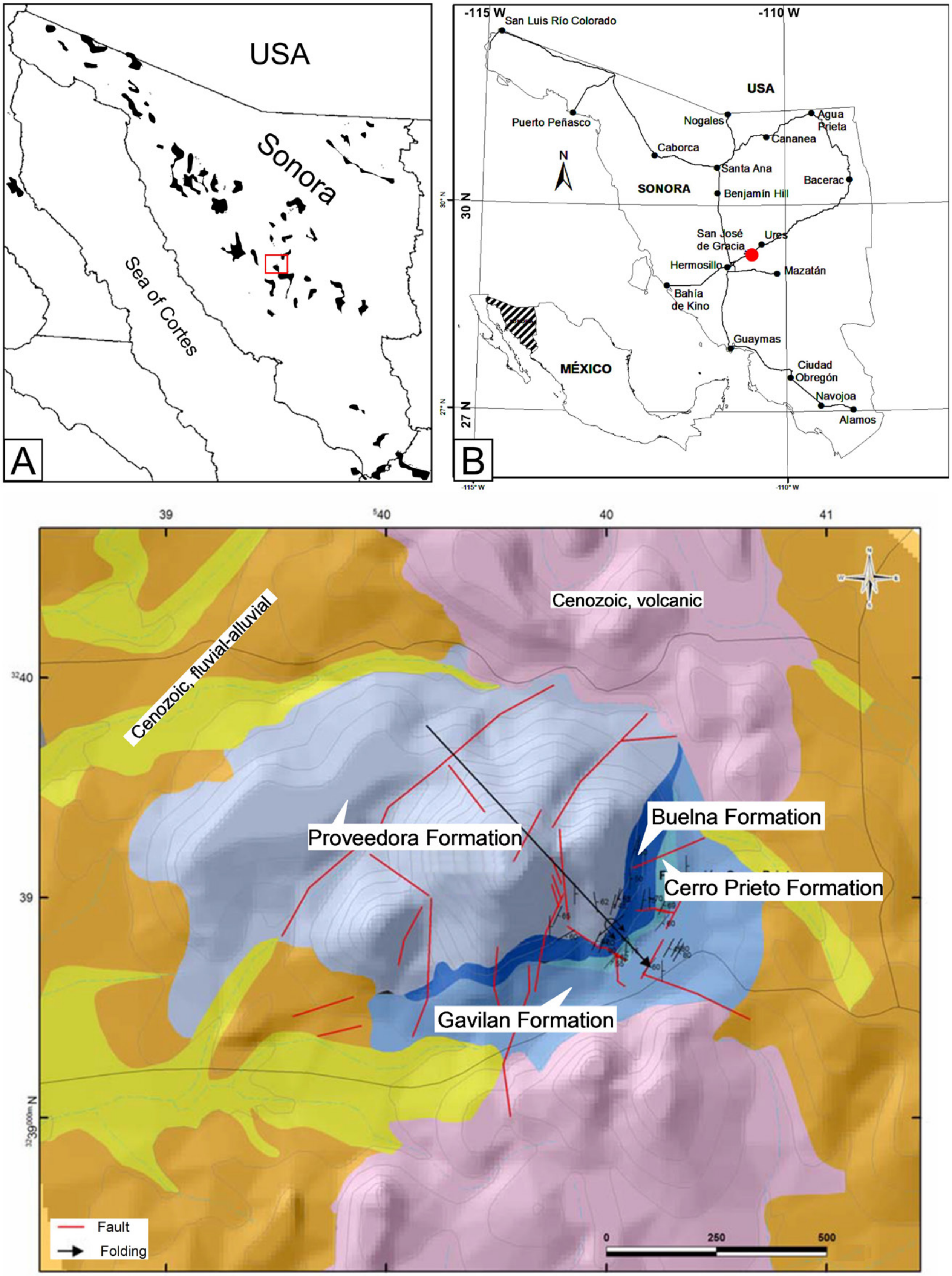

Figure 1. A. Map of Cambrian outcrops (shaded areas) in Northern Mexico. Most of them are volcanogenic. Outcrop extension was exaggerated to achieve visual scale. The box indicates the location of San José de Gracia (SJG). B. Location of the Chihuarruita Hill in SJG. C. Geologic map of the Chihuarruita Hill, approximately 2.5 km East of San José de Gracia, Sonora, Mexico. Oncolites studied here belong to the Buelna Formation.

Vázquez (1989) wrote about the Cambrian-Ordovician outcrops in the Arivechi region, where oncolites have been found but not studied. Later, Riva and Ketner (1989) and Debrenne *et al*. (1989) provided new descriptions of Cambrian and Ordovician graptolites and archaeocyathids from the Caborca region, further refining the age and biostratigraphy of those rocks. Nardin *et al*. (2009) described the eocrinoids of Lower to Middle Cambrian of SJG, which was a pioneer study of the area. Cuen *et al*. (2013, 2016) redefined the geology of SJG and Buitrón-Sánchez *et al*. (2016) studied its ichnofossil content. This, altogether, has rendered a much clearer idea about the fossil content of these Lower Cambrian rocks and their paleoenvironmental and paleoecological meaning.

2.1. The Chihuarruita Hill in San José de Gracia

Oncolites studied in this paper come from Chihuarruita Hill, located in the vicinity of SJG, ~40 km East of Hermosillo (Figure 1). The fossil assemblages found at Chihuarruita Hill vary from Lower to Middle Cambrian, and represent well constituted marine communities of mature ecosystems. These communities include sponge-like animals (*Chancelloria* sp., *Diagoniella* sp.), acute-shelled molluscs (*Hyolithes* sp., *Haplophrentis* sp.), eocrinoids (*Gogia* sp.), brachiopods (*Acrothele* sp., *Dictyonina* sp.), trilobites (*Peronopsis* sp., *Ptychagnostus praecurrens*, *Bristolia* sp., *Olenellus* sp., *Oryctocephalites* sp., *Elrathina* sp., *Ogygopsis* sp., *Pentagnostus* sp.), and several types of ichnofossils (*Skolithos* isp., *Planolites* isp., *Arenicolites* isp., *Thalassinoides* isp., *Asterosoma* isp., *Palaeophycus* isp.; Buitrón-Sánchez *et al*., 2016). Their stratigraphic occurrence is indicated in Fig. 2 and some examples are shown in Figure S1. Oncolites are of course part of these assemblages, and coexisted for some time (> 1 Ma, judging by the thickness of the strata) with many shelled animals represented as fragments within the limestone matrix, and as nuclei of oncolites and within their laminae. Those shelled organisms were obviously reworked skeletal particles, commonly found in carbonate banks all throughout the Phanerozoic. The coexistence of oncolites with metazoans is unclear, given the absence of complete skeletons within the oncolitic limestone. Complete skeletons, however, are found in adjacent strata.

Four Cambrian rock units can be recognized at Chihuarruita Hill (figures. 1C, S2). From base to top they are the Proveedora, Buelna, Cerro Prieto, and El Gavilan formations (Cuen *et al*., 2016). The Proveedora Formation consists of cross-bedded quarzarenites with ichnofossils representative of the '*Skolithos* ichnofacies' (Buitrón-Sánchez *et al*., 2016). This formation was likely deposited in an intertidal to shallow subtidal, siliciclastic environment. Comparable lithology, ichnofacies and environmental interpretation has been proposed for the Proveedora Formation in the northern Caborca region (Rivera-Carranco, 1988a).

The second unit is the oncolite-bearing Buelna Formation that overlies the Proveedora Formation and grades up from mixed silicilastic-carbonate units to detrital limestone interbedded with shale. The oncolitic limestone is a ~1 m-thick, well indurated, calcitic limestone toward the mid section of the succession (figures 1, 2, S2). Toward the top of the oncolitic limestone a ~30 cm thick tempestite with abundant mud intraclasts crowns the last stage of the Buelna Formation and is in gradational contact with the overlying Cerro Prieto Formation in SJG. In the upper section there are abundant mollusks *Hyolithes sonora* and *Haplophrentis reesei*. These are associated with olenellid trilobites, identified as *Olenellus* sp. and *Bristolia bristolensis*, as well as *Gogia eocrinoids*, which indicate an age of 515–510 Ma (Levi-Setti, 1995; Cuen *et al*., 2016). The depositional environment of these strata is interpreted as shallow marine, with dominant low energy but with frequent high-energy storms and terrigenous input, perhaps in subtidal setting above the storm wave base (Cuen *et al*., 2016). We infer that the oncolites were accumulated within a carbonate bank flanked by a protected shallow area toward the shore.

The third unit, the Cerro Prieto Formation, consists of massive, dolomitized, oolitic limestone, with prominent cliffs and pronounced karstic features. Oolites are less than 1 mm in diameter (commonly 100 μm). Crystals of hematite and pyrite are common. The genesis and deposition of these oolites likely occurred in a high-energy, carbonate-supersaturated, shallow marine environment. High tide activity in a subtidal to intertidal environment can be envisioned for these facies. This Formation bears oncolites in the Caborca region (Cooper *et al*., 1952; Cuen *et al*., 2016) but not in SJG.

The fourth unit is the uppermost El Gavilán Formation. This top unit is composed dominantly of red shale interbedded with dark gray limestone, both with abundant trilobites, inarticulate and articulate brachiopods, sponge-like spicules, chancellorids, and hyolithids, among others (Figure 2, S1). Toward its base, brachiopods *Acrothele* sp. and *Linnarssonia* sp. are more common. The middle shale beds bear a wide variety of trilobites, including *Peronopsis bonnerensis*, *Pagetia resseri*, *Oryctocephalus* sp., *Oryctocephalites walcotti*, *Elrathina antiqua*, *Ogygopsys typicalis* and *Bathyuriscus* sp. (Cuen *et al*., 2016). Toward the top, sponge-like spicules of *Chancelloria eros* and *Diagoniella* sp. have been found (Cuen *et al*., 2013). The lithology and fossil composition suggest deposition within a middle to outer shelf. This formation bears oncolites in Nevada, USA (Cuen *et al*., 2016).

Overall, the sedimentary succession in SJG, depicts a change from silicilastic sandstone-dominated, to limestone-dominated, to shale-limestone lithologies. This could represent the deepening of the shelf, from coastal sands (Proveedora Quartzite), to a shallow carbonate ramp (Buelna and Cerro Prieto formations) and ending with episodes of deeper shelf environments (El Gavilan Formation) where fine sediment (shale) was deposited, interrupting periodically carbonate deposition.

3. Methods

3.1. Sample collection

Oncolites were collected from a ~1 m-thick, oncolitic limestone unit (Figs. 2, S2) that is heavily recrystallized and less prone to erosion than the adjacent strata. Oncolite samples were chosen in situ after inspection with hand lenses to determine their degree of preservation, internal lamination, and non-laminated textures in order to have assorted representatives along a ~100 m stretch. Selected samples used for laboratory analyses were hammered out from the rock after being labeled with permanent markers (GPS location and spatial position within the stratum), and sealed in plastic bags.

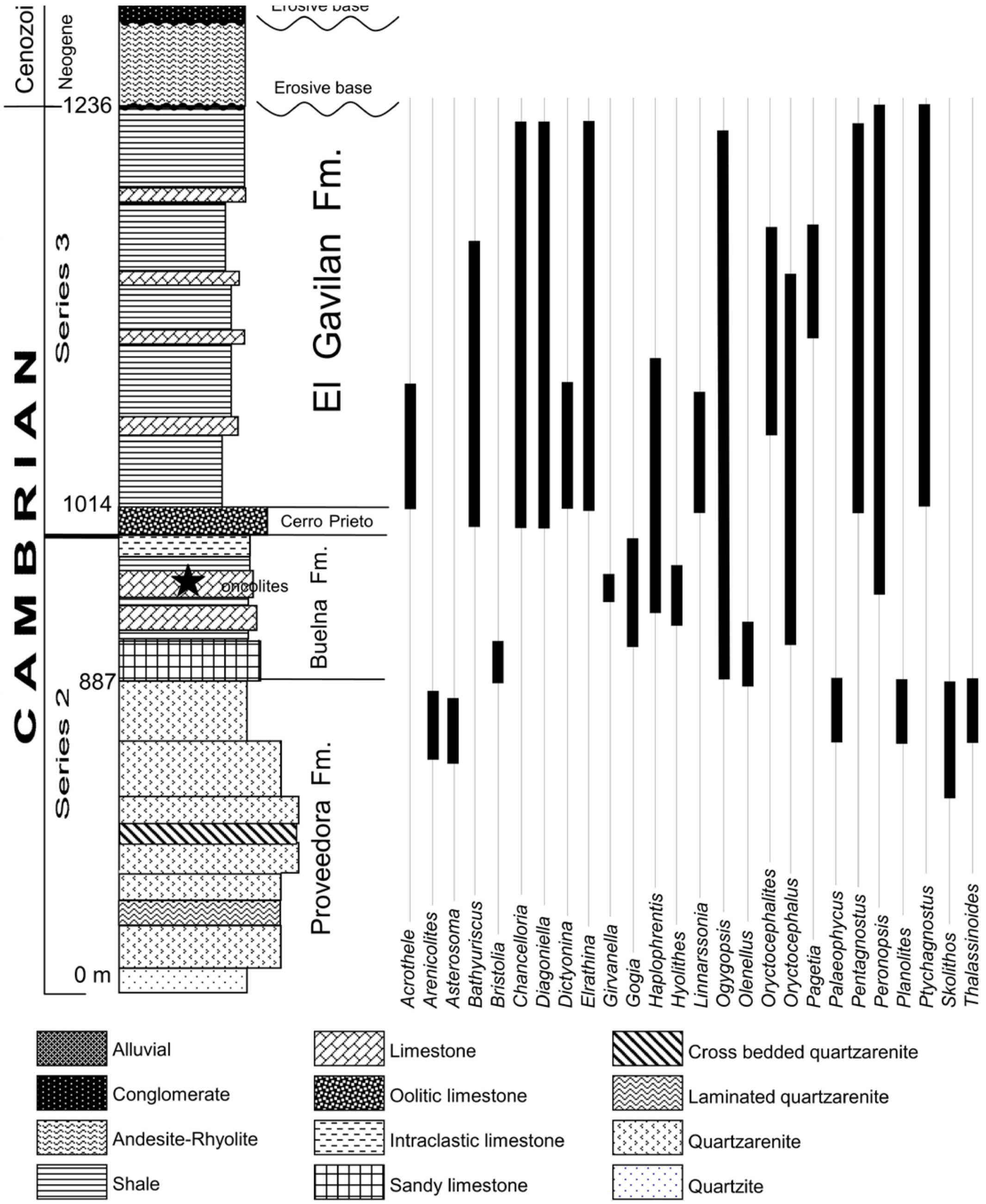

Figure 2. Stratigraphic succession of the Chihuarruita Hill indicating the approximate distribution of fossil fauna and ichnofossils. Some of this fauna is depicted in Fig. S1).

3.2. Size and density distribution

Measurements of oncolite diameters and areal density counts were quantified from 45 scaled images taken on the field along a ~100 m stretch of the stratum bearing oncolites, using a Canon D20 digital camera and the ImageJ free software v. 1.6 (https://imagej.nih.gov/ij). Areal density was calculated as the number of oncolites per unit area. Diameters were measured as the major axis of each oncolite in 2D at the rock surface (Figure S3).

3.3. Thin petrographic sections and polished surfaces

Polished surfaces and thin petrographic sections were used to observe diagenetic features (recrystallization, cementation, deformation, infillings, pressure marks, etc.), morphologies of aggregates, fossil content, and textures. These were made from 6 selected samples that were spread along the ~100 m stretch. They were observed and imaged in a Zeiss Axiozoom stereoscopic microscope, a Zeiss Axio Imager M2 brightfield microscope, and an Olympus BX51 petrographic microscope. The width of fossil filaments was measured from scaled images using the ImageJ software v. 1.6. Thin sections and fresh fractured samples were also observed with a Scanning Electron Microscope.

3.4. Raman analysis

Raman analyses were used to aid in the interpretation of possible organic remnants, such as graphitized contents in the oncolites and organic matter associated with iron compounds. Analyses were made from thin sections. A dispersive Nicolet-AlmegaXR (Thermo Electron Scientific Instruments LLC, Madison, WI USA) laser Raman setup was used, coupled with a BX51 Olympus microscope for focusing the beam repeatedly on a same target and averaging the peaks. The scattered light was collected in a 180-degree backscattering configuration. Raman spectra were accumulated over 25 s with a resolution of ~4 cm−1, the excitation source was 532 nm radiation from a Nd:YVO4 laser (frequency-doubled) and the laser power on the sample was 10 mW. The spectra were analyzed in Microsoft Excel v. 2003. The area under the peaks was calculated and the peaks were matched with a physical standard and standard curves from an owned CCADET-UNAM database.

3.5. X-Ray Diffraction and Fluorescence analyses

The bulk mineralogy and elemental composition of the samples was assessed with X-ray diffraction and X-ray fluorescence from powdered oncolites and bulk rock using a portable XRD-XRF Terra instrument (In Xitu Inc.; Bish *et al*., 2007), with a Cobalt X-ray tube at 40 Kv and a fixed 5 to 50-degree 2Θ and a resolution of 0.3 degree 2Θ. Detected X-rays were integrated by default into a histogram of number of photons and photon energies that produced a XRF pattern of the sample. Data analysis was made using the JADE software v 7.0 (MDI, Pleasanton, CA) and the ICDD (www.icdd.com) and AMCSD (http://www.geo.arizona.edu/xtal-cgi/test) library data.

3.6. Scanning electron microscopy with elemental analyses

Thin sections, fresh fractures, and HCl-etched fragments of oncolites were observed, uncoated, in a variable-pressure Zeiss EVO10-MA Scanning Electron Microscope, equipped with a Bruker Flash X electron dispersive spectrometer (EDX), to image the samples at the nano-scale and to observe fine microscopic details, as well as the elemental composition depicted by X-ray elemental mapping.

4. Results

Abundant (201–996 oncolites/m^2; average = 465; Table S1) grey to black oncolites, semispherical and concentrically-laminated, were enclosed in a hematized matrix of skeletal grains, oolites, and, locally dolomitized, calcite (Figure S3). Their diameter ranged from 2 to 44 mm (n = 2226; Table S1), being more frequent from 8 to 15 mm (Fig. S3). These measurements may be biased, as the exposed cross sections from which measurements were made may not represent the central axis of symmetry of the oncolites, but rather oblique cuts. Regardless, it is a numerical value useful for comparisons against other Cambrian oncolites.

Most of the oncolites were nucleated on mollusc shells (*Hyollites* sp.), which appeared filled with micrite and thin and assorted, broken skeletal grains (figures 3, 4). The oncolites and the matrix (60–80% skeletal grains) were pervasively hematized (figures 3, 4), although some portions were enriched in silica (figures S4A, S5). Skeletal grains were mostly calcitic, but displayed heterogeneous composition (figures S4–S9). Carbonate recrystallization and cementation often displayed drusy habits (Figure 3 D), which indicate a synsedimentary or early diagenetic process of cavity filling. A small percentage (< 5%) of terrigenous particles (floating quartz grains and Fe-rich, clay-sized aggregates; figures 3 B, D, F) were also observed. Hematization may have been selective, as some buried contents display heterogeneous hematization (figures 3 E, F). This pattern suggests that some hematization processes were syndepositional or early diagenetic. Some oncolites displayed corroded surfaces (karstic textures) and small pits, which were then covered by a new laminae (figures 4 C–D, 5). These could have been produced by erosion or bioerosion (grazing, cyanobacterial boring, etc.). Some oncolites displayed relatively large burrows perpendicular to the concentric lamination, sometimes distorting it (Figure 4 C). The burrows were usually filled with slightly finer sediment than the surrounding matrix (figures 4 C–D, 5). Bioerosion

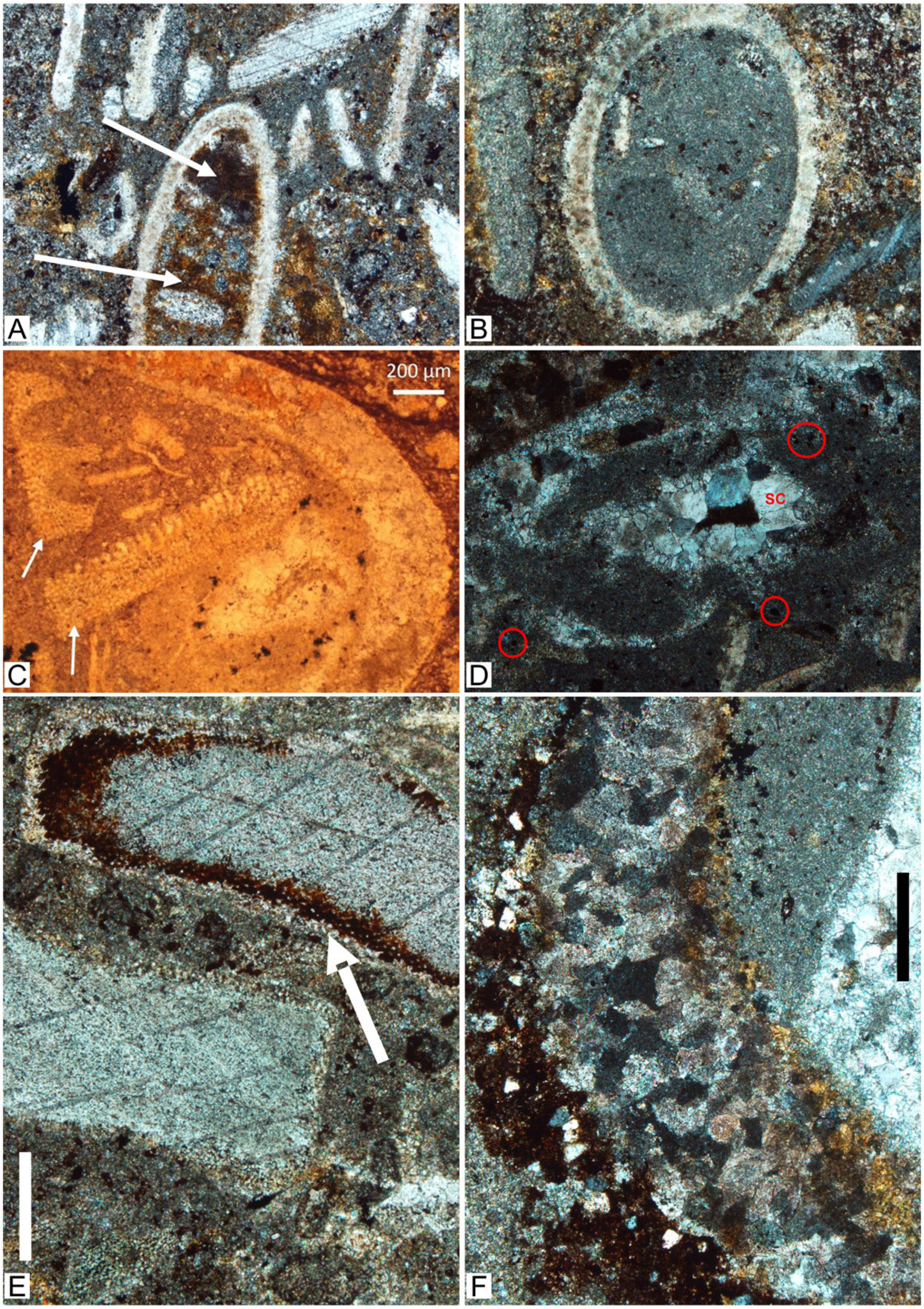

Figure 3. Cambrian oncolites from San José de Gracia at the mm to cm scale. A. Oncolites embedded in a hematized limestone-dolostone. The 'packstone' matrix is dominated by eocrinoid, trilobite, mollusc, and brachiopod fragments. M = mollusc nucleus; O = Oncolite. Mx = matrix. Scale = 10 mm. B. Close up of an oncolite to show its concentric laminations (L), the previously-filled mollusc nucleus (N), the skeletal packstone matrix (M), and the pervasive hematization all throughout. Note corroded surfaces and interiors (arrows), and the cross-cut lamination (curved lines). Scale bar = 5 mm. C. Dominant skeletal grains. Large fragment of an eocrinoid (e), along with smaller brachiopod, and trilobite (t) fragments. The oncolite surface displays accreted sediment wrapped by an outer lamina. Distorted lamination can be produced by grazing and burrowing of other organisms. Scale bar = 5 mm. D. Naked (m) and encrusted (o) mollusc shells, along with fragments of eocrinoids (e) and trilobites (t). Scale bar = 5 mm.

at different metric scales is plausible, and was likely made by different biological groups (*e.g.* bacteria, fungi, protozoa, and animals), which were present at the moment, according to the fossil record of the Chihuaurrita Hill.

Concentric, usually discontinuous, sub-millimetric, micritic laminae outlining the oncolites could be seen at macro and microscopic scales (figures 4–6). Laminae could be thin (3–20 μm), medium (20–200 μm), or thick (> 200 μm), smooth or contorted, and sometimes appeared cut by other laminae, indicating erosion events (figures 4 B, 6 A–D). In many cases, biofilm-like textures were present, usually lined up by several episodes of laminar development

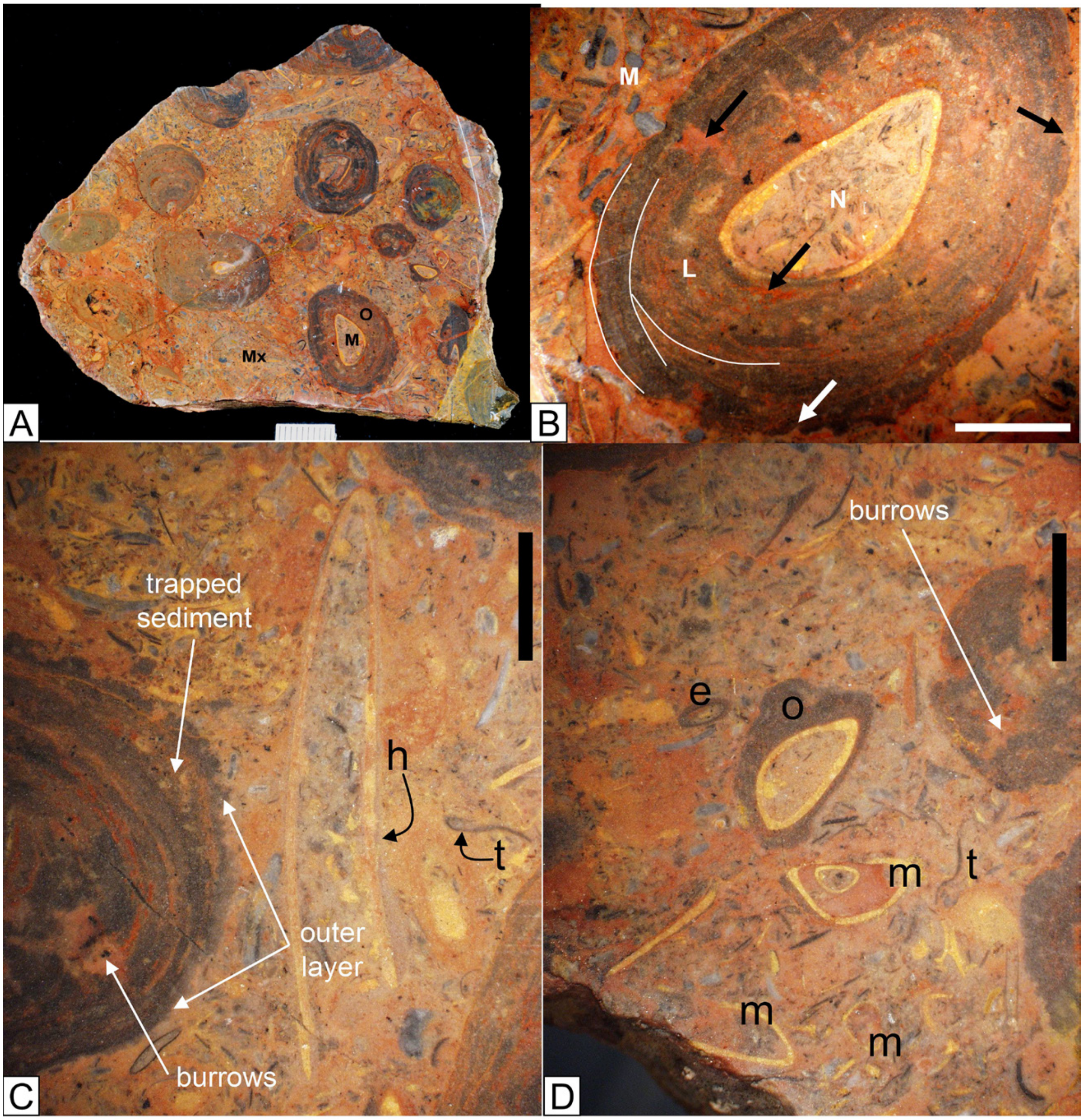

Figure 4. Distinct filling of skeletal grains and hematization. A. note the selective hematization (arrows) inside the largest eocrinoid shell, compared to the less hematized exterior matrix. B. Finer, micritic, and less hematized sediment inside the elyptical eocrinoid shell, compared to the coarser and heavily hematized exterior matrix with terrigenous particles. C. Eocrinoid fragments (arrows) inside the nucleus of an oncolite. D. Pore spaces being filled with sparry calcite with drusy habit (SC). Note micritic matrix with scattered terrigenous particles (circles). E. close up to eocrinoid fragments showing their characteristic twinning lamellae. Note degradation and hematization toward the edges of the fragments (arrow). F. close up to a brachiopod shell, showing exterior and interior coating of walls (dark). Terrigenous particles can be seen otside the shell as part of those coatings. Scales in A and B = 5 mm. Scales in C and D = 250 μm.

(Figure 6 B–D). Biofilm fragments and accumulations of dark kerogenous material were also present in the best preserved samples (Figure 6 E–F). Such organic materials could be seen coating grains, forming clumps and ripped biofilms, and were constituted by different densities, porosities, and textures, either in biofilm-biofilm contact or in biofilm-sediment contacts (figures 6–8). In some cases, fenestral porosity infilled with sparry calcite (figures 7 E–F, 8 C–D) were similar to biogenic, gas-like accumulations (see figures 3–4 in Wilmeth *et al*., 2015).

Girvanella-like filaments were pervasive in most samples (figures 9–10), along with other tubular filamentous structures (Figure 11). Some of them had sinuous morphology and irregular width (Figure 9 D), which might be compatible with fungal hyphae. These did not display diagnostic features, such as sporangia or other reproductive structures, perhaps because the entire length was not observed in full, but in fragments only. The *Girvanella*-like filaments were 2.7 to 13 µm in width and > 100 µm in length, with an average width of 5.8 µm and a median of 4.6 µm (n = 50). No filament branching was observed, although the intrincate nature of the contorted filaments holds doubt on this fact. In cases where filaments could be 'followed' in length, a fairly constant diameter was observed. Some filaments appeared to be septate (Figure 9 D–H), but lack of consistency in supposedly 'septal' walls may imply crystal growth within the filament cavity rather than true original septa. This needs further studies to be confirmed.

Secondary and backscatter SEM images of different portions of oncolites (figures12–14) revealed the presence of tubular, subspherical, and amorphous, biogenic-looking structures that were partially preserved. Most of them were siliceous in composition (figures S4–S9) and often enriched in iron. Other Fe-rich, isolated structures were also found within the oncolitic lamination (figures S4 A, C, S5 B, S6 A-B, S8 B–C). In cases where Al-enriched areas were more prominent, Fe was scarcer or absent. The Carbon signal from EDX seemed to be associated largely with Ca, indicating its presence in the form of $CaCO_3$ of the shells, the rock matrix, and the oncolites. However, it sometimes appeared concentrated in structures of uncertain, but likely biogenic origin (Figure S5 D). Raman spectra with clear G and D bands obtained from the samples were consistent with the presence of kerogenous material within the structure of the oncolites (figures S10–S11), and argues for some original organic material to be present in the rocks, as is the case in other fossil examples of older and younger ages (Schopf and Kudryavtsev, 2009; Beraldi-Campesi *et al*., 2015). XRD analysis detected 80% calcite in bulk rock matrix and oncolites separately, with minor (< 20%) quartz and muscovite (Figure S12). XRF analyses (Figure S12) showed the presence of Ca, Mn, Fe, and Co, from which Ca, Fe, and Mn were measured also with EDX (figures S7 B, S8 A, S9 A). Mg was also detected with EDX (figures S7 A, S8 A) but not with XRF. Further studies may require analysis with a different methodology (*e.g*. solvent extraction, mass

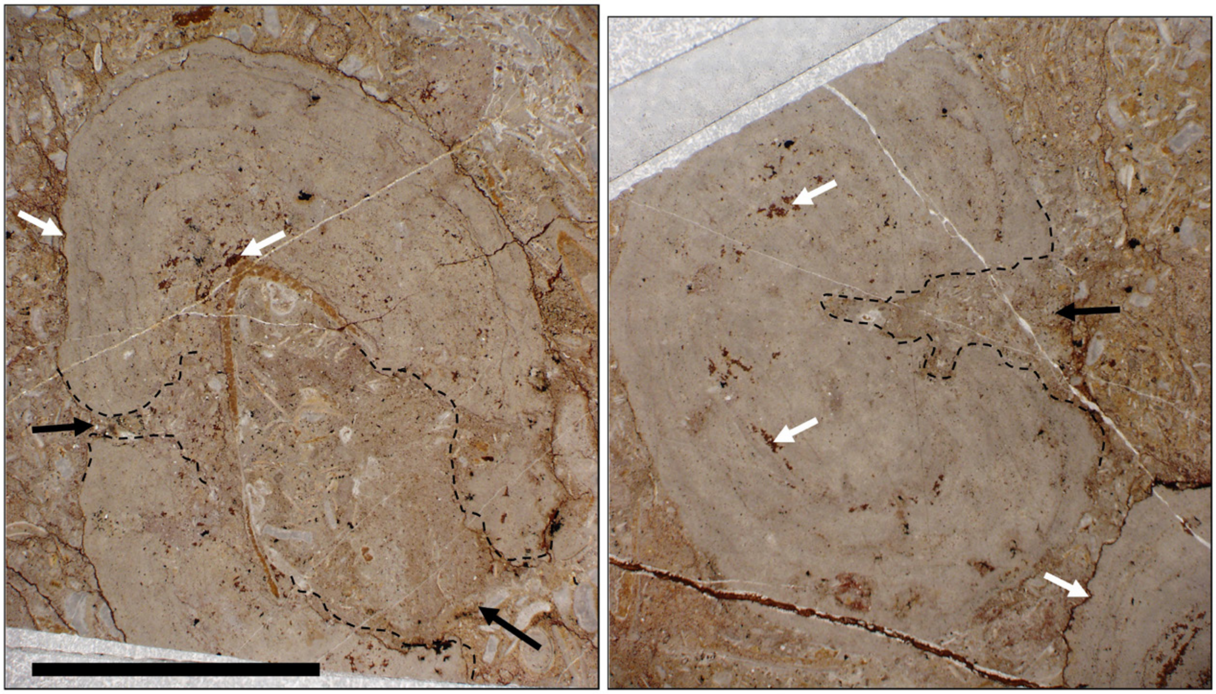

Figure 5. Pits and burrows in oncolites. A nucleated (left) and non-nucleated (right) oncolite displaying burrows, inner pits, and corroded surfaces. Dashed lines show the burrows and black arrows show their entrances. Eroded (karstic) or bored surfaces and pits are shown with white arrows. Scale bar = 1 cm for both images.

spectrometry) to better analyze organic compounds and metals.

5. Discussion

5.1. Environmental significance of oncolites

The presence of oncolites in the sedimentary Cambrian of Mexico demonstrates the wide geographical distribution that such microbialites attained in the past, and therefore, the significant importance of microbes in sedimentary and biogeochemical processes throughout time. Fossil oncolites are known from the Precambrian (3500 Ma) to the Recent, in a variety of environments (Henderson, 1975; Dunlop *et al*., 1978; Lowe, 1983; Knoll *et al*., 1989; Winsborough *et al*., 1994). The studied oncolites mark an important episode of microbial-sediment development in this part of southern Laurentia in the Lower Cambrian.

Oncolites may constitute good indicators of microbially-induced mineral precipitation rates in relation to their size in non-saturated solutions. Thus, the presence of relatively

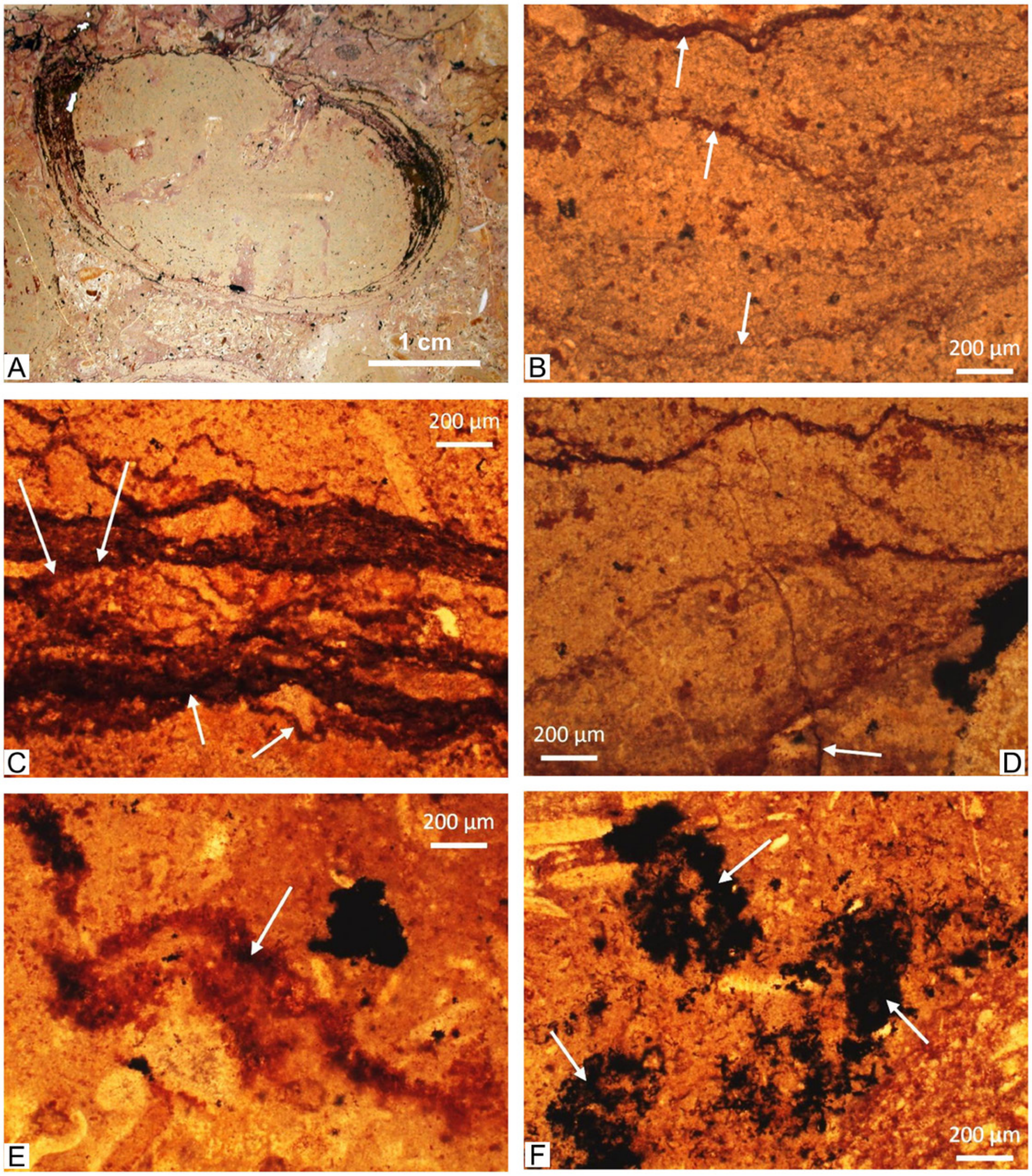

Figure 6. Oncolite lamination and biofilms. A. Oncolite with a muddy core (no shell nucletion) and well developed biofilm lamination toward the surface. B. Oncolite lamination showing biofilms (arrows) spaced by relatively long intervals of sediment accumulation. C. Biofilm lamination showing relatively short intervals of sediment accumulation. Example of erosive surfaces of biofilms are indicated with arrows. Each lamina indicates an event of biofilm formation. D. Fractures crossing oncolite lamination. Fluids can migrate easier through fractures and transport organics and metals. E. Ripped piece of biofilm of ferruginous organic matter. F. Graphitized and ferruginous organic matter. Note some grains coated with it.

large, marine carbonate oncolites would imply high rates of mineral precipitation, likely associated with microbial productivity, in particular high rates of photosynthetic CO_2 sequestration (Kah and Riding, 2007), which is important for the CO_2–CO_3 balance in the oceans and essential in the global carbon cycle. It also may imply high rates of microbial sulfate reduction, as it appears to be one of the main process of lithification in modern, marine, carbonate stromatolites (Dupraz and Vischer, 2005). These features are highlighted in the studied oncolites, which are relatively large and abundant, implying an important sink for carbon by this time.

Regarding the local environmental conditions, the great abundance of reworked and fragmented skeletal grains in the matrix and inside the studied oncolites, suggests episodes of high-energy and reworking capable of grinding shells. This high-energy is consistent with the energy required to overturn the oncolites and promote their concentrically, laminated growth. Smaller, reworked skeletal grains filling larger shells (Figure 3A), suggest that there were

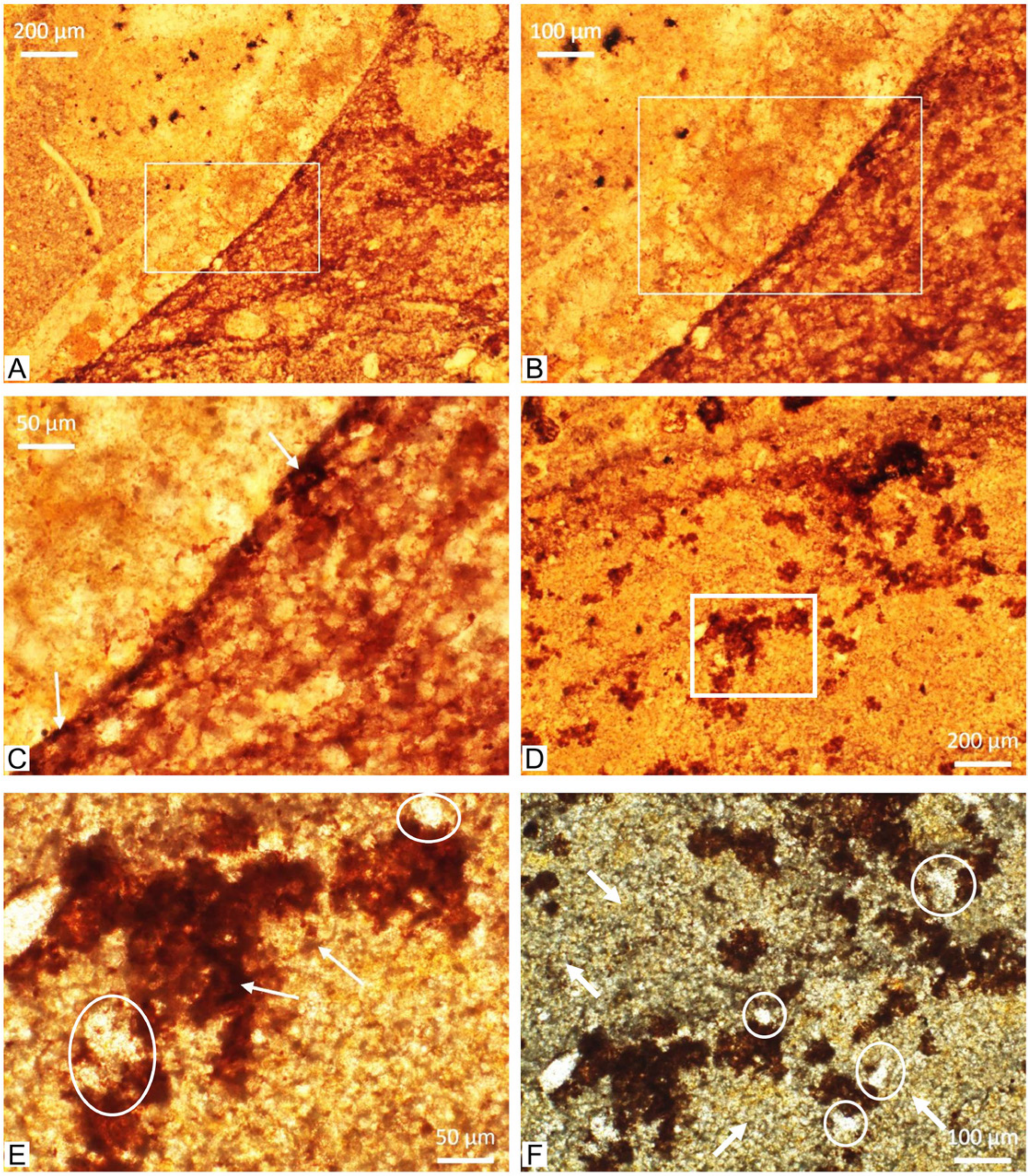

Figure 7. Oncolite biofilms and their interaction with *Girvanella*-like filaments. A. Well preserved oncolite nuclear boundary. B. Close up of box in A showing the and organic-rich layer. C. Close up of box in B. Coated grains (arrows) in the organic matrix can be seen in contact with the mollusc shell. D. Clumped organic material distributed along the oncolite laminae. E. Close up of box in D showing filament-like structures associated with organic clumps. Fenestral porosity filled with sparry calcite (circles) indicate gas-like voids. F. Same clumps shown in D and E, in polarized light. Note the abundance of *Girvanella*-like filaments (arrows) occupying spaces between clumps. Circles indicate fenestral porosity formed through gas accumulation.

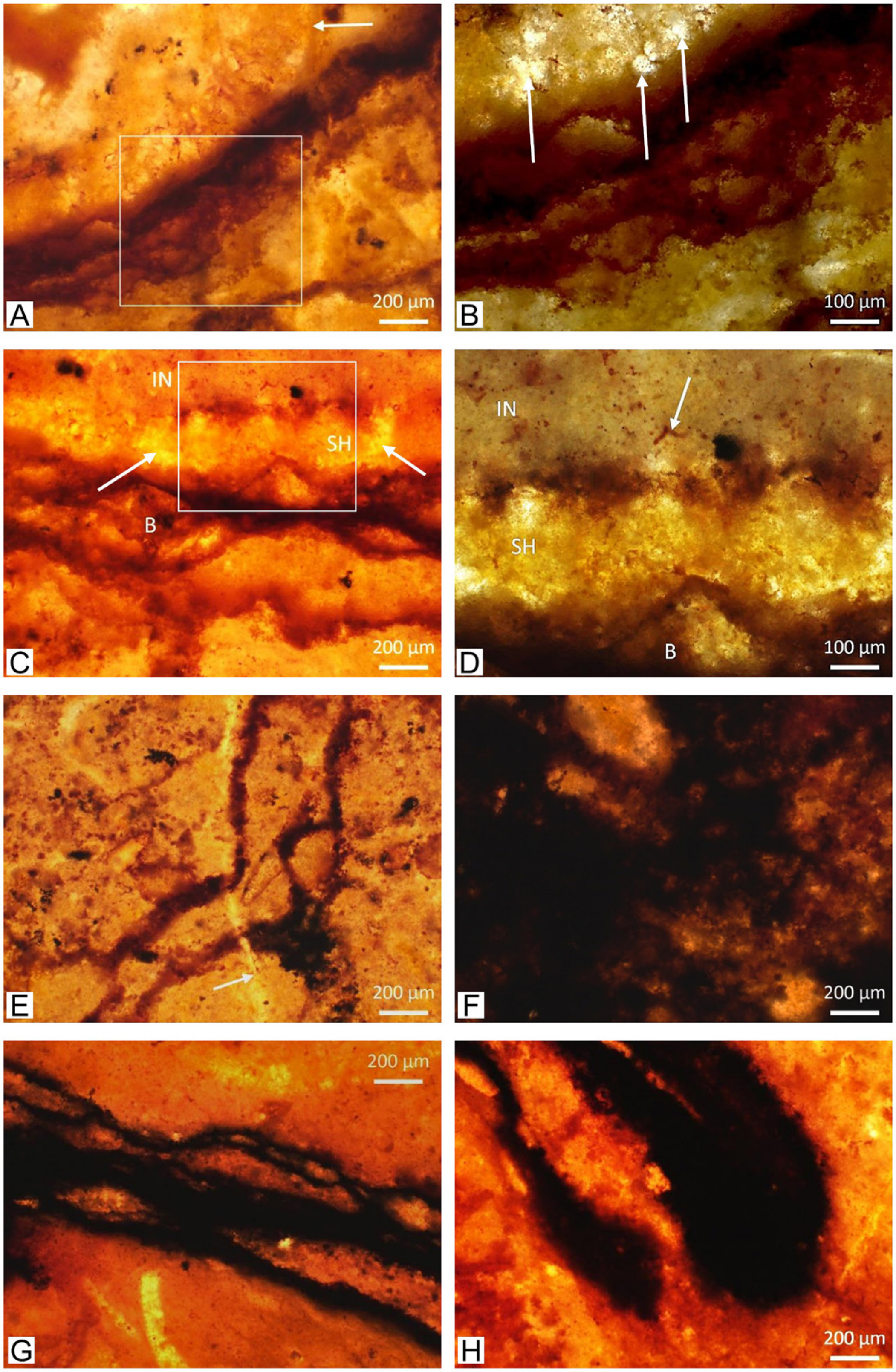

Figure 8. Oncolite biofilms. A. Biofilm at the boundary of a lamina, showing abundant microbe-like structures (arrow). B. Close up of box in A showing dark laminations developed by biofilms and the mineral grains embedded in them. Arrows show fenestral porosity, likely derived from metabolic gas production. C. Laminated biofilms (B) covering a shell fragment (SH) and the sedimentary fill of the interior (IN) of the nucleus. Arrows point to gas-generated fenestral porosity filled with sparry calcite. D. Close up of the filament shown in C. Mucilaginous cover and cells are overdrawn with a dashed line. E. Peculiar lamination crossed by a fracture (arrow). F. Sometimes organics are concentrated. G. Well stained ripped laminated biofilm. H. Rounded end of biofilm shown in C. Thread-like structures may be seen departing from the main structure by the bottom end.

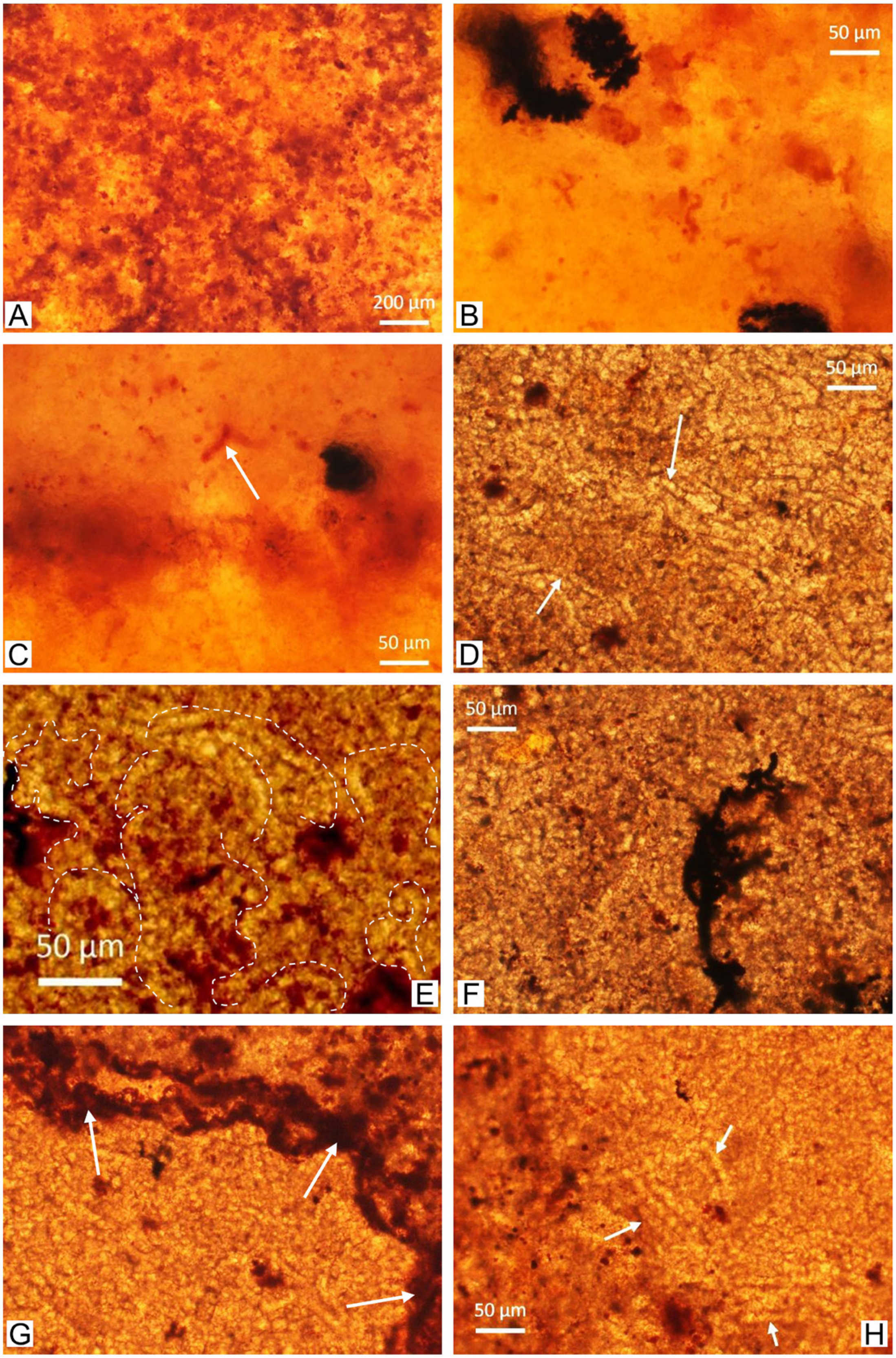

Figure 9. Filamentous structures. A. Filament-like structures that form part of an oncolite lamina. B. Close up of isolated filament-like structures shown in A. C. Isolated and contorted filament-like structures (arrow). D. *Girvanella*-like filaments displaying an overall NW-SE alignment. E. Close up of the lower left area in D, displaying *Girvanella*-like filaments with marked curvature (dashed lines). F. Dark fungal-like structure surrounded by *Girvanella*-like filaments. G. *Girvanella*-like filaments delimited by a biofilm (arrows). H. *Girvanella*-like filaments showing septation (arrows).

previous episodes of sedimentation, early diagenesis, and reworking, before they were deposited in the basin. Riding (1975) has stated that *Girvanella* (likely cyanobacteria) can develop in shallow waters (< 30 m), with depth ranges that may vary from a few meters to several hundred meters or more. The amount and density of oncolites in SJG can be better explained in a high energy environment with wave oscillation for their overturning. This would require a shallower environment less than 30 m deep. Even in clear, oligotrophic waters, where photosynthesis could have operated in deeper waters, no sufficient energy would have been available for the rolling needed to form oncolites.

Remnants of semi-preserved organic matter (figures. S6 C–F, 8, S10) indicate that a rapid process of entombment occurred, perhaps in oxygen-deficient conditions within the sediment, which prevented its oxidation (Bauld, 1981; Zonneveld *et al*., 2010). Cavities with patterns of microbe-sediment-gas interactions preserved within the oncolitic lamination (Figure 8 B–D), could be correlated with deformation of the original biofilm by gas entrapment (Wilmeth *et al*., 2015). This is plausible given the existence of conspicuous biofilms and colonial filaments (figures 6–11) that likely produced gasses within the oncolite lamination while this was developing. We infer that abundant microbial communities, including cyanobacteria, were responsible for the development of the SJG oncolites, that they developed in a carbonate, shallow bank with episodes of storms and high-energy currents, and that fine sediment accumulated rapidly and entombed a large proportion of specimens, where anoxic conditions and early diagenesis occurred.

SEM analyses support the idea that some microbial remains were fossilized and are still present in the samples. Despite the degree of obliteration due to diagenetic processes (including replacement and recrystallization), carbon peaks in EDS of some biogenic-looking structures and clear G and D bands in Raman spectra, indicate the presence of organic matter localized in specific regions of the samples. Some of these organic remains appear to have been silicified and enriched in Fe. Complexation of metals by sorption on microbial EPS is common in most environments, and it keeps those metals bound or chelated (Sander and Koschinsky, 2011) and even dissolved for several days (Theis and Singer, 1974). Combined processes of metal sequestration and early diagenesis may be reflected in specimens where oncolite lamination was highly enriched in Fe (Figure S8 C). The selective hematization in some cases (Figure 3 E–F) is also indicative of this process, by the chemical alteration of isolated fragments that experienced diagenesis before being transported and redeposited where the oncolites were forming. Infilling of pores with sparry calcite in drusy habit suggests episodic transitions from saturated conditions below the water table, to unsaturated conditions within the vadose zone, where cavities could have been infilled with calcite. It is possible that sea level fluctuations (tides) or prolonged seasons of subaerial exposure in the carbonate bank influenced the early diagenetic history of the oncolitic deposit.

The SJG oncolites also display features that may be of ecological relevance. Corroded and perforated fabrics (pits) observed in our oncolites (figures 4–5) may be indicative of microbial boring, which is common in these environments (*e.g*. Garcia-Pichel *et al*., 2010), and also indicative of feeding processes of grazers on soft or semi-lithified surfaces. Metazoans (especially eocrinoids, mollusks and trilobites) could have fed on microbial biofilms and mats. The absence of stromatolites in the SJG but large amounts of oncolites may have been influenced by grazing. Sesile microbialites could have been easily targeted by metazoans contrary to the mobile oncolites. The different size of the cavities may reflect grazing intensity and body size of grazers and borers. In addition to bioerosion, karstic dissolution (whenever exposed to the atmosphere) and abrasion caused by rolling of the oncolites are likely to have occurred as well. These small-scale interactions require further studies.

5.2. Interpretation of *Girvanella*

The genus *Girvanella* was first described by Alleyne Nicholson and Robert Etheridge in 1878 from Upper Ordovician exposures near Girvan, on the Ayrshire coast, UK (Nicholson and Etheridge, 1878). The description reads: “Microscopic tubuli with arenaceous or calcareous (?) walls, flexuous or contorted, circular in section, forming loosely compacted masses. The tubes apparently simple cylinders, without perforation in their sides, and destitute of internal partitions or other structures of similar kind” (Nicholson and Etheridge, 1878). Microbes influence the development of oncolites, either by promoting mineral nucleation and precipitation, or by affecting the porosity, lamination, and other internal fabrics, as well as the three-dimensional development of the structure. Although many microbes can be present in oncolite-biofilm communities, cyanobacteria are the typical type found in association with this type of structures in shallow marine and freshwater environments (Winsborough *et al*., 1994; Wade and Garcia-Pichel, 2003; Alshuaibi *et al*., 2012). It is probable that cyanobacteria dominated these environments and were dominant drivers of oncolite-associated biofilms (Riding, 1975, 1977). The presence of *Girvanella*-looking filaments in these Sonoran oncolites supports this hypothesis but makes no reference to any specific taxa at the moment. Proof of their biological origin is the abundance of filamentous structures that, given their curvature and spatial arrangement, fit the minimum criteria for biogenicity, along with their contextual provenance, indigenousness, and syngenicity (Buick, 1990; Schopf, 1993). We assume that cyanobacteria were present in the environment where SJG oncolites formed, that they had a crucial role in oncolite formation, and that they were responsible for much of the primary productivity at the time.

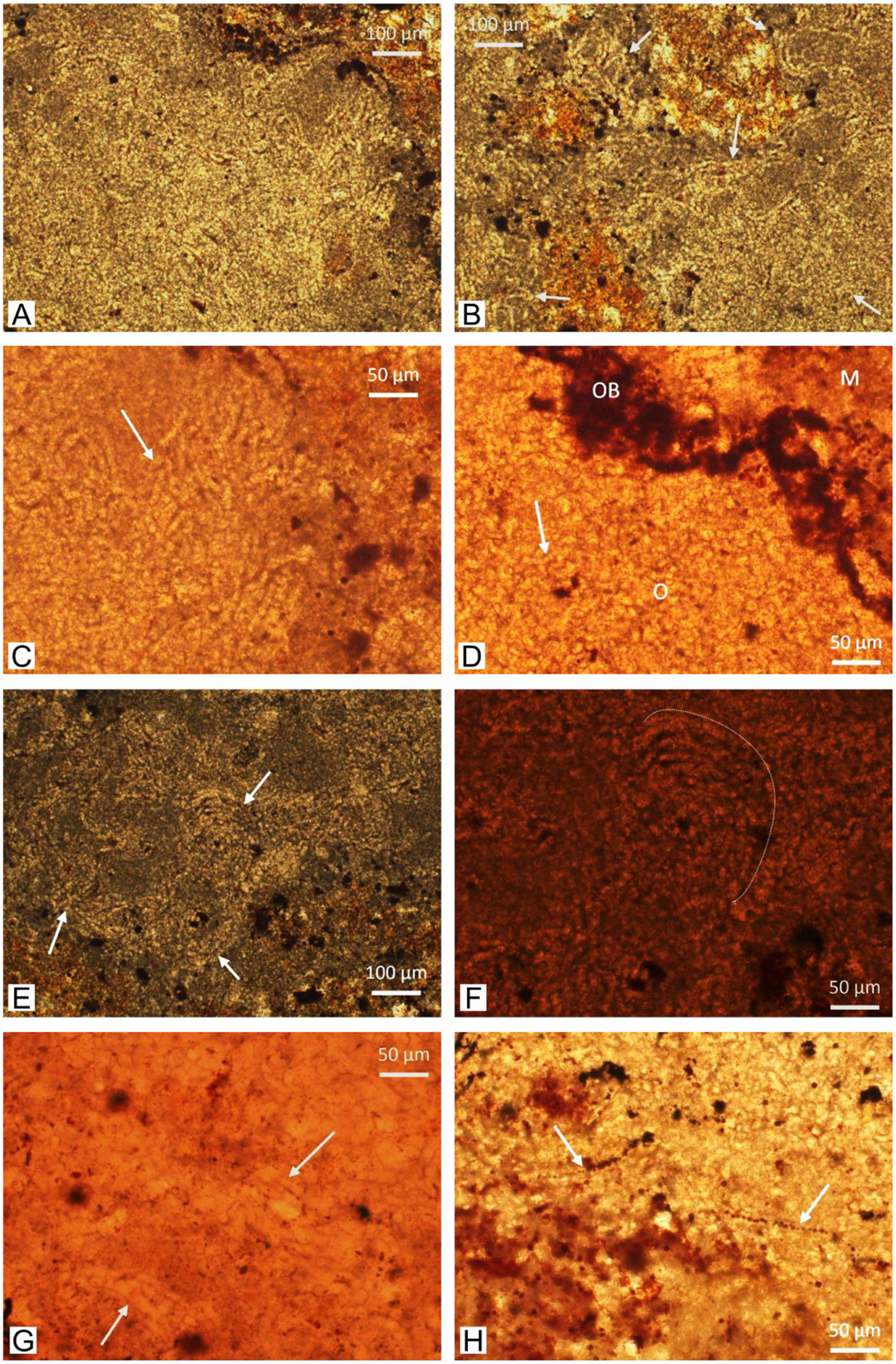

Figure 10. *Girvanella*-like filaments. A. *Girvanella*-like filaments filling a space inside an oncolite. B. *Girvanella*-like filaments (arrows) near hematized areas (reddish). C. Close up of the *Girvanella*-like filaments shown in A and B. D. Septated *Girvanella* filaments (O) (arrow) next to the organic-rich biofilm (OB), separating them from the matrix (M). E. *Girvanella*-like filaments forming a coil in polarized light. F. Close up of a *Girvanella* coil in transmitted light. G. *Girvanella*-like filaments forming coils in groups. H. *Girvanella*-like filaments sharing space with larger, and morphologically different types of filaments.

Stratigraphically, *Girvanella* is found in the Neoproterozoic and throughout the Paleozoic and Mesozoic (Riding, 2006). It tended to grow in shallow marine and coastal environments, where it was pervasive in microbialite-building communities. Their physiology and metabolic consequences for the environment (biogeochemistry), along with their capacity to interact with minerals, must have been significant as geobiological agents. The *Girvanella*-oncolite association seems to be common in the Lower Cambrian of Sonora and other parts of the world.

The *Girvanella*-like filaments found in SJG may differ from the original description by the apparent presence of septa in most of the filaments (Figure 9 D–H), but are similar in size and spatial arrangement. It should be noted that septate-looking and branching *Girvanella* (which by definition should be non-septated and non-branched) have been reported from the Ordovician of Scotland (Wood, 1957). The physiological nature of these microfossils is uncertain, but a cyanobacterial origin cannot be discarded (Wood, 1957; Riding, 1977; Laval *et al*., 2000; Planavsky *et al*., 2009). Filaments forming coils (figures 9 E, 10 E–F) may portray behavioral traits also observed in cyanobacteria (Shepard and Sumner, 2010; Sim *et al*., 2012). Some biomorphs (filaments, blobs, subspherical features) within

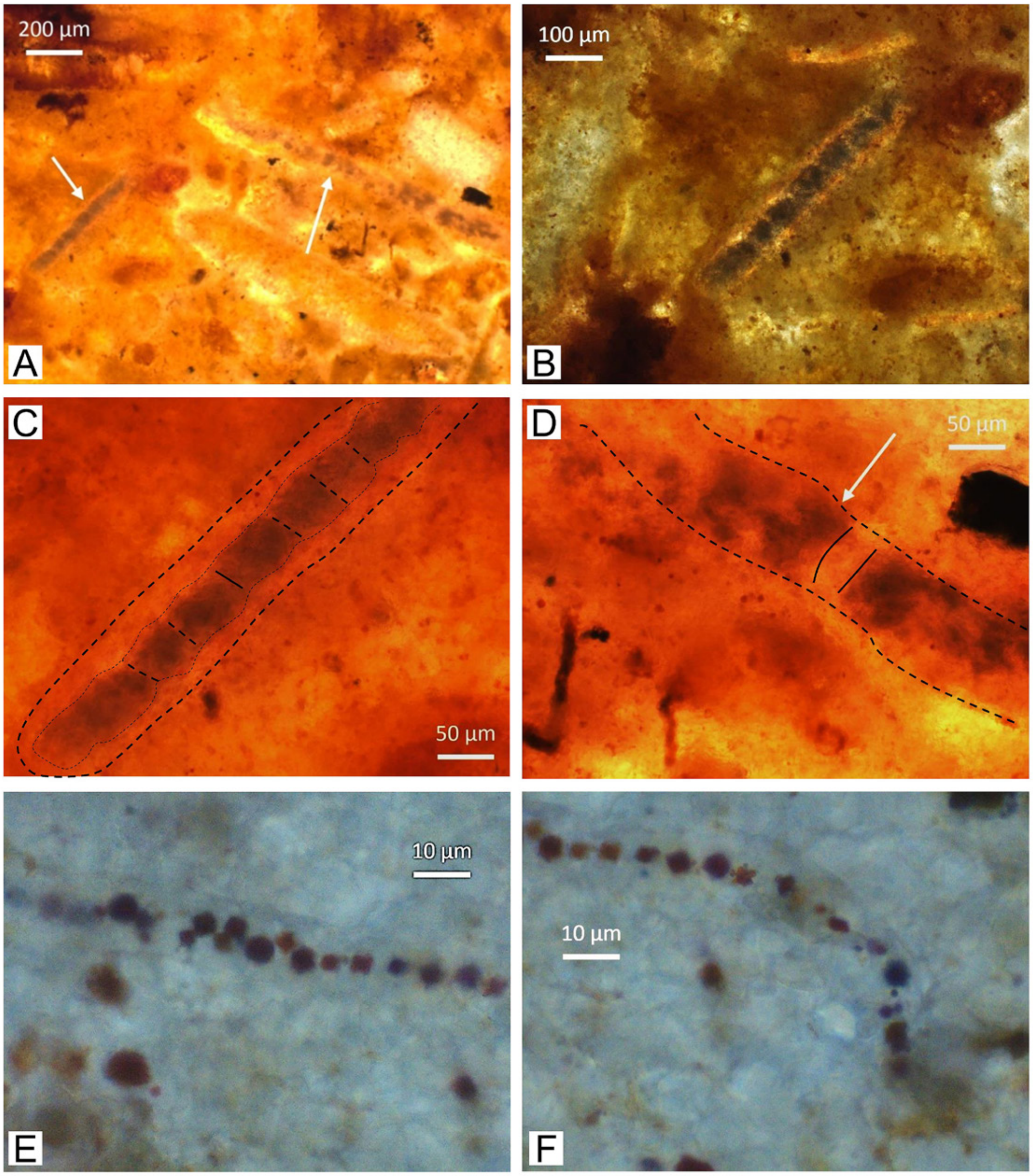

Figure 11. Other types of filaments. A. Filamentous structures (arrows) in the matrix between oncolites. B. Filamentous structure with septation and mucilage-like cover surrounding the trichome-like arrangement. C. Close up of the filament shown in B. Mucilaginous cover and cells are overdrawn with a dashed line. D. Close up of filament (dashed lines) shown in A. Cell-like bodies (arrow) seem to be separated by a septum (solid lines). Fungi-like organisms are also present (bottom left quadrant). E. Close up of filaments shown in B. F. Close up of a filament displaying flexibility.

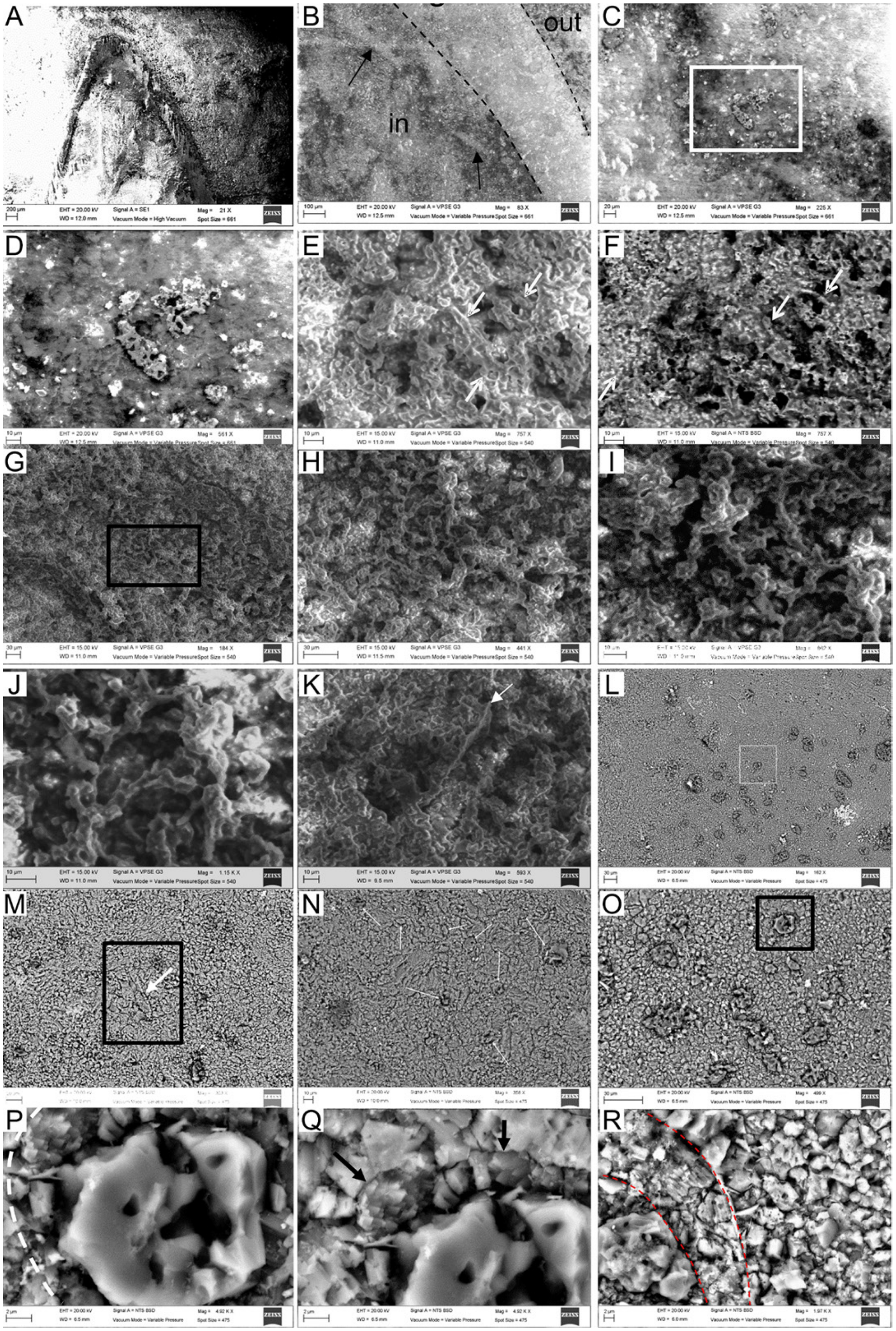

Figure 12. SEM photographs of the oncolitic structure. A. Fresh fracture of an oncolite displaying its nuclear mollusc shell, the inner filling with skeletal fragments, and the outer oncolite massive texture. B. Brachiopod shell (dashed lines) between inner filling with skeletal grains (arrows) and outer oncolite body. C. Oncolite matrix and part of the internal lamination (dark), displaying cross sections of filament-like structures. White box shown in D. D. Detail of the acid-etched cross section of a filament-like stucture. EDS of a similar structure is in Fig S4A. E–F. Oncolite matrix with clumps of calcite and occasional filamentous structures (downward arrows), sometimes with buddying-like structures (upward arrows). F = secondary electrons. G = backscatter electrons. G–H–I–J. Different magnifications on biogenic-looking features. K. Calcitic matrix of a fractured oncolite (arrow). L–M–N–O–P–Q. Different magnifications of a portion inside the oncolite matrix. Silicified cross sections of filament-like structures appear in the surrounding. Note the cell wall-like structure in P and Q (dashed line and arrows). See figure S4 for EDS analysis of the filament-like structures. R. Crystal size, not composition, makes cell wall-like structures visible (dashed lines).

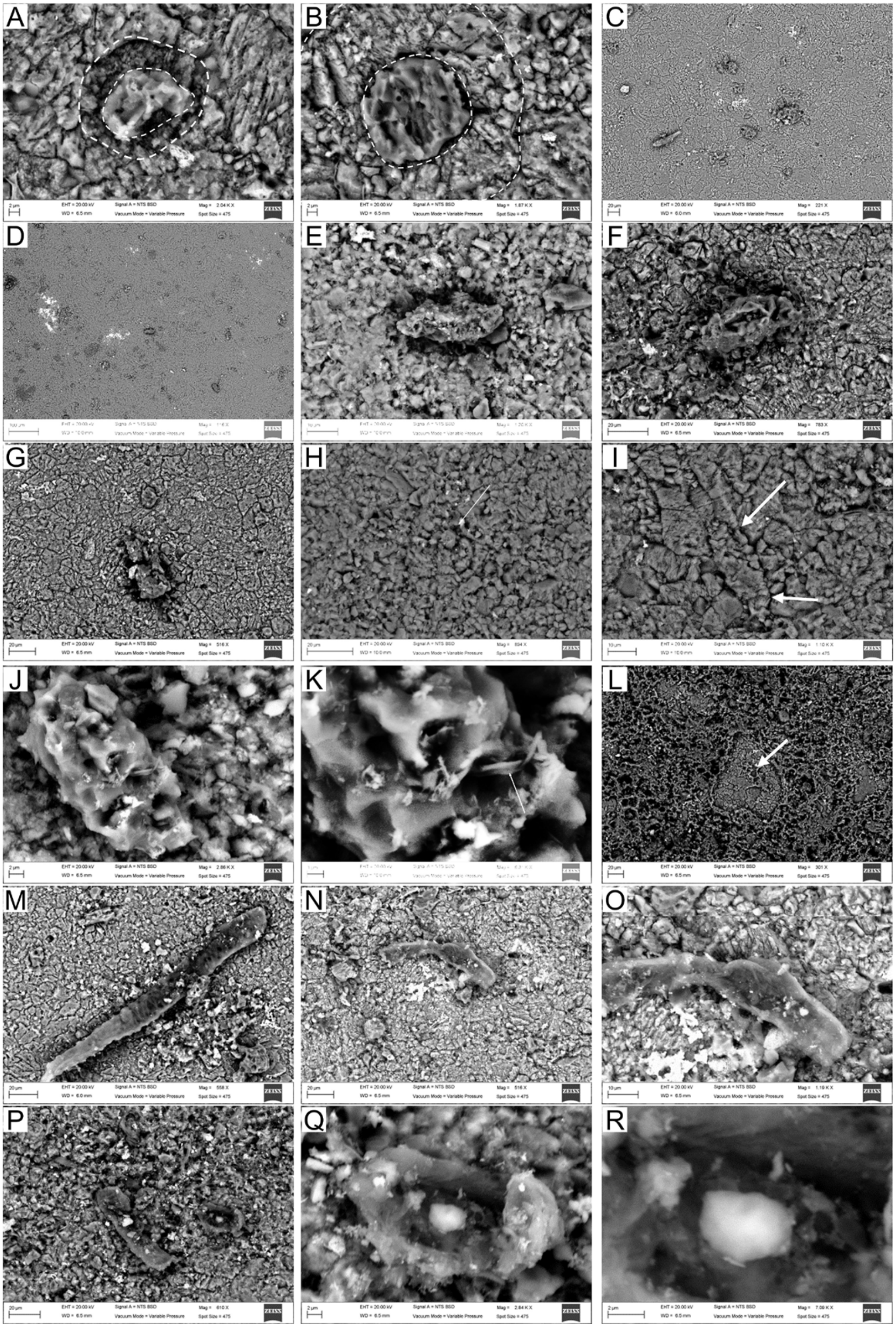

Figure 13. SEM photographs of the inner oncolite structure. A–B. Cell wall-like structures around filament-like structures in cross section. C–D. Limestone matrix with filament-like structures in cross section. E–F–G. Close up of filament-like structures in cross section in D. Cell wall-like structures are absent. H–I. *Girvanella*-like filament (arrows). J–K. Siliceous core of a filament-like structure showing porosity and clay minerals. L. Calcified and carbonaceous body (arrow) surrounded by silicified structures in a honeycomb-like texture. See Fig. S7 for EDS elemental analysis. M–N–O–P. Close up of carbonaceous, tube-like structures. Q–R. Cross section of a tube-like structure with a siliceous core.

Sonoran oncolites could be compared with reminiscences of calcifying biofilms seen in ancient (Riding, 2006) and modern marine microbialites (Planavsky *et al*., 2009). If cyanobacteria inhabited these biofilms, they must have been responsible of important biogeochemical cycling and ecological and geobiological functioning.

5.3. Stratigraphic significance

The Cambrian outcrops of the Chihuarruita Hill site bear important index fossils for biostratigraphy and age correlation (Figure 2). For instance, the eocrinoid *Gogia granulosa* has been reported also from northern Utah and south-eastern Idaho (Robison, 1965; Sprinkle, 1973; Nardin *et al*., 2009) and indicates an Early to Middle Cambrian time span. Trilobites are abundant and diverse in Sonora and useful for global age correlations. Numerous genera of agnostoid arthropods (*Peronopsis* and *Pagetia*) have been identified in Sonora, India, Australia, Canada and the United States; *Oryctocephalus* has been reported in the United States, Asia, South America, and Europe; *Bathyuriscus* is found in the northeastern United States and England; and *Elrathina* is found in Greenland, the United States and Canada. Brachiopods are also an important group found in the Chiuharruita Hill, and are represented by the genera *Acrothele*, found also in Europe, Asia, North America,

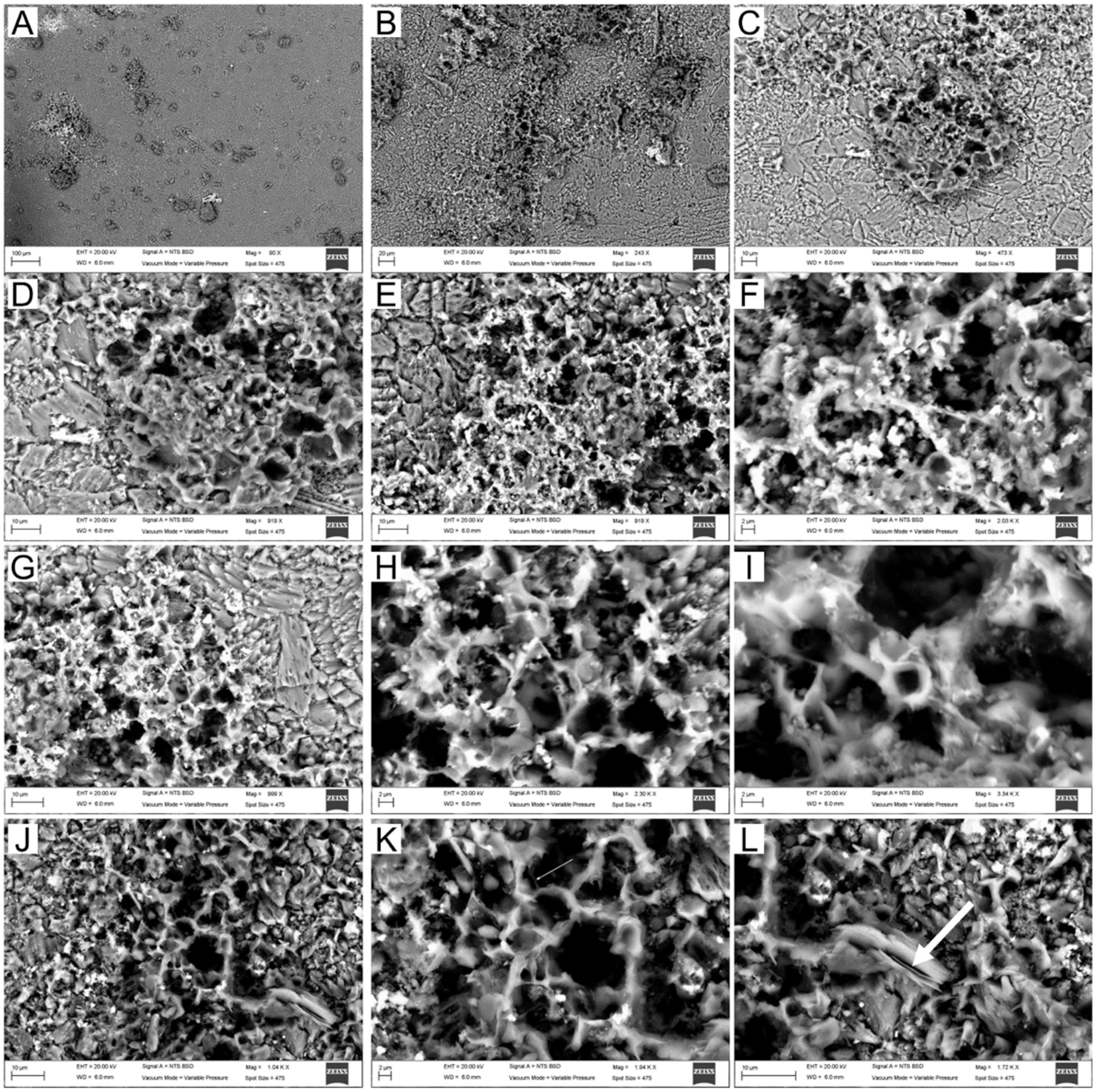

Figure 14. SEM photographs of reticulated structures within the rock matrix (outside the oncolitic structure). A, B, C, D. Incremental magnifications of reticulated structures show the overall circular shape in cross section (A, C, D), and the contrasting difference in texture with the surrounding matrix (C). Although similar to structures in Fig. 14 (L–R), these display a reticulated texture but are similar in composition (Fig. S9 A–B). E, F, G, H. These reticulated structures often display thread-like filaments that are < 2 µm in diameter and make up the bulk of the structures in cross section. I, J, K, L. Tubular structures (I; ~2 µm in diameter) and clays (J, L) are also present within these reticulated structures.

Australia, and North Africa; the genus *Dictyonina* is found in North America, Asia, and Europe; the genus *Prototreta* is found in Europe, America, and Asia; and *Linnarssonia* is found in North America and Europe. These fossils give the Cambrian of Sonora a worldwide stratigraphic context.

Paleogeographic reconstructions of North America (Scotese, 2002) place the platform where this fauna developed in Sonora in the tropics during the Early Cambrian. This was open to the Iapetus Ocean, with large landmasses (Baltica, Siberia, Avalonia, and northern Gondwana) relatively close by and located more or less in the tropics as well. Ongoing work is dealing with whether Lower Cambrian oncolites developed under similar conditions along that stretch of the Iapetus coastal areas, under the premise that oncolite markers exist in many strata of the world, and that they can be useful when used together with index fossils and lithology. Oncolites are present in stratigraphic ages other than the Cambrian and thus are not index fossils, but ambiguous stratigraphic markers by themselves (Rezak, 1957). However, when other, well-known index fossils are present they result in useful stratigraphic markers for close geographical regions, which is the case with the Caborca-SJG correlation. Regardless of the similarity in morphology, Cambrian oncolites are known from China (Hicks and Rowland, 2009; Zhang *et al*., 2015), Australia (Youngs, 1978; Walter, 1972), Jordan (Shinaq and Bandel, 1992; Elicki *et al*., 2002), Spain (Álvaro *et al*., 2000; Perejón *et al*., 2012), Antarctica (Rees *et al*., 1989), Argentina (Bordonaro, 2003; Gomez *et al*., 2007), Iran (Bayet-Goll *et al*., 2014), and Canada (Powell *et al*., 2006), which highlights the expansion of oncolites in the Cambrian as a global phenomena, with implications for paleoenvironmental and geobiological significance.

Localities from the USA are particularly important for correlations with the Chihuarruita Hill given their proximity and the extension of Cambrian outcrops to the south. The SW USA shares a lot in common with rocks and fossils from Sonora. Oncolites from Nevada, California, and Arizona (Johnson, 1952; Hose, 1961; Halley, 1975; Gilbert and Donovan, 1982; Rees, 1986) have particular characteristics according to their geographical location, particularly size, shape and color, which implies similar lithology and diagenesis. They tend to be darker than the matrix, can occur in hematizied horizons, their size ranges in ~20–50 mm, and most are nucleated and have concentric lamination. Some have been recovered from fine-grained carbonate rocks in the Chambless Formation and the Lower Cambrian Mule Spring Limestone, Nevada, USA, which have similar color, size, shape, style of lamination and depositional style than those from Caborca and SJG. In California, the Thimble Limestone Member of the Carrara Fm. (Palmer and Halley, 1979) bears *Bristolia bristolensis* and *Olenellus* sp. fragments and can thus be correlated with the oncolite-bearing Buelna Formation. Other index fossils found in SJG, such as molluscs *Hyolithes* and *Haplophrentis* and sponge-like spicules of *Chancelloria* and *Diagoniella*, are also found in the SW USA (Levi-Setti, 1995; Nardin *et al*., 2009; Cuen *et al*., 2013). The correlation between the Chihuarruita Hill and the Caborca region can be conceived as an extension of southern, Cambrian marine environments of Laurentia.

6. Conclusions

The overall geology of Chihuarruita Hill, the fossil content of the succession, and the composition of the rocks and their components is interpreted as a shallow, marginal marine carbonate platform, perhaps with a protected, back reef lagoon-type of setting, which is consistent with the studies by Cuen *et al*. (2016). Sand banks could have formed, given the intercalations with storm-deposited sandstones. Warm temperatures are thought to have enhanced carbonate deposition in waters with normal salinity (~3.5 %) and a steady source of Ca^{2+} and carbonate ions. The oncolites of SJG, are visually abundant in one rock unit of the Buelna Formation, but are known from northern localities in Sonora, and are similar to Cambrian oncolites from SW USA. They were important components of a larger biotic association in ecosystems that covered hundreds of square kilometers in the southern shores of Laurentia. Abundant skeletal grains in the limestone matrix and within oncolites depict a diverse fauna of a mature ecosystem with well established trophic chains. The absence of complete bodies of animals in the oncolitic limestone may indicate that the sediment was reworked in high energy, wave environment, where perhaps living metazoans were absent most of the time. Perhaps less metazoan grazing occurred in that area of the carbonate bank, allowing the oncolites to attain large diameters (44 mm). They formed clast-supported conglomerates in coastal facies of shallow marine environments through active nucleation around skeletal grains, promoted by microbial growth and carbonate precipitation. Microscopic features that resemble biological remains, such as coherent filamentous biofilms that are found within the oncolites, are consistent with a biological origin of the structures.

Trilobites, brachiopods, eocrinoids, sponges (hexactinellid) and molluscs (hyolitids) are found in strata that represent tenths of millions of years of deposition. Some index fossils (*e.g. Bristolia* sp., *Olenellus* sp.) indicate an age of ~510 Ma. The overall geology of the Chiuharruita Hill depicts a coastal paleoenvironment, with clastic shores and a carbonate, off-shore platform. The amount of carbonate suggests tropical, warm and well oxygenated waters (Cuen *et al*., 2016), and clastic sediments represent offshore platform environments. The oncolites themselves and the associated fauna, especially trilobites and ichnofossils, suggest a continental-scale continuum faunistic province in this part of North America. Further studies of Cambrian oncolites around the world could provide a better view of their extension, paleogeographical distribution, and role in ecology and evolution.

Acknowledgments

Research was funded by CONACyT grant No.165826, UNAM-DGAPA-PAPIIT grant No. IN101512 and ECOS FRANCIA-MEXICO grant No. M13-U01. We thank Kathleen B. Pigg (ASU), Teresa Pi Puig, Laura Luna González, Enoch Ortiz Montejo, Iris Suárez Quijada, Jaime Díaz Ortega, Rafael López Martínez, Margarita Reyes Salas, Sonia Ángeles García, Consuelo Macias Romo, Sergio Cevallos-Ferriz, Leticia Alba Aldave, and Fernando Nuñez Useche (Instituto de Geología, UNAM), David F. Blake (NASA-JPL), Chris Mavris (UCL), José Manuel Saniger Blesa and José Guadalupe Bañuelos (Laboratorio Universitario de Caracterización Espectroscópica - LUCE; Centro de Ciencias Aplicadas y Desarrollo Tecnológico - CCADET, UNAM), and Adriana Espino del Castillo (Rotoplas) for their contributions to this work. We thank Alberto Blanco Piñón and an anonymous reviewer for their useful comments. FCR acknowledges the Posgrado en Biocencias (DICTUS-UNISON) for providing facilities to carry out research aided with financial and technical support from CONACyT project No. 205981.

References

Almazán-Vázquez, E., 1989, El Cámbrico-Ordovícico de Arivechi, en la región centro-oriental del estado de Sonora: Revista del Instituto de Geología, Universidad Nacional Autónoma de México, 8(1), 58–66.

Alshuaibi, A., Duane, M.J., Mahmoud, H., 2012, Microbial-Activated Sediment Traps Associated with Oncolite Formation Along a Peritidal Beach, Northern Arabian (Persian) Gulf, Kuwait: Geomicrobiology Journal, 29(8), 679–696.

Álvaro, J.J., Vennin, E., Moreno-Eiris, E., Perejón, A., Bechstädt, T., 2000, Sedimentary patterns across the Lower–Middle Cambrian transition in the Esla nappe (Cantabrian Mountains, northern Spain): Sedimentary Geology, 137, 43–61.

Baldis, B.A.J., Bordonaro, O.L., 1981, Vinculación entre el Cámbrico del noroeste de México y la Precoordillera Argentina, en Porto Alegre, Brasil, II Congreso Latinoamericano de Paleontología, Annals. 1–10.

Balson, P.S., Taylor, P.D., 1982, Palaeobiology and systematics of large cyclostome bryozoans from the Pliocene Coralline Crag of Suffolk: Palaeontology, 25, 529–554.

Bauld, J., 1981, Geobiological role of cyanobacterial mats in sedimentary environments: production and preservation of organic matter: BMR Journal of Australian Geology and Geophysics, 6, 307–317.

Bayet-Goll, A., Geyer, G., Wilmsen, M., Mahboubi, A., Reza, S., Harami M., 2014, Facies architecture, depositional environments, and sequence stratigraphy of the Middle Cambrian Fasham and Deh-Sufiyan Formations in the central Alborz, Iran: Facies, 60(3), 815–841.

Beraldi-Campesi, H., Mann, D.G., Cevallos-Ferriz, S.R.S., 2015, Life cycle of 70 Ma-old non-marine pennate diatoms: Cretaceous Research, 56, 662–672.

Bish, D.L., Blake, D., Sarrazin, P., Treiman, A.H., Hoehler, T., Hausrath, E.M., Midtkandal, I., Steele, A., 2007, Field XRD/XRF mineral analysis by the MSL CheMin instrument: LPSC XXXVIII, Abstract #1163.

Bordonaro, O.L., 2003, Evolución paleoambiental y paleogeográfica de la cuenca cámbrica de la Precordillera argentina: Revista de la Asociación Geológica Argentina, 58(3), 329–346.

Buick, R., 1990, Microfossil recognition in Archean rocks; an appraisal of spheroids and filaments from a 3500 m.y. old chert-barite unit at North Pole, Western Australia: PALAIOS, 5, 441–459.

Buitrón-Sánchez, B.E., Vachard, D., Almazán-Vázquez, E., Palafox, J.J., 2012, A Carboniferous to lower Permian cratonic sequence exposed in El Tule hills, northeastern Sonora, Mexico: Revista Mexicana de Ciencias Geológicas, 29(1), 39–62.

Buitrón-Sánchez, B., Corona-González, N., Cuen, F.J., Palafox-Reyes, J.J., Ramírez-Guerrero, G., 2016, Icnofósiles del Cámbrico Inferior de San José de Gracia, Sonora: Paleontología Mexicana, 5(1), 33–40.

Cooper, G.A., Arellano, A., Jhonson, J., Okulitch J., Stoyanow, A. Lochman, C., 1952, Cambrian stratigraphy and paleontology near Caborca, northwestern Sonora, México: Smithsonian Miscellaneous Collections, 119(1), 1–178.

Cuen, F.J., Beresi, M.S., Montijo, A., Buitrón, B.E., Minjarez, I., De la O, M., 2013, Chancelloriida Walcott, 1920 y Reticulosa Reid, 1958 del Cámbrico medio de San José de Gracia, Sonora, México: Boletín de la Sociedad Geológica Mexicana, 65(3), 581–590.

Cuen, F.J., Valdez, J.E., Buitrón, B.E., Monreal-Saavedra, R., Sundberg, F., Montijo-González, A., Minjarez-Sosa, I., 2016, Cambrian stratigraphy of San José de Gracia, Sonora, México: El Gavilán Formation, a new middle Cambrian lithostratigraphic unit of open shelf environment: Boletín de la Sociedad Geológica Mexicana, 68(3), 429–441.

Debrenne, F., Gandin, A., Rowland, S.M., 1989, Lower Cambrian bioconstructions in northwestern Mexico (Sonora) - Depositional setting, paleoecology and systematics of archaeocyaths: Geobios, 22(2), 137–195.

Dunlop, J.S.R., Muir, M.D., Milne, V.A., Groves, D.I., 1978, A new microfossil assemblage from the Archaean of Western Australia: Nature, 274, 676–678.

Dupraz, C., Visscher, P.T., 2005, Microbial lithification in marine stromatolites and hypersaline mat: Trends in Microbiology, 13, 429–438.

Elicki, O., Schneider, J., Shinaq, R., 2002, Prominent facies from the Lower/Middle Cambrian of the Dead Sea area (Jordan) and their palaeodepositional significance: Bulletin de la Société Géologique de France, 173, 547–552.

Flügel, E., 2004, Microfacies of Carbonate Rocks. Analysis, Interpretation and Application: Springer-Verlag, Berlin, 976 pp.

Garcia-Pichel, F., Ramirez-Reinat, E., Gao, Q., 2010, Microbial excavation of solid carbonates powered by P-type ATPase-mediated transcellular Ca^{2+} transport: Proceedings of the National Academy of Sciences, 107, 21749–21754.

Gilbert, M.C., Donovan, R.N. (eds), 1982, Geology of the Eastern Wichita Mountains, Southwestern Oklahoma: Oklahoma Geological Survey Guidebook, 21, 160 pp.

Gomez, F.J., Ogle, N., Astini, R.A., Kalin, R.M., 2007, Paleoenvironmental and carbon–oxygen isotope record of Middle Cambrian Carbonates (La Laja Formation) in the Argentine Precordillera: Journal of Sedimentary Research, 77, 826–842.

Halley, R.G., 1975, Peritidal lithologies of Cambrian carbonate islands, Carrara Foramtion southern Great Basin, *in* Ginsburg, R.N. (ed.): Tidal Deposits, Springer, Berlin, 279–288.

Henderson, J.B., 1975, Archean Stromatolites in the Northern Slave Province, Northwest Territories, Canada: Canadian Journal of Earth Sciences, 12(9), 1619–1630.

Hicks, M., Rowland, S.M., 2009, Early Cambrian microbial reefs, archaeocyathan inter-reef communities, and associated facies of the Yangtze Platform: Palaeogeography, Palaeoclimatology, Palaeoecology, 281(1–2), 137–153.

Hillmer, G., Scholz, J., Wolf-Christian, D., 1996, Two types of bryozoan nodules from the Gulf of Aqaba, Red Sea, *in* Gordon, D.P., Smith, A.M., Grant-Mackie, J.A. (eds.): Bryozoans in Space and Time, NIWA, Wellington, 125–130.

Hose, R.K., 1961, Physical characteristics of Upper Cambrian stromatolites in western Utah: US Geological Survey, Professional Paper, 424-D, Washington, USA, 245–248.

Johnson, J.H., 1952, *Girvanella*, *in* Cooper, G.A., Arellano, A.R.V., Johnson, J. H., Okulitch, V.J., Stoyanow, A., Lochman, C. (eds.). Cambrian stratigraphy and paleontology near Caborca, northwestern Sonora, Mexico: Smithsonian Miscellaneous Collections, 119(1), 24–26.

Kah, L.C., Riding, R., 2007, Mesoproterozoic carbon dioxide levels inferred from calcified cyanobacteria: Geology, 35, 799–802.

King, R.E., 1940, Pre-Tertiary history of the Sierra Madre Occidental of Sonora and Chihuahua and some adjacent parts of central Sonora, México: Sexto Congreso Científico, Proceedings, 1, 217–222.

Knoll, A.H., Swett, K., Burkhardt, E., 1989, Paleoenvironmental Distribution of Microfossils and Stromatolites in the Upper Proterozoic Backlundtoppen Formation, Spitsbergen: Journal of Paleontology, 63(2), 129–145.

Laval, B., Cady, S.L., Pollack, J.C., McKay, C.P., Bird, J.S., Grotzinger, J.P., Ford, D.C., Bohm, H.R., 2000, Modern freshwater microbialite analogues for ancient dendritic reef structures: Nature, 407(6804), 626–629.

Levi-Setti, R., 1995, Trilobites: The University of Chicago Press, 2nd ed., 342 pp.

Lowe, D.R., 1983, Restricted shallow-water sedimentation of Early Archean stromatolitic and evaporitic strata of the Strelley Pool Chert, Pilbara block, Western Australia: Precambrian Research, 19, 239–283.

McMenamin, N.M., 1985, Basal Cambrian small shelly fossils from La Ciénega Fm. NW, Sonora: Journal of Paleontology, 59, 1414–1425.

McMenamin, N.M., 1987, Lower Cambrian zonation and correlation of the Puerto Blanco, Fm. Sonora: Journal of Paleontology, 4, 738–749.

Nardin, E., Almazán-Vázquez, E., Buitrón-Sánchez, B.E., 2009, First report of *Gogia* (Eocrinoidea, Echinodermata) from de Early-Middle Cambrian of Sonora (México), with bioestratigraphical and palaecological comments: Geobios, 42, 233–242.

Nicholson, H.A., Etheridge, R., 1878, Silurian fossils of the Girvan District in Ayrshire. With special reference to those contained in the "Grey Collection": William Blackwood and Sons, Fasciculus 1, Edinburgh and London, 135 pp.

Palmer, A.R., Halley, R.B., 1979, Physical stratigraphy and trilobite biostratigraphy of the Carrara Formation (Lower and Middle Cambrian) in the southern Great Basin: US Geological Survey, Professional Paper, 1047 pp.

Perejón, A., Moreno-Eiris, E., Bechstädt, T., Menéndez, S., Rodríguez-Martínez, M., 2012, New Bilbilian (Early Cambrian) archaeocyath-rich thrombolitic microbialite from the Láncara Formation (Cantabrian Mts., northern Spain): Journal of Iberian Geology, 38, 313–330.

Peryt, T.M., 1981, Phanerozoic oncoids: an overview: Facies, 4, 197–214.

Pickford, M., Senut, B., Hipondoka, M., Person, A., Segalen, L., Plet, C., Jousse, H., Mein, P., Guerin, C., Morales, J., Mourer-Chauvire, C., 2009, Mio-Plio-Pleistocene geology and palaeobiology of Etosha Pan, Namibia: Communications of the Geological Survey of Namibia, 14, 95–139.

Planavsky, N., Reid, P., Lyons, W., Myshrall, L., Visscher, P., 2009, Formation and diagenesis of modern marine calcified cyanobacteria: Geobiology, 7, 566–576.

Powell, W.G., Johnston, P.A., Collom, C.J., Johnston, K.J., 2006, Middle Cambrian brine seeps on the Kicking Horse Rim and their relationship to talc and magnesite mineralization and associated dolomitization, British Columbia, Canada: Economic Geology, 101, 431–451.

Rees, M.N., 1986, A fault-controlled trough through a carbonate platform: The Middle Cambrian House Range embayment: Geological Society of America Bulletin, 97, 1054–1069.

Rees, M.N., Pratt, B.R., Rowells, A.J., 1989, Early Cambrian reefs, reef complexes, and associated lithofacies of the Shackleton Limestone, Transantarctic Mountains: Sedimentology, 36, 341–361.

Reimer, T.O., 1975, Paleogeographic significance of the oldest known oolite pebbles in the Archaean Swaziland Supergroup (South Africa): Sedimentary Geology, 14(2), 123–133.

Rezak, R., 1957, *Girvanella* not a guide to the cambrian: Bulletin of the Geological Society of America, 68, 1411–1412.

Rider, J., Enrico, R., 1979, Structural and functional adaptations of mobile anascan ectoproct colonies (ectoproctaliths), *in* Larwood, G.P., Abbott, M.B. (eds.): Advances in Bryozoology Systematics Association, Special Volume 13, Academic Press, London, 297–319.

Riding, R., 1975, *Girvanella* and other algae as depth indicators: Lethaia, 8, 173–179.

Riding, R., 1977, Calcified *Plectonema* (blue–green algae), a recent example of *Girvanella* from Aldabra Atoll: Palaeontology, 20, 33–46.

Riding, R., 2006, Cyanobacterial calcification, carbon dioxide concentrating mechanisms, and Proterozoic–Cambrian changes in atmospheric composition: Geobiology, 4, 299–316.

Riva, J., Ketner, K.B., 1989, Ordovician graptolites from the northern Sierra de Cobachi, Sonora, Mexico: Transactions of the Royal Society of Edinburgh, Earth Sciences, 80, 71–90.

Rivera-Carranco, E., 1988a, Condiciones Paleoambientales de depósito de las Formaciones Cámbricas del área de Caborca, Sonora: Revista Mexicana de Ciencias Geológicas, 7(1), 22–27.

Rivera-Carranco, E., 1988b, Génesis de la Formación Proveedora (Cámbrico Inferior) del área de Caborca, Sonora: noroccidental: Revista Mexicana de Ciencias Geológicas, 7(2), 163–167.

Robison, R.A., 1965, Middle Cambrian Eocrinoids from Western North America: Journal of Paleontology, 39, 355–364.

Sander, S.G., Koschinsky, A., 2011, Metal flux from hydrothermal vents increased by organic complexation: Nature Geoscience, 4(3), 145–150.

Scholz, J., 2000, A field theory of bryozoans, microbial mats and sediment surfaces: Proceedings of the Senckenberg Nature Research, Waldemar Kramer, Gesellscaft, Frankfurt, 552, 1–193.

Schopf, J.W., 1993, Microfossils of the early Archean Apex Chert—new evidence of the antiquity of life: Science, 260, 640–646.

Schopf, J.W., Kudryavtsev, A.B., 2009, Confocal laser scanning microscopy and Raman imagery of ancient microscopic fossils: Precambrian Research, 173, 39–49.

Scotese, C.R., 2002, http://www.scotese.com, (PALEOMAP website), *viewed in* September, 2016.

Shepard, R.N., Sumner, D.Y., 2010, Undirected motility of cyanobacteria produces reticulate mats: Geobiology, 8, 179–190.

Shinaq, R., Bandel, K., 1992, Microfacies of Cambrian Limestones in Jordan: Facies, 27(1), 263–283.

Sim, M.S., Liang, B. Petroff, A.P., Evans, A., Klepac-Ceraj, V., Flannery, D.T., Walter, M.R., Bosak, T., 2012, Oxygen-Dependent Morphogenesis of Modern Clumped Photosynthetic Mats and Implications for the Archean Stromatolite Record: Geosciences, 2, 235–259.

Sprinkle, J., 1973, Morphology and evolution of blastozoan echinoderms: Harvard University, Museum of Comparative Zoology Special Publication, 1–284.

Stewart, J.H., McMenamin, A.S., Morales-Ramirez, J.M., 1984, Upper Proterozoic and Cambrian Rocks in the Caborca Region, Sonora, México. Physical Stratigraphy, Biostratigraphy, Paleocurrent Studies and Regional relations: US Geological Survey Professional Paper 1309, 36 pp.

Stewart, J.H., Amaya-Martínez, R., Palmer, A.R., 2002, Neoproterozoic and Cambrian strata of Sonora, México: Rodinian supercontinent to Laurentian Cordilleran margin, *in* Barth, A. (ed.), Crustal evolution in the southwest USA: Geological Society of America Special Paper 365, 5–48.

Theis, T.L., Singer, P.C., 1974, Complexation of iron(III) by organic matter and its effect on iron(II) oxygenation: Environmental Sciences and Technology, 8, 569–572.

Wade, B.D., Garcia-Pichel, F., 2003, Evaluation of DNA Extraction Methods for Molecular Analyses of Microbial Communities in Modern Calcareous Microbialites: Geomicrobiology Journal, 20(6), 549–561.

Walter, M.R., 1972, Stromatolites and the biostratigraphy of the Australian Precambrian and Cambrian: Special Papers in Palaeontology, 11, 1–190.

Wilmeth, D.T., Corsetti, F.A., Bisenic, N., Dornbos, S.Q., Oji, T., Gonchigdorj, S., 2015, Punctuated growth of microbial cones within Early Cambrian oncoids, Bayan Gol Formation, Western Mongolia: Palaios, 30(12), 836–845.

Winsborough, B.M., Seeler, J.S., Golubic, S., Folk, R.L., Maguire, Jr. B., 1994, Recent fresh-water lacustrine stromatolites, stromatolitic mats and oncoids from northeastern Mexico, *in* Bertrand-Sarfati, J., Monty, C.L.V. (eds.) Phanerozoic Stromatolites II. The Netherlands: Kluwer Academic Publishers, 71–100.

Wood, A., 1957, The type-species of the genus *Girvanella* (Calcareous algae): Palaeontology, 1(1), 22–28.

Youngs, B.C., 1978, The petrology and depositional environments of the Middle Cambrian Wirrealpa and Aroona Creek limestones (South Australia): Journal of Sedimentary Petrology, 48, 63–74.

Zhang, W., Shi, X., Jiang, G., Tang, D., Wang, X., 2015, Mass-occurrence of oncoids at the Cambrian Series 2–Series 3 transition: Implications for microbial resurgence following an Early Cambrian extinction: Gondwana Research, 28, 432–450.

Zonneveld, K.A.F., Versteegh, G.J.M., Kasten, S., Eglinton, T.I., Emeis, K.C., Huguet, C., Koch, B.P., De Lange, G.J., De Leeuw, J.W., Middelburg, J.J., Mollenhauer, G., Prahl, F.G., Rethemeyer, J., Wakeham, S.G., 2010, Selective preservation of organic matter in marine environments; processes and impact on the sedimentary record: Biogeosciences, 7, 483–511.

Manuscript received: May 6, 2018.
Corrected manuscript received: June 3, 2018.
Manuscript accepted: June 4, 2018.

Supplementary materials

Figure S1. Examples of fossils and ichnofossils from the Chihuarruita Hill in SJG. Their stratigraphical distribution is indicated in Fig. 2 of the main text. A. Cast of the trilobite *Elrathina antiqua* Palmer and Halley, 1979. B. Torax and pigidium of *E. antiqua*. C. Cranidia and torax of E. antiqua. D. *Pentagnostus* (*Meragostus*) *bonnerensis* (Resser, 1939) Naimark, 2012. E. Thorax and pygidium of the trilobite *Oryctocephalites walcotti*. F. Burrows of *Palaeophycus* isp. in oblique view. G. Galleries of *Skolithos* isp. in cross view. H. Plan view of *Arenicolites* isp. burrows. I. Galleries of *Thalassinoides* isp. J. Large *Skolithos* isp. gallery. K–L. Plan view of *Asterosoma* isp. burrows. M. Plan view of a *Skolithos* isp. gallery. N. Complete skeleton of a large *Elrathina antiqua*. O. Skeleton of the trilobite *Ptychagnostus praecurrens*. P. Oblique view of *Skolithos* isp. standing up from the eroded matrix. Q. *Arenicolites* isp. in vertical cross section.

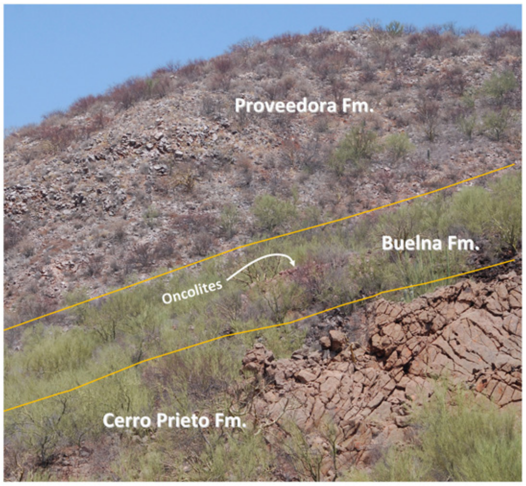

Figure S2. Field view of the Proveedora, Buelna, and Cerro Prieto formations. An oolitic block of the Cerro Prieto Fm. stands in the lower right, followed by inclined terrain of the Buelna Fm. that extends > 120 m before coming in contact with the Proveedora Fm. at its base. The massive oncolitic limestone unit can be seen close to the Buelna-Cerro Prieto contact.

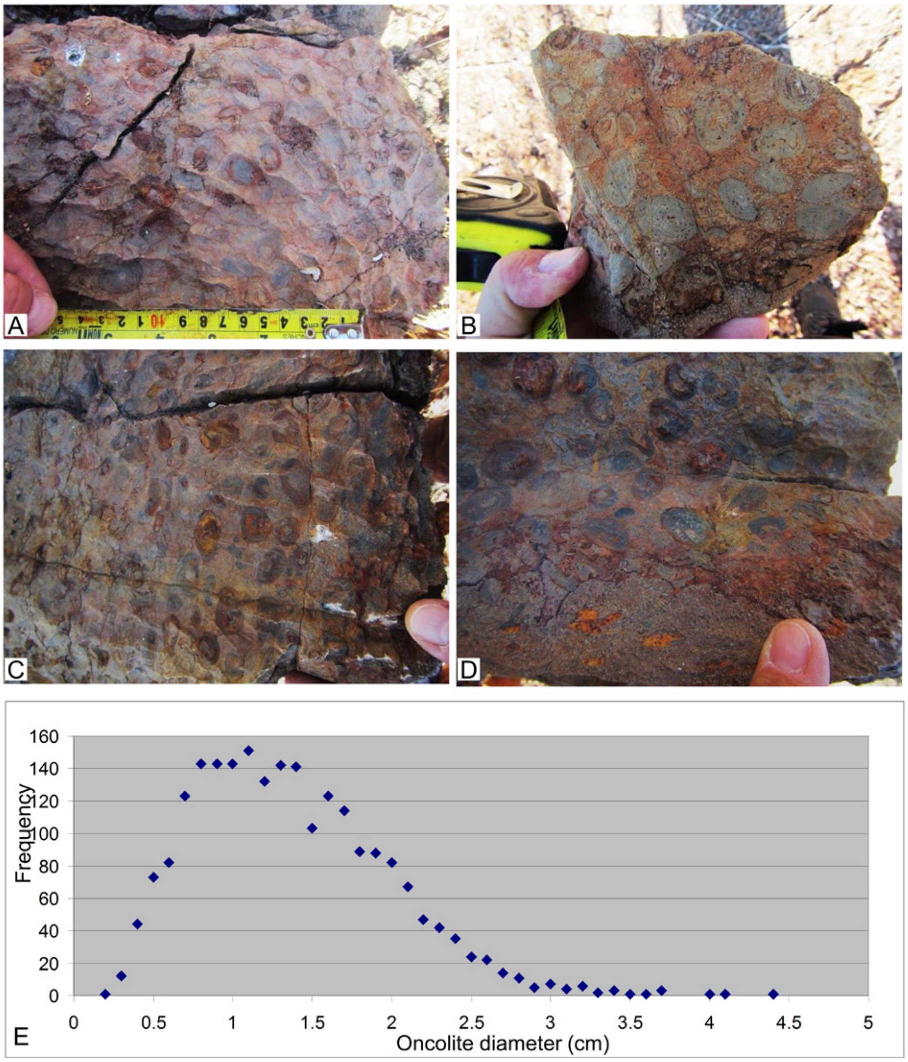

Figure S3. Field view of oncolites. A. Clast-supported oncolites. B. Matrix-supported oncolites. C. Graded oncolites. The base of the stratum is to the right and it grades up in size to the top (left). D. Oncolites in a packstone matrix, overlying a ferruginous sandstone bank. E. Frequency distribution of oncolite diameters (n = 2226).

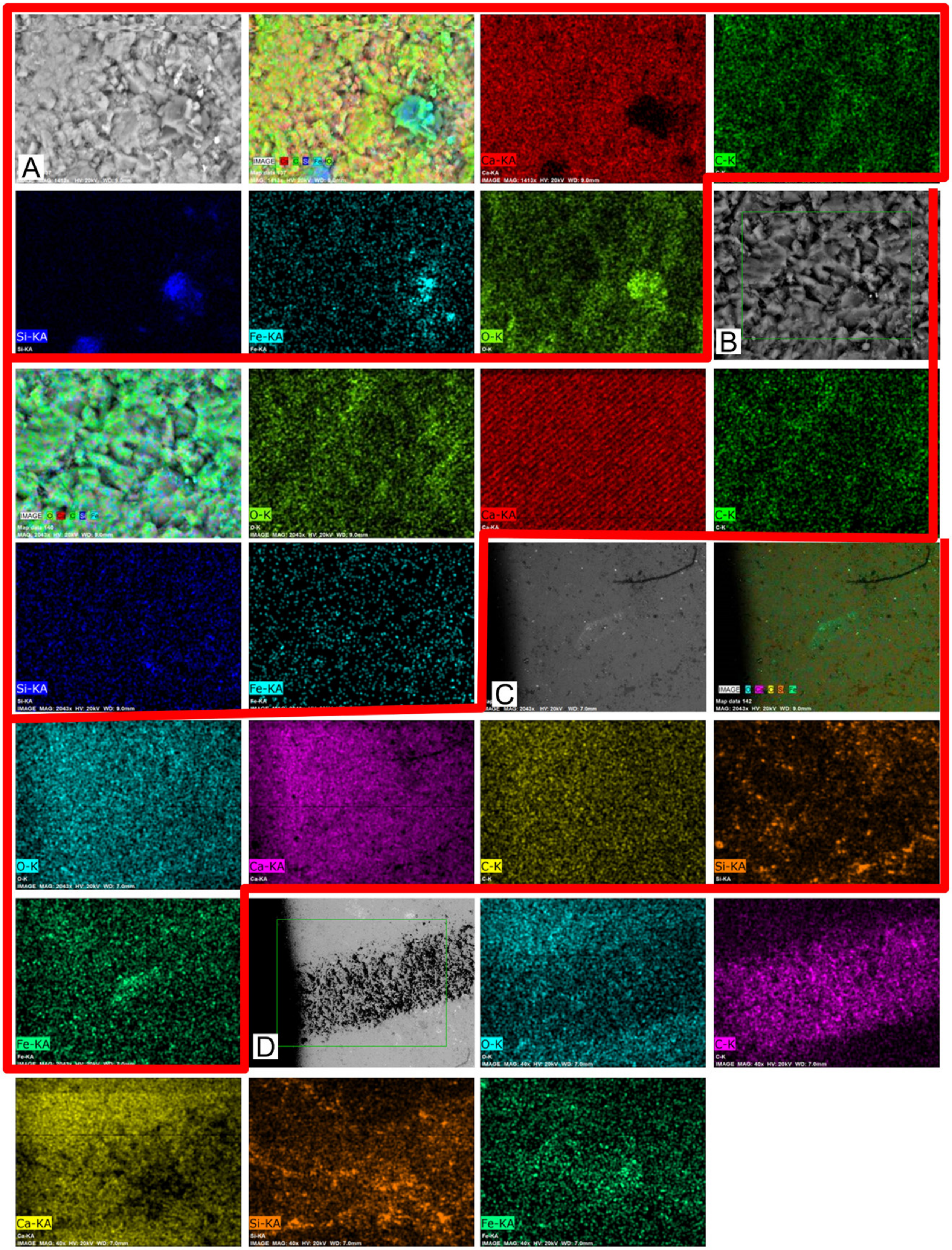

Figure S4. EDX spectra obtained with an electron microscope (see methods). Colors show the spectral composition of chemical elements. A. Silicified structures in the matrix of the rock between oncolites. B. Filament-like structures found in the matrix, outside an oncolite. C. Fe-rich structures in the rock matrix between the oncolites. D. Pencil strike on a clear portion (no skeletal or detrital fragments at the surface) of the limestone matrix to show the signal of graphite.

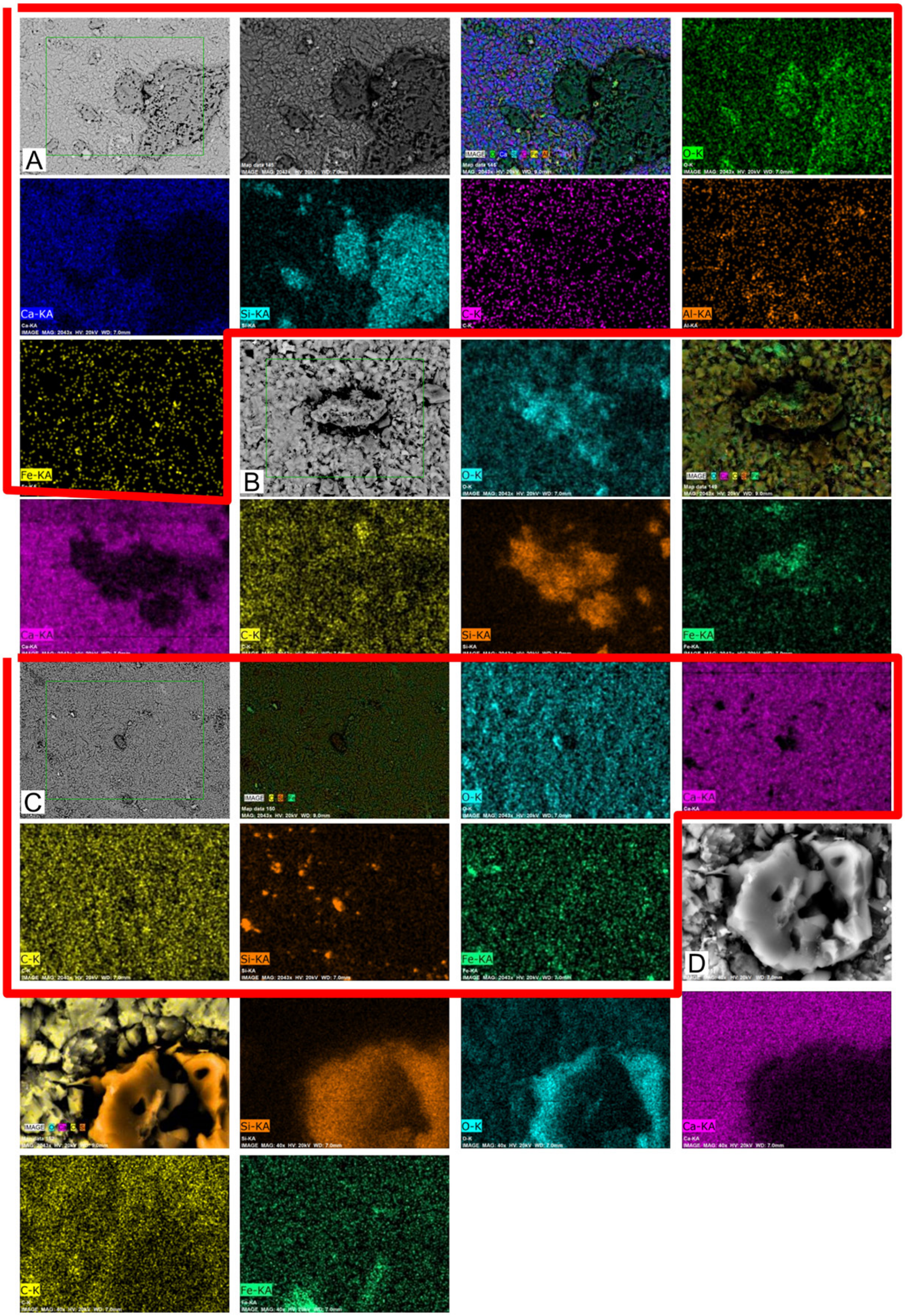

Figure S5. EDX spectra obtained with an electron microscope (see methods). Colors show the spectral composition of chemical elements. A. Silicified blobs found in the rock matrix between oncolites. B. Ellipsoidal structure rich in silica and iron, found in the rock matrix. C. General view of Si-rich and Fe-rich scattered objects shown in B. D. Close up of a silicified filamentous structure in cross section. Figure 14 L–R shows details of these structures.

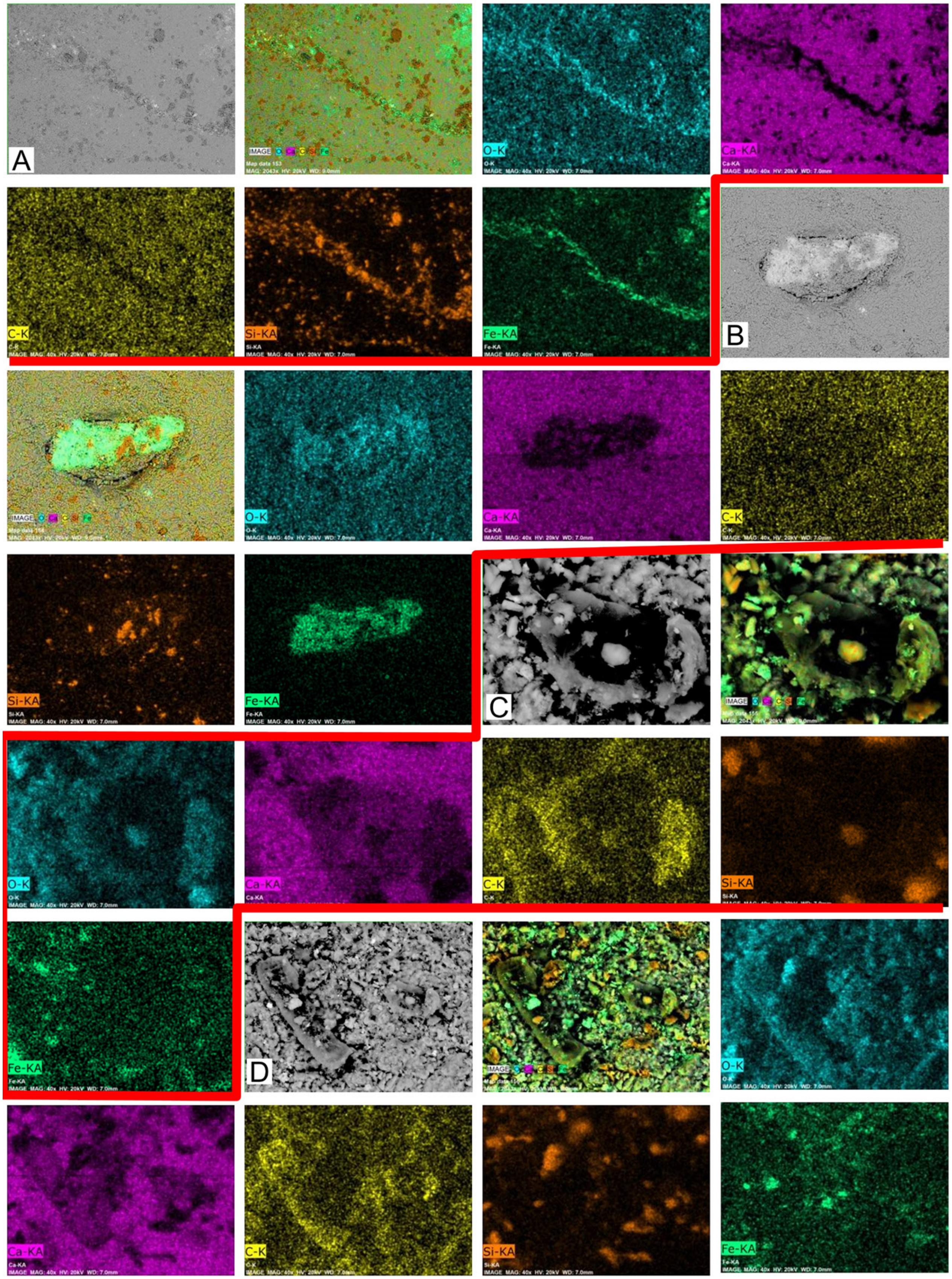

Figure S6. EDX spectra obtained with an electron microscope (see methods). Colors show the spectral composition of chemical elements. A. Section of an Fe-rich and Si-rich lamina of an oncolite, sandwiched between thicker calcitic laminae. B. Fe-rich structures within the oncolite lamination. C. Calcitic, filament-like structure in cross section, with a silicified nucleus. D. Carbonaceous structure loosely attached to the surface of the oncolitic matrix.

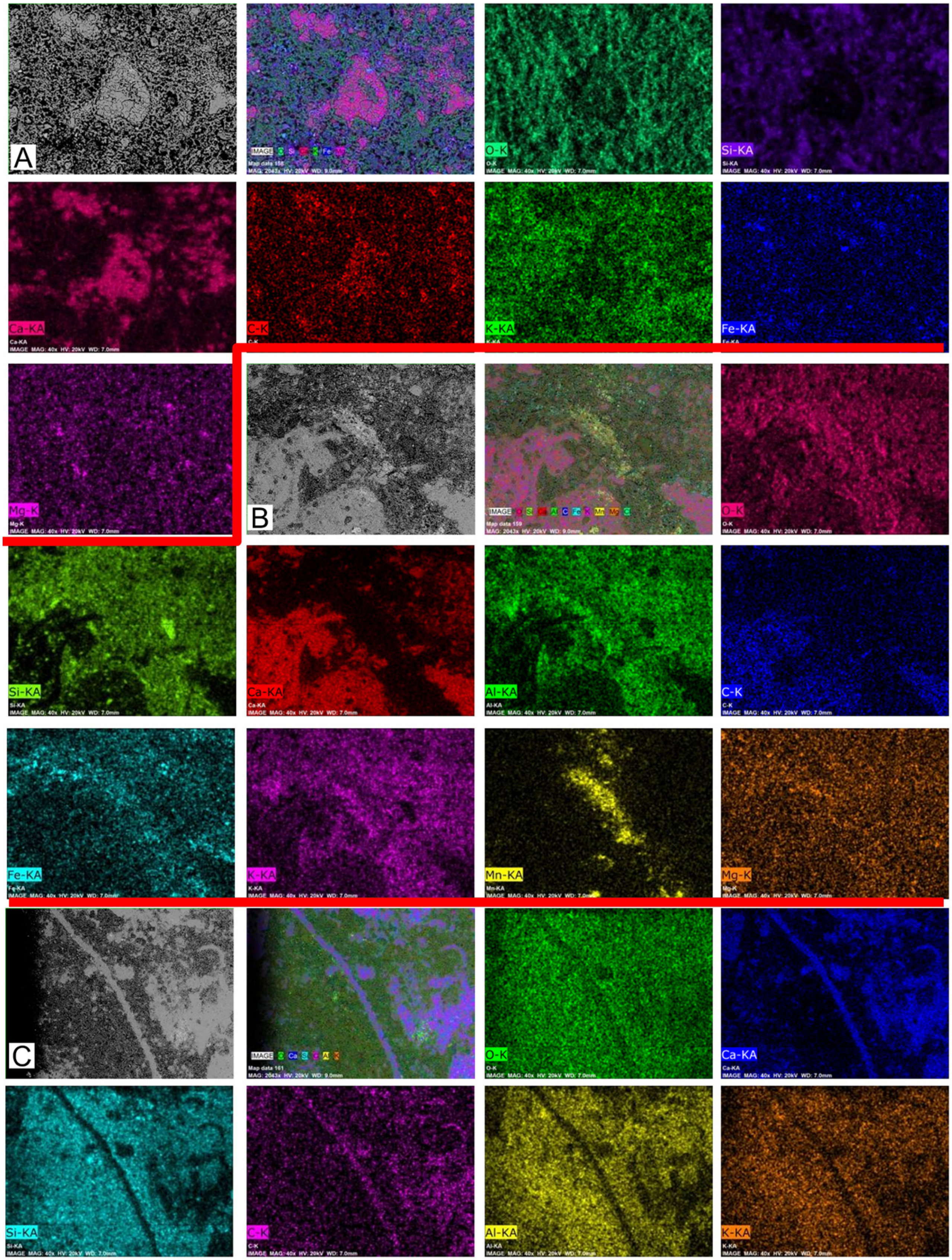

Figure S7. EDX spectra obtained with an electron microscope (see methods). Colors show the spectral composition of chemical elements. A. Ca-rich structures within a K-rich portion of the oncolitic matrix. B. Ca-rich skeletal particles within a portion of silicified matrix rich in Al and K. Note a Mn-rich particle at the center of the image. C. Calcitic skeletal grains embedded in a Si-Al-K-rich portion of the rock matrix.

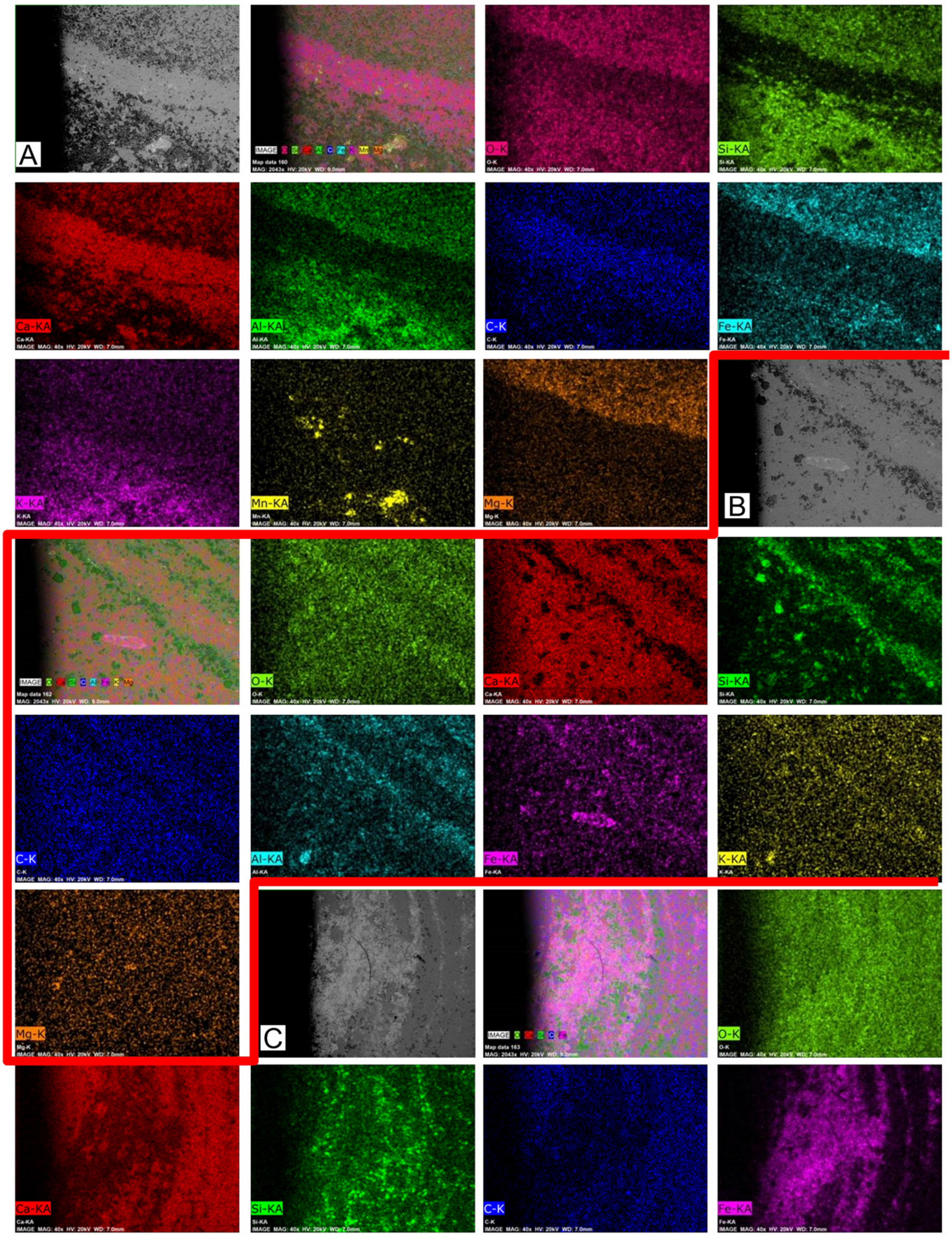

Figure S8. EDX spectra obtained with an electron microscope (see methods). Colors show the spectral composition of chemical elements. A. Oncolitic lamination showing calcitic laminae within a silicified portion of the oncolite, and scattered Mn-rich particles. B. Contrary to A, some lamination of the oncolites appeared rich in silica, and surrounded by a calcitic matrix. C. Fe-rich laminae of an oncolite surrounded by a calcitic matrix.

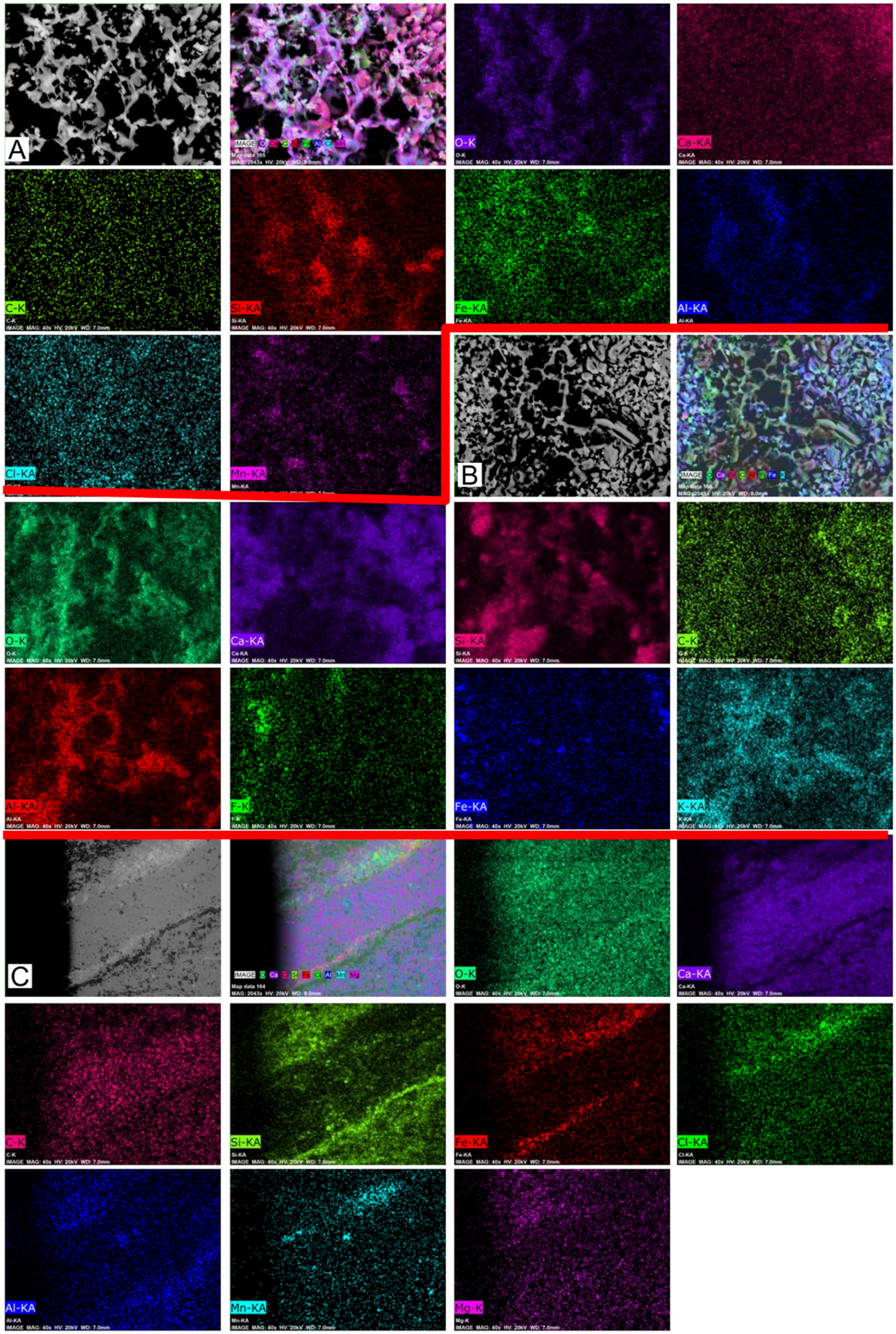

Figure S9. EDX spectra obtained from the oncolitic lamination. Colors show the spectral composition of chemical elements. A. Silicified reticulated structures within an oncolite. B. Another reticulated structure enriched in Al. C. Si- and Fe-rich lamination within an oncolite.

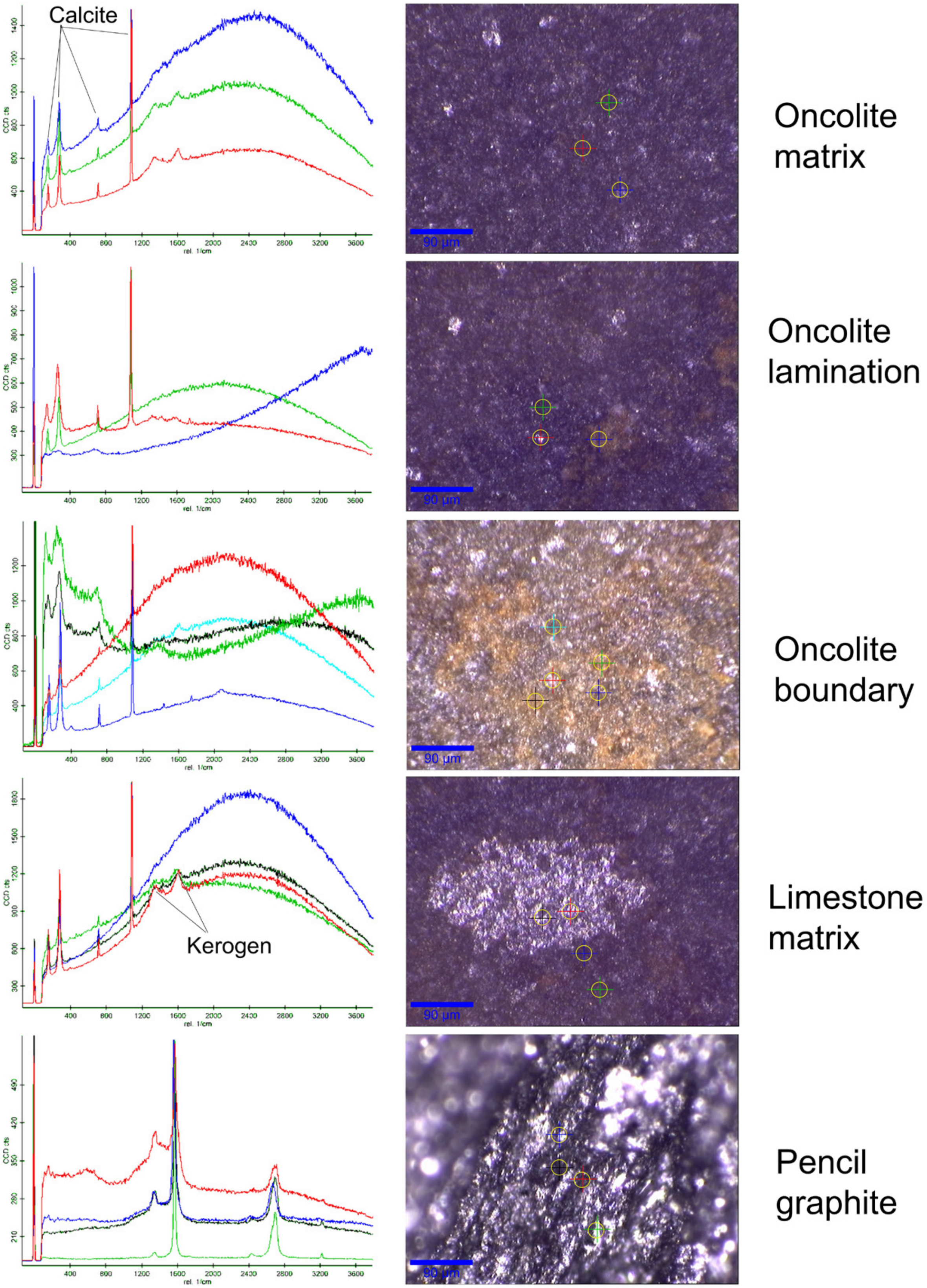

Figure S10. Raman spectra of different areas within the oncolite lamination, the limestone matrix, and pencil graphite to show the signal of kerogenous material within the rock samples. Colored circles on images indicate the measured points. Scale bars on images = 90 µm.

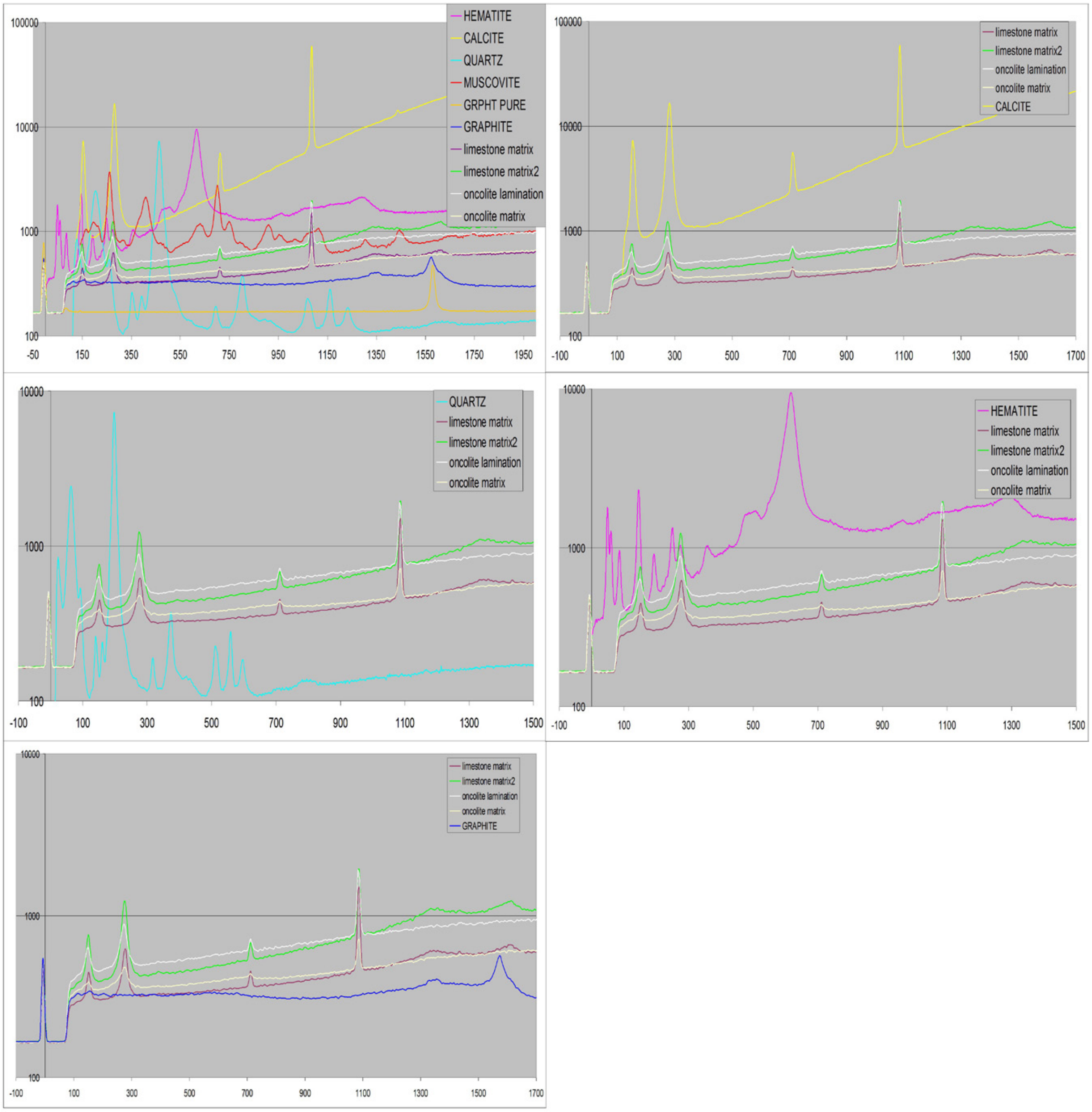

Figure S11. Raman spectra of standard minerals and samples from San José de Gracia. Standard curves *vs.* physical standard.

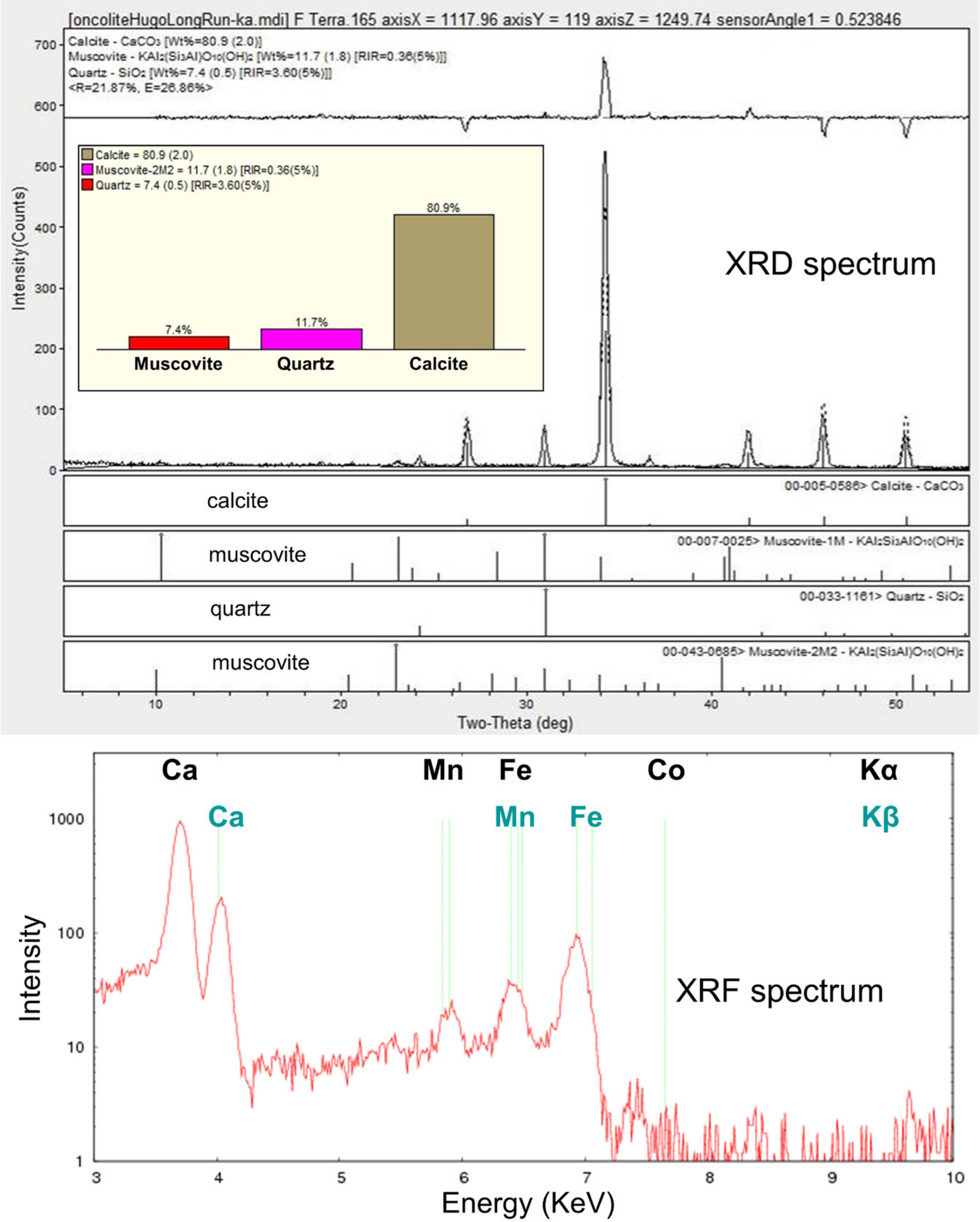

Figure S12. XRD and XRF analyses of a powdered oncolite. More than 80% is calcite, with minor amounts of quartz and muscovite. Ca, Mn, and Fe were present as impurities. XRF indicated the presence of Ca, Mn, Fe and Co.

PALEONTOLOGÍA MEXICANA
VOLUMEN 7, NÚM. 1, 2018, P. 57 – 72

Micropaleontological study of Lower Cretaceous rocks (Barremian-Albian) near La Soledad, Nuevo León, northeastern Mexico

Alejandro Monier-Castillo[a,*], Isabel López-Palomino[b], Julio Reyes Romo-Ramírez[c], Arturo Palma-Ramírez[b], Diana Contreras-Cruz[d]

[a] Léxico Estratigráfico de México, Gerencia Regional Sur, Servicio Geológico Mexicano, Desviación a San Lorenzo Cacaotepec km 0.5 San Pablo Etla, C.P. 68258, Oaxaca, México.
[b] Léxico Estratigráfico de México, Departamento de Estratigrafía, Servicio Geológico Mexicano, Blvd. Felipe Ángeles km. 93.50-4, Col. Venta Prieta, C.P. 42083, Pachuca, Hidalgo, México.
[c] Gerencia Regional Centro, Servicio Geológico Mexicano, Av. Mariano Jiménez 465, Col. Alamitos, C.P. 78280, San Luis Potosí, S.L.P., México.
[d] Instituto de Geología, Universidad Nacional Autónoma de México, Ciudad Universitaria, C.P. 04510, Ciudad de México, México.

[*] alejandromonier@sgm.gob.mx

Abstract

A micropaleontological study was conducted to provide information about the microfossil fauna in the Lower Cretaceous rocks of the Cupido, La Peña, and Cuesta del Cura formations cropping out near the town of La Soledad, southern of Nuevo León state. For the Cupido Formation were recognized the Barremian-middle Aptian *Globigerinelloides blowi*, *Hedbergella sigali*, *H. similis*, *H. roblesae*, and *Hedbergella* sp. For the La Peña Formation the association comprises the late Aptian *Globigerinelloides ferreolensis*, *Paraticinella rohri* (= *Ticinella bejaouaensis*), *Hedbergella* sp., *H. sigali*; and other pelagic microfossils such as *Microcalamoides diversus* and *Colomiella recta*. In the Cuesta del Cura Limestone we recorded *Muricohedbergella delrioensis*, *Bishopella ornelasae*, *B. alata*, *Ticinella* sp., and *Favusella washitensis*, Albian in age, in association with calcareous-hyaline calcispheres and *Microcalamoides diversus*. The micropaleontological analysis allows clarifying the stratigraphy of the study area. The information presented will contribute to a better known of the microfauna studied and therefore of paleoenvironmental conditions, under which these rocks were deposited. In addition, this study will allow correlations to local and regional level.

Keywords: Microfossils, Barremian-Albian, Nuevo León, Mexico.

Resumen

Se realizó un estudio micropaleontológico para proporcionar información sobre los microfósiles presentes en las rocas del Cretácico Inferior de las formaciones Cupido, La Peña y Cuesta del Cura; expuestas cerca de La Soledad, al sur del estado de Nuevo León. Para la Formación Cupido se reconocieron Globigerinelloides blowi, Hedbergella sigali, H. similis, H. roblesae y Hedbergella sp. del Barremiano-Aptiano medio. Para la Formación La Peña la asociación comprende Globigerinelloides ferreolensis, Paraticinella rohri (= Ticinella bejaouaensis), Hedbergella sp., H. sigali; y otros microfósiles pelágicos como Microcalamoides diversus y Colomiella recta, correspondientes al Aptiano tardío. En la Caliza Cuesta del Cura se registraron Muricohedbergella delrioensis, Bishopella ornelasae, B. alata, Ticinella sp. y Favusella washitensis, del Albiano; asociadas a calcisferas hialinas calcáreas. El análisis micropaleontológico permite aclarar la estratigrafía del área de estudio. La información presentada aquí, contribuirá a una mejor comprensión de la microfauna y, por lo tanto, de las condiciones paleoambientales bajo las cuales se depositaron estas rocas, además de permitir establecer correlaciones a nivel local y regional.

Palabras clave: Microfósiles, Barremiano-Albiano, Nuevo León, México.

1. Introduction

In Mexico, Lower Cretaceous rocks are outstanding from the stratigraphic and paleontological point of view. Due to their extensive outcrops and rich fossil content, these rocks allow performing detailed studies on their fauna. The recognition of the stratigraphic distribution of these fossil-bearing units is very useful for accurate determination of the age of the rocks. In particular, the simultaneous use of different groups increases the resolution and reliability of the geological and paleontological interpretations, and therefore the global and regional biostratrigraphic correlations. For chronostratigraphic purposes, planktonic foraminifers are among the most important groups of microfossils used in biostratigraphic studies. In the south-central portion of the state of Nuevo León, Lower Cretaceous rocks have been the subject of stratigraphic and paleontological studies, highlighting among the latter those carried out by Méndez-Franco (2003), Barragán-Manzo and Méndez-Franco (2005), and Ángeles-Villeda *et al*. (2005). Ángeles-Villeda *et al*. (2005) recognized the Cupido, Tamaulipas Superior, Cuesta del Cura, Agua Nueva, and San Felipe formations based on the microfacies and the micropaleontological associations, identified a platform, upper slope, and basin paleoenvironments with abundant benthic foraminifers, rudists, ostracods, echinoderms and algae; slope with predominance of planktonic foraminifers, radiolarians, ostracods; and basin with planktonic foraminifers, radiolarians, echinoderms and mollusks. Around six years ago, a field campaign was carried out by geological field survey mappers from the Mexican Geological Survey (SGM by its Spanish initials) where the microfossils herein studied were collected. The rock for thin-sections collection was performed without bed by bed sampling control. However, the samples were taken considering the position within the Cupido, La Peña, and Cuesta del Cura formations, such as lower, middle, and upper parts of each studied unit. Despite the lack of bed by bed sampling control, the microfossil herein studied are interesting for several reasons among them: the first time that planktonic microfossils are reported in the studied area, their presence allowed to corroborate chronostratigraphically the age of the lithological units, and furthermore, this age control will provide baseline data for forthcoming micropaleontological studies. The purpose of this work was to identify the microfossil fauna present in the outcrops of the Cupido, La Peña, and Cuesta del Cura formations exposed at Los Mimbres, southeastern Nuevo León state. The biostratigraphic information obtained from this microfauna, besides the geological framework established in the studied units, will be useful for subsequent correlation with other areas, as well as in paleogeographic reconstructions.

2. Study area

The study area is located in a mountain range in the southern part of the Nuevo León state, northeastern Mexico, between 24°02’13”-24°02’16” North and 100°02’54”-100°03’16” West. The studied rocks are exposed at Los Mimbres locality, placed in the neighborhood of La Soledad town, approximately 1100 m to the south of Los Mimbres stream (Figure 1). Geologically, it belongs to the physiographic sub-province of the Sierras Bajas, which is part of the Sierra Madre Oriental Province (Raisz, 1964).

3. Materials and methods

The material analyzed come from 3 stratigraphic outcrops measured and sampled in Los Mimbres, Nuevo León. The 15 rock hand samples were collected from each section, exercising caution of the lithological features and stratigraphical relations among sequences. The micropaleontological study was carried out on 30 thin sections from limestone samples. These thin sections were prepared by SGM’s staff at Centro Experimental Oaxaca and later examined using a petrographic microscope in order to determine its micropaleontological content. In this study, we followed the criteria of Caron (1985), Sliter (1989), Premoli-Silva and Verga (2004), Huber and Leckie (2011), and Ando *et al*. (2013) for Cretaceous planktonic foraminifers. In the case of colomielids, we followed Trejo (1975, 1980); while for calcisphaerulids and Microcalamoides we adopt Trejo (1983).

4. Results

4.1. Lithostratigraphy

Geological units exposed in the studied area correspond to the Cupido, La Peña, and Cuesta del Cura formations (Figure 2).

The Cupido Formation. Imlay (1937) named the Cupido limestone from later Hauterivian-Barremian rocks in the middle and west parts of the Sierra de Parras, Coahuila. Humphrey (1949) included Imlay’s lower limestone member of the La Peña Formation within this unit, and Humphrey and Díaz (2003) redefined it as the Cupido Formation. Based on the stratigraphic position of this formation, Mayer-Pérez (1967) and Humphrey and Díaz (2003) proposed a Barremian-early Aptian, and Hauterivian-late Aptian age, respectively. According to its paleontological content, Hauterivian-Aptian age has been assigned by PEMEX (1988) and Ángeles-Villeda *et al*. (2005); while Barragán-Manzo and Díaz-Otero (2004) assigned a Barremian-early Aptian age. At Los Mimbres,

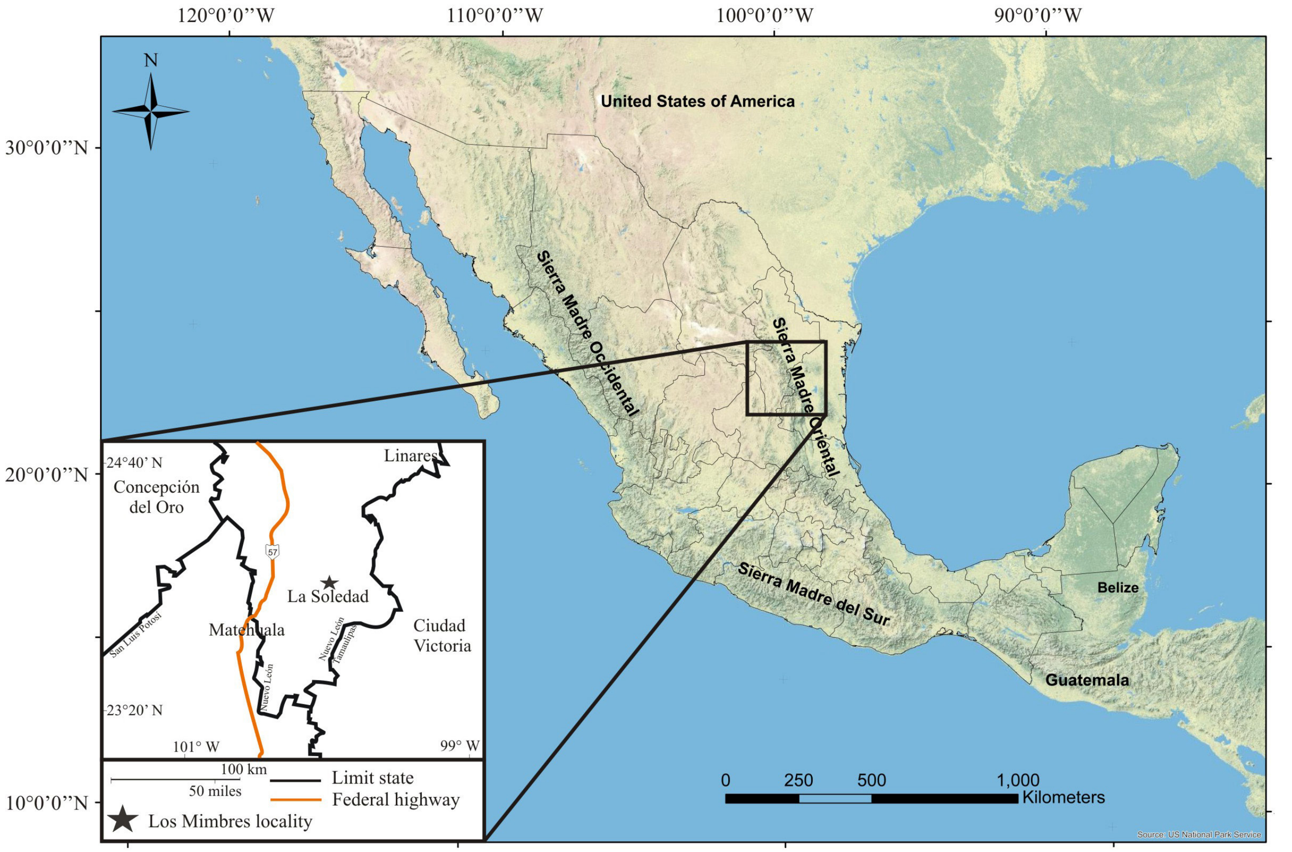

Figure 1. Geographical location. Location of the study area in the Sierra Madre Oriental, at Los Mimbres locality, near of La Soledad, southern of Nuevo León. (Taken from Geo Info Mex. http://mapasims.sgm.gob.mx/GeoInfoMexDb/).

the Cupido Formation about 50 m thick, conformably underlies the La Peña Formation (Figure 3 A), and consists of light gray argillaceous limestone in fresh sample and light-white-yellowish gray in weathering sample, with mudstone-wackestone texture in sets of thin-to-medium beds which thickness is in a range of 0.05 m to 0.50 m (Figure 3 B). Occasionally, laminar argillaceous limestone beds with stylolites, light gray to dark gray chert nodules and lenses, calcite stringers and veins, as well as hematite nodules, can be found. Five hand samples were taken from the limestone layers of this unit to prepare thin sections for micropaleontological analysis.

The La Peña Formation. The La Peña Formation was originally described by Imlay (1936) from an upper Aptian outcrop in the Sierra de Parras, Coahuila, conformed by a lower unit of limestone and an upper shale unit. Humphrey (1949) restricted the term La Peña Formation to the upper shale unit and included the lower limestone within the Cupido Formation. Barragán-Manzo and Méndez-Franco (2005) according to ammonite vertical distribution in this unit, established an age corresponding to the uppermost part of the early to late Aptian. In Los Mimbres this formation, about 20 m thick, consists of gray limestone in fresh sample, that weathers to light-reddish-pinkish limestone, with mudstone or mudstone-wackestone texture in beds from 0.10 m to 0.40 m thick, alternating with laminar reddish limestone. Dark gray chert occurs in nodules and bands (Figure 3 C). Interbedding shale and laminar argillaceous limestone, as well as stylolites, calcite stringers and veins, and nodules of hematite are present. For micropaleontological study, six rock hand samples were collected from this formation.

The Cuesta del Cura Limestone. The term Cuesta del Cura Limestone was proposed by Imlay (1936) to describe an Albian rocks exposed in Sierra de Parras, Coahuila, constituted by interbedded limestone, clay and chert bands. Based on its stratigraphic position, the age of this unit was restricted to upper part of the Albian (Imlay, 1937), but several subsequent works focused on its paleontological content determined an Albian-Cenomanian age (Gandolfi, 1942 in Ángeles-Villeda *et al*., 2005; Pantoja-Alor, 1962; Tardy *et al*., 1975; Bacon, 1978; Stinnesbeck, 1983; PEMEX, 1988; Barboza-Gudiño *et al*., 2004; Arvizu-Gutiérrez, 2006; Villarreal-Fuentes, 2007), and Albian-Turonian age (Pérez-Rul, 1967). Locally, the Cuesta del Cura Limestone, 80 m thick, is constituted by gray limestone in fresh samples that weathers to light-white gray colors with mudstone-wackestone texture. Calcite veins and oxides

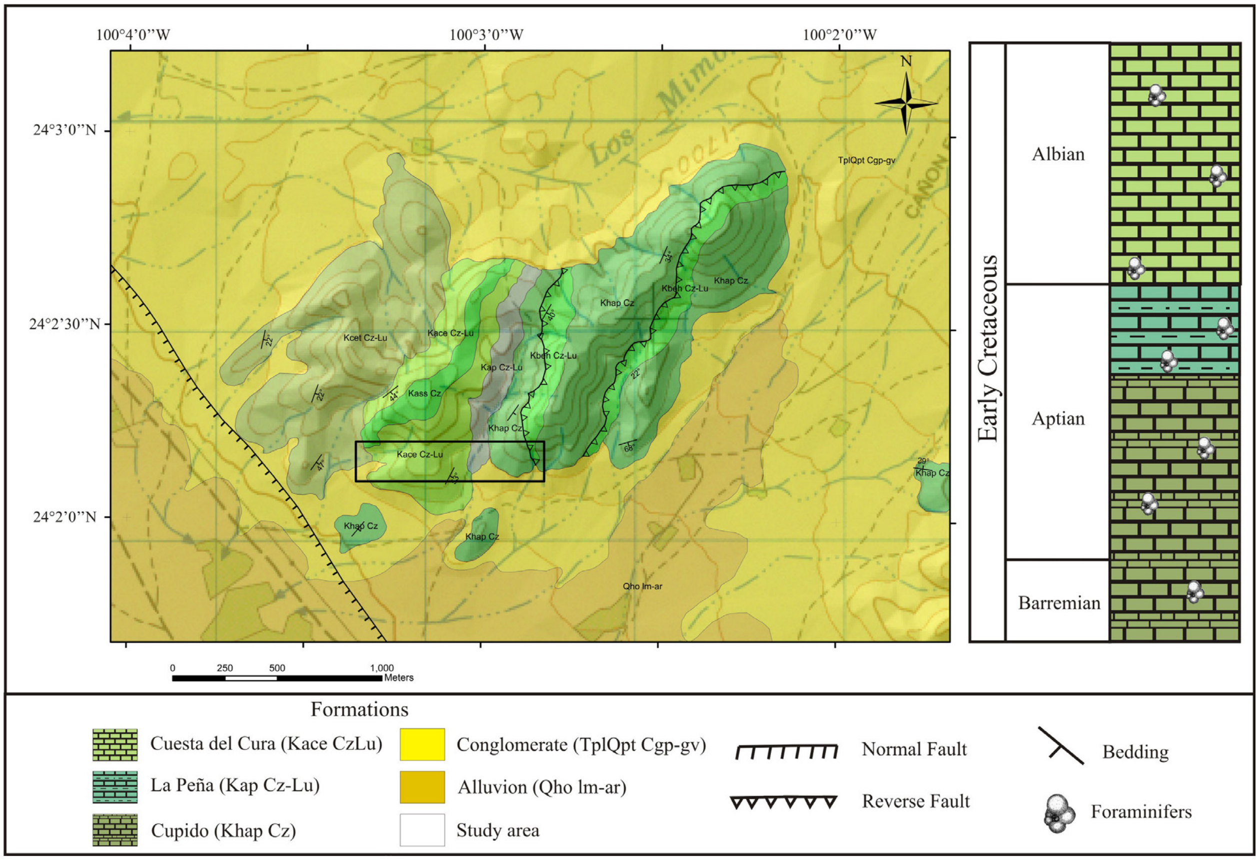

Figure 2. Geological map and generalized stratigraphic column in the studied region. Modified from Romo-Ramírez and Padilla-Islas (2012).

dissemination are present. Medium-to-thick beds from 0.10 m to 0.60 m conformed by dark gray chert nodules and bands, as well as laminar argillaceous limestone interbedded with reddish shale can be observed (Figure 3 D). For micropaleontological analysis, four rock hand samples were collected from the limestone layers of this unit.

4.2. Systematic Paleontology

Order Foraminiferida Eichwald, 1830
Suborden Globigerinina Delage and Hérouard, 1896
Superfamily Planomalinacea Bolli, Loeblich and Tappan, 1957
Family Globigerinelloididae Longoria, 1974
Subfamily Globigerinelloidinae Longoria, 1974

Genus *Globigerinelloides* Cushman and Ten Dam, 1948

Type species. *Globigerinelloides algeriana* Cushman and Ten Dam, 1948.

Diagnosis. Test planispirally enrolled, biumbilicate, involute to evolute, lobulate in outline, chambers globular to somewhat elongate in partially evolute species, sutures depressed; wall calcareous, perforate, optically radial; aperture equatorial and interiomarginal, hordered by a narrow imperforate lip, broad and low to moderately arched, the lateral portians remaining open as relict supplementary apertures around the umbilicus when new chambers are added.

Globigerinelloides blowi (Bolli, 1959)
(Figure 4 A)

1959 *Planomalina blowi* Bolli, p. 260, pl. 20, figs. 2–6.
1974 *Globigerinelloides blowi* (Bolli); Longoria, p. 82, pl. 4, figs. 4, 7, 11–13.
1978 *Globigerinelloides blowi* (Bolli); Caron, p. 658, pl. 6, figs. 11, 12.
1979 *Globigerinelloides blowi* (Bolli); Butt, p. 258, pl. 3, figs. 14–17.
1981 *Globigerinelloides*? *blowi* (Bolli); Tronchetti, p. 121, pl. 32, figs. 1–2.
1988 *Blowiella blowi* (Bolli); Banner and Desai, p. 170, pl. 4, figs. 5–8.
1992 *Globigerinelloides blowi* (Bolli); Sliter, fig. 6.4.
1999 *Globigerinelloides blowi* (Bolli); Sliter, p. 334, pl. 2, fig. 2.
2004 *Globigerinelloides blowi* (Bolli); Premoli-Silva and Verga, p. 239, pl. 9, figs. 9–10.
2005 *Globigerinelloides blowi* (Bolli); Omaña, González-Arreola and Ramírez-Garza, p. 93, fig. 3.6.

Figure 3. Outcrops of Lower Cretaceous rocks at Los Mimbres locality, Nuevo León. A) Contac between the Cupido and La Peña formations, B) Light gray argillaceous limestone in thin-to-medium strata with interbedded shale horizons of the Cupido Formation, C-D) Dark gray limestone with medium-to-thick beds of the Cuesta del Cura Limestone.

Description. Test small with planispiral coiling; globular to sphaerical chambers in final whorl, increasing rapidly in size; wall calcareous.

Ocurrence. Sample PSJ-246, the Cupido Formation, Los Mimbres locality.

Stratigraphic range. Aptian (Caron, 1985; Sliter, 1989); late Barremian to uppermost Aptian (Premoli-Silva and Verga, 2004); early Barremian to Aptian (Huber and Petrizzo, 2016).

Globigerinelloides ferreolensis (Moullade, 1961)
(Figure 4 B)

1961 *Biticinella ferreolensis* Moullade, p. 214, pl. 1, figs. 1–5.
1974 *Globigerinelloides ferreolensis* (Moullade); Longoria, pl. 5, figs. 7, 8; pl. 8, figs. 1–3, 8–15; pl. 14, figs. 7, 8; pl. 27, figs. 3, 5, 12.
1975 *Globigerinelloides ferreolensis* (Moullade); Longoria, pl. 1, fig. 7.
1985 *Globigerinelloides ferreolensis* (Moullade); Caron, p. 47, figs. 29.12–13; 10, 12, 15.
1992 *Globigerinelloides ferreolensis* (Moullade); Sliter, figs. 6.5, 6.6.
2004 *Globigerinelloides ferreolensis* (Bolli); Premoli-Silva and Verga, p. 239, pl. 9, figs. 13–15.
2009 *Globigerinelloides ferreolensis* (Moullade); Longoria and Monreal, p. 282.
2017 *Globigerinelloides ferreolensis* (Moullade); Brovina, p. 524, pl. 1, fig.7.

Description. In axial view, medium sized and planispiral test, slightly thick wall with smooth surface. Globular chambers are visible; the last one increased in size with respect to the others. Inside the visible chambers, a dark layer inside the wall. Moderately preserved specimen.

Ocurrence. Sample PSJ-242, the La Peña Formation, Los Mimbres locality.

Stratigraphic range. Aptian (Sliter, 1989; Premoli-Silva and Verga, 2004; Huber and Petrizzo, 2016); late Aptian (Caron, 1985; BouDagher-Fadel, 2015).

Superfamily Rotaliporacea Sigal, 1958
Family Hedbergellidae Loeblich and Tappan, 1961
Subfamily Hedbergellinae Loeblich and Tappan, 1961

Genus *Hedbergella* Brönnimann and Brow, 1958

Type species. *Anomalina lorneiana*, d'Orbigny var. *trochoidea* Gandolfi, 1942.

Diagnosis. Test with globular and gradually enlarging chambers in a low trochospiral coil, narrow umbilicus on the umbilical side, sutures radial, depressed; wall calcareous, finely perforate optically radial, surface smooth to hispid, without a poreless margin; aperture an interiomarginal, umbilical-extraumbilical arch, with a narrow lip or flap.

Hedbergella sigali Moullade, 1966
(Figure 4 C)

1966 *Hedbergella sigali* Moullade, p. 87, pl. 7, figs. 20–25.
1985 *Hedbergella sigali* Moullade; Bolli, Saunders and Perch-Nielsen, p. 59, figs. 25.21–22; 10, 12, 15.
1992 *Hedbergella sigali* Moullade; Sliter, figs. 7.1–2.
1999 *Hedbergella sigali* Moullade; Sliter, p. 333, pl. 1, figs. 2–3.
2002 *Hedbergella sigali* Moullade; Moullade, Bellier and Tronchetti, p. 128.
2004 *Hedbergella sigali* Moullade; Premoli-Silva and Verga, p. 251, pl. 21, fig. 12.
2005 *Hedbergella* gr. *sigali* Moullade; Omaña, González-Arreola and Ramírez-Garza, p. 93, fig. 3.3.

Description. Test small, trochospiral, in equatorial section, with 4 – 4½ globular to reniform chambers in final whorl; final chamber globular to slightly ovate.

Ocurrence. Sample PSJ-246, PSJ-247, the Cupido Formation, Los Mimbres locality.

Stratigraphic range. Early Cretaceous, Barremian-early Aptian (Caron, 1985), Barremian to Albian (Sliter, 1989); late Valaginian to early Albian (Premoli-Silva and Verga, 2004); and late Valanginian to uppermost Aptian (Huber and Petrizzo, 2016).

Hedbergella similis Longoria, 1974
(Figure 4 D)

1974 *Hedbergella similis* Longoria, p. 68, pl. 16, figs. 10–21; pl. 18, figs. 12, 13; pl. 23, figs. 14–16.
1988 *Lilliputianella similis* (Longoria); Banner and Desai, p. 169, pl. 8, figs. 8, 9.
1999 *Hedbergella similis* Longoria; Michalík, Reháková, Lintnerová, Boorová, Halásová, Kotulová, Soták, Peterèáková, Hladíková and Skupien, p. 177, pl. 4, fig. 3.
1999 *Hedbergella similis* Longoria; Sliter, p. 335, pl. 3, figs. 6, 13.
2005 *Hedbergella similis* Longoria; Omaña, González-Arreola and Ramírez-Garza, p. 93, figs. 3.1a, 3.1b.
2014 *Hedbergella similis* Longoria; Mweneinda, p. 125, pl. 3.6, figs. 3a–d.

Description. Test medium, trochospiral, in equatorial section with 5 globular chambers in the final whorl. The final chamber is ovate to slightly elongated.

Ocurrence. Sample PSJ-247, the Cupido Formation, Los Mimbres locality.

Stratigraphic range. Aptian (Sliter, 1989); early Barremian to late Aptian (Premoli-Silva and Verga, 2004); late Hauterivian to Aptian (Huber and Petrizzo, 2016).

Hedbergella roblesae (Obregón de la Parra, 1959)
(Figure 4 E)

1959 *Globigerina roblesae* Obregón de la Parra, p. 149, pl. 4, fig. 4.
1974 *Hedbergella roblesae* (Obregón de la Parra); Longoria, p. 65–66, pl. 16, figs. 1–3, 4–6; pl. 20, figs. 10, 11.
1997 *Lilliputianella roblesae* (Obregón de la Parra); BouDagher-Fadel, Banner, Whittaker, and Simmons, 173, pl. 9.3, figs. 1–7.
1998 *Praehedbergella roblesae* (Obregón de la Parra); Moullade, Tronchetti, Kuhnt and Masse, p. 208.
2002 *Praehedbergella roblesae* (Obregón de la Parra); Moullade, Bellier and Tronchetti, p. 128.
2013–2014 *Lilliputianella roblesae* (Obregón de la Parra); Barchetta, p. 79, pl. 4, figs. 3a–b.

Description. Test medium sized, in equatorial section, trochospirally coiled with 5 chambers in outer whorl; chambers initiality globular to subglobular, the last three elongate. Wall calcareous and smooth.

Remarks. The equatorial section of this species is comparable with the illustration of Premoli-Silva and Verga (2004).

Ocurrence. Sample PSJ-246, the Cupido Formation, Los Mimbres locallity.

Stratigraphic range. Barremian to uppermost Aptian (Premoli-Silva and Verga, 2004); late Hauterivian to Aptian (Huber and Petrizzo, 2016).

Hedbergella spp.
(Figure 4 F)

Description. Test medium sized and trochospiral in axial view. Wall thin and finely perforate. Chambers globular to subglobular. Umbilical area narrow and deep. Moderately preserved specimen.

Ocurrence. Sample PSJ-243, the La Peña Formation; Sample PSJ-247, the Cupido Formation, Los Mimbres locality.

Stratigraphic range. Early Barremian-early Santonian (Caron, 1985), late Valanginian-late Aptian (Premoli-Silva and Verga, 2004), late Aptian-Paleocene (BouDagher-Fadel, 2015), late Valanginian-late Albian (Huber and Petrizzo, 2016).

Genus *Muricohedbergella* Huber and Leckie, 2011

Type species. *Muricohedbergella delrioensis* (Carsey, 1926).

Diagnosis. Test wall moderately thick, multilamellar, finely perforate, wall pores variably spaced in adult chambers, surface moderately to coarsely muricate or pustulose, never with a keel, raised sutures or imperforate peripheral margin. Test small to moderate in size, coiled in a very low to low trochospire, spiral side evolute, umbilical side mostly involute; chambers globular, never elongated radially, increasing slowly to moderately in size, with 4.5–7 in the final whorl; aperture a low interiomarginal, umbilical-extraumbilical arch that is bordered by a thick lip or flap that may extend partly into the umbilical region.

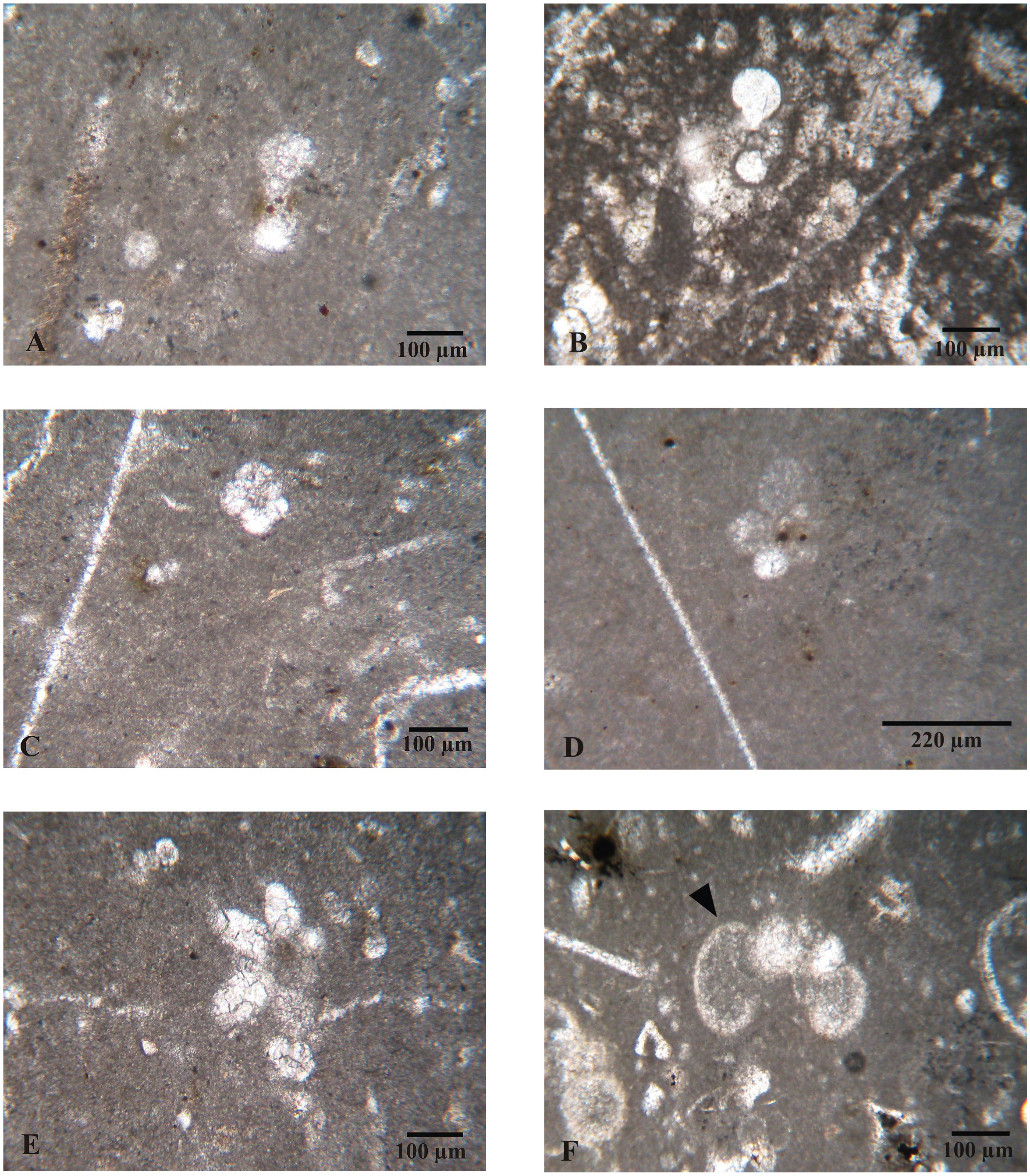

Figure 4. A) *Globigerinelloides blowi* (Bolli), axial section; B) *Globigerinelloides ferreolensis* (Moullade), axial section; C) *Hedbergella sigali* Moullade, equatorial section; D) *Hedbergella similis* Longoria, equatorial section; E) *Hedbergella roblesae* (Obregón de la Parra), equatorial section; F) *Hedbergella* sp., axial section.

Remarks. According to Huber and Leckie (2011) the "murico" definition is added to pre-existing *Hedbergella* genus, because of the presence of moderate to thick pustules or muricas on test surface.

Muricohedbergella delrioensis (Carsey, 1926)
(Figure 5 A)

1926 *Globigerina cretacea* d'Orbigny var. *delrioensis* n. var. Carsey, p. 43.
1937 *Globigerina infracretacea* Glaessner, p. 28, text-fig. 1.
1966 *Hedbergella delrioensis* (Carsey); Butt, p. 173–174, pl. 2, figs. 1–8.
1967 *Hedbergella delrioensis* (Carsey); Pessagno, p. 282–283, pl. 48, figs. 1, 2, 3–5.
1970 *Hedbergella delrioensis* (Carsey); Eicher and Worstell, p. 302, pl. 9, figs. 10, 11a–b.
1971 *Hedbergella delrioensis* (Carsey); El-Naggar, pl. 6, figs. a–c, 37.
1972 *Hedbergella delrioensis* (Carsey); Barr, p. 13, pl. 2, fig. 1a.
1973 *Hedbergella delrioensis* (Carsey); Dailey, p. 82, pl. 17: a.
1974 *Hedbergella delrioensis* (Carsey); Herb, p. 752, pl. 3, figs. 15–18.
1974 *Hedbergella delrioensis* (Carsey); Longoria, pl. 10, figs. 1–3.
1975 *Hedbergella delrioensis* (Carsey); North and Caldwell, pl. 4, figs. 16a, 18a–c.
1975 *Hedbergella delrioensis* (Carsey); Luterbacher, pl. 1, fig. 8.
1975 *Hedbergella delrioensis* (Carsey); Heller, pl. 2, fig. 12.
1976 *Hedbergella delrioensis* (Carsey); Masters, p. 328, pl. 2, figs. 1–3.
1979 *Hedbergella delrioensis* (Carsey); Robaszynski, Caron and others, p. 123, pl. 22, figs. 1–2; pl. 23, figs. 1–3.
1980 *Hedbergella delrioensis* (Carsey); Peryt, p. 54, pl. 10: 1a–c.
1983 *Hedbergella delrioensis* (Carsey); Belford, p. 15, pl. 5, figs. 11–16.
1983 *Hedbergella delrioensis* (Carsey); Peryt, p. 447, pl. 30: 8, 10.
1984 *Hedbergella delrioensis* (Carsey); Leckie, p. 598, pl. 1, fig. 12; pl. 9, figs. 1–4, 8.
1985 *Hedbergella delrioensis* (Carsey); Caron, p. 57, figs. 25.6–7.
2006 *Hedbergella delrioensis* (Carsey); Petrizzo and Huber, p. 185, pl. 7, figs. 3–4.
2011 *Muricohedbergella delrioensis* (Carsey); Huber and Leckie, p. 84.
2013 *Muricohedbergella delrioensis* (Carsey); Egger, Mohamed and Rögl, p. 100, figs. 10/8–9.
2017 *Muricohedbergella delrioensis* (Carsey); Flores-Cadenas, p. 36–38, fig. 8D.

Description. Test small to medium, low trochospiral, globular to subglobular chambers; wall calcareous and thin.

Ocurrence. Sample PSJ-243, the La Peña Formation, Los Mimbres locality.

Stratigraphic range. The stratigraphic range varies depending the criterious of each autor, for example, Barremian to Campanian (Master, 1977); early Aptian to Coniacian (Caron, 1985); early Aptian to early Santonian (Sliter, 1989); late Albian to early Santonian (Patterson *et al.*, 2004); early Albian to late Coniacian (Premoli-Silva and Verga, 2004); Albian to Turonian (Loeblich and Tappan, 1961; Salaj and Samuel, 1966; Longoria, 1974; Pflamann and Krasheninnikov, 1977; Chronos, 2006); late Albian to early Turonian (Huber and Petrizzo, 2016).

Family Favusellidae Longoria 1974

Genus *Favusella* Michael 1972

Type species. *Globigerina washitensis* Carsey, 1926.

Diagnosis. Test trochospirally coiled, globular chambers rapidly enlarging, 4–5 in each of the 2–3 whorls, sutures radial, depressed; wall calcareous, perforate, without keels, surface with a distinct honeycomblike pattern of costellae.

Favusella washitensis (Carsey, 1926)
(Figure 5 B1)

1926 *Globigerina washitensis* Carsey, p. 44, pl. 7, fig. 10.
1931 *Globigerina washitensis* Carsey; Plummer, p. 193, pl. 13, figs. 12a–b.
1972 non *Favusella washitensis* (Carsey); Michael, p. 61, pl. 4, figs. 7–9.
1974 *Favusella washitensis* (Carsey); Longoria, pl. 26, figs. 4–6.
1985 *Favusella washitensis* (Carsey); Bolli, Saunders and Perch-Nielsen, p. 45, figs. 25.25–26, 10, 12, 15.
2009 *Favusella washitensis* (Carsey); Longoria and Monreal, p. 281, pl. 2, fig. 7.
2013 *Favusella washitensis* (Carsey); Soleimani, Bahadori and Meng, p. 1168, fig. 4.6.
2016 *Favusella washitensis* (Carsey); Omaña, Alencaster and Buitrón, p. 485, fig. 5g.

Description. Test high with trochospiral coil. Chambers sphaerical to subsphaerical. Wall calcareous ornamented.

Ocurrence. Sample PSJ-241, the Cuesta del Cura Limestone, Los Mimbres locality.

Stratigraphic range. According to Caron (1985) and Premoli-Silva and Verga (2004) the age is Lower Cretaceous (Albian) to Upper Cretaceous (lower Cenomanian); while Longoria and Monreal (2009), BouDagher-Fadel (2015), and Huber and Petrizzo (2016) assigned from Early Cretaceous (late Aptian) to Late Cretaceous (Cenomanian).

Family Rotaliporidae Sigal, 1958
Subfamily Ticinellinae Longoria 1974

Genus *Ticinella* Reichel, 1950

Type species. *Anomalina roberti* Gandolfi, 1942.

Diagnosis. Test trochospiral, biconvex to planoconvex, umbilicate, chambers globular to ovate, sutures curved on the spiral side, radial on the umbilical side, depressed, periphery rounded and without a keel or poreless margin, peripheral outline lobulate; wall calcareous, optically radial, surface smooth, finely perforate, secondary lamellae emphasizing the surface rugosity and obscuring some pores but enlarging others.

Ticinella sp.
(Figure 5 C1)

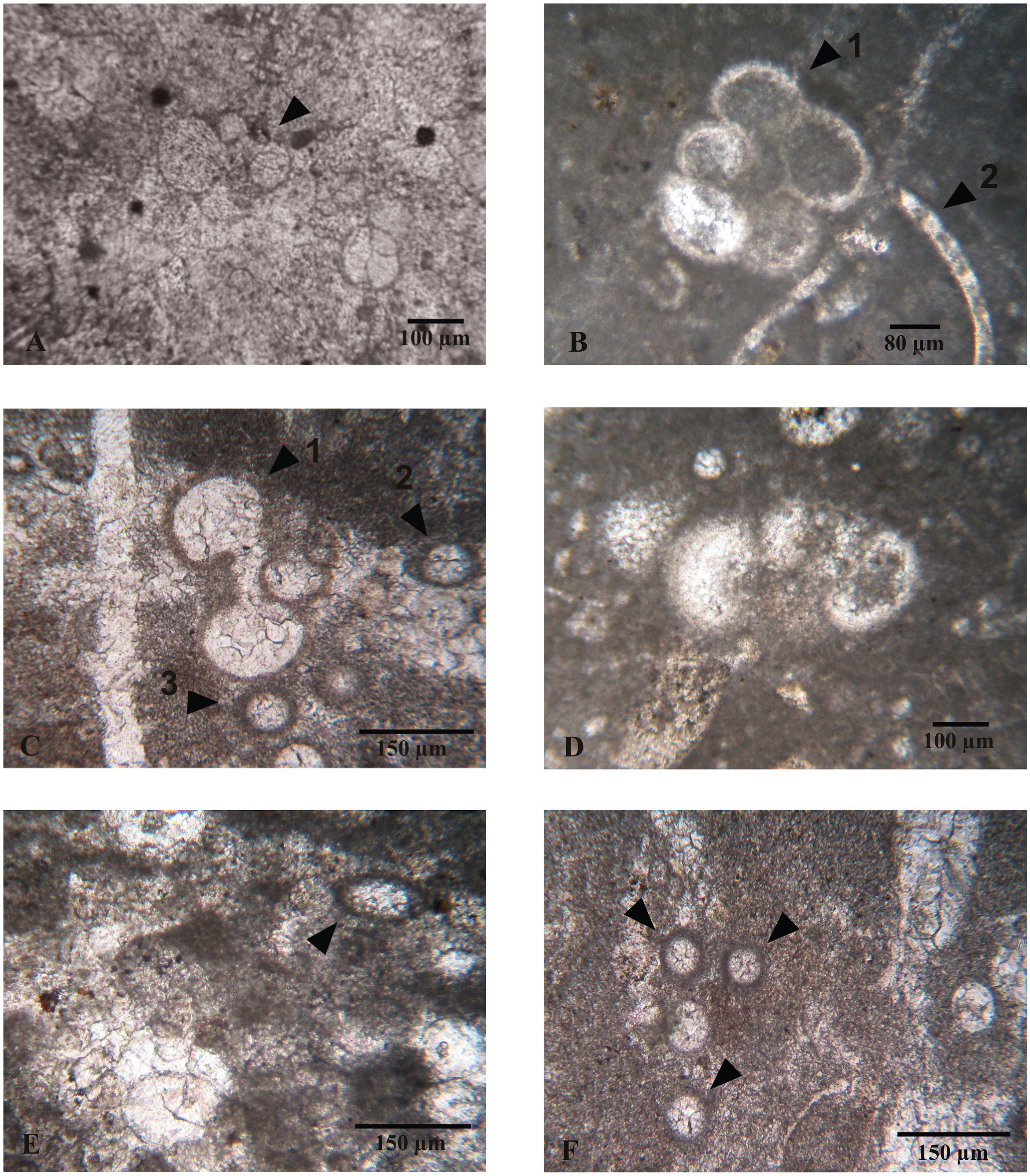

Figure 5. A) *Muricohedbergella delrioensis* (Carsey), axial section; B) *Favusella washitensis* (Carsey), equatorial section (1), *Microcalamoides diversus* Bonet (2); C) *Ticinella* sp., axial section (1), *Bishopella alata* (2), *Bishopella ornelasae* (3); D) *Paraticinella rohri* (Bolli), axial section; E) *Bishopella alata* Trejo; F) *Bishopella ornelasae* Trejo.

Description. Test trochospiral, chambers globular to ovate, periphery rounded without keels; wall calcareous, surface smooth, finely perforate.

Ocurrence. Sample PSJ-240, the Cuesta del Cura Limestone, Los Mimbres locality.

Stratigraphic range. Late Aptian to late Albian (Caron, 1985); Aptian to early Cenomanian (Loeblich and Tappan, 1988); Albian (Sliter, 1989; Premoli-Silva and Verga, 2004; Huber and Petrizzo, 2016).

Genus *Paraticinella* Premoli-Silva, Caron, Leckie, Petrizzo, Soldan and Verga, 2009

Type species. *Ticinella eubejaouaensis* Randrianasolo and Anglada, 1988, and *Ticinella bejaouaensis* as emmended by Moullade 1966.

Diagnosis. Low trochospiral, generally slightly lobate in outline, numerous chambers (7–11) in the last whorl, globular, sutures straight and depressed on both sides; wall finely perforate; wall surface rugose to smooth, with rugosities masking the inner whorl, then covering the first chambers of the last whorl, frequently organized in irregularly sized ridges that may cover the pores and run parallel to the spiral suture; surface of later-formed chambers may bear volcano-like perforation cones that progressively attenuate toward the ultimate chamber; shallow umbilical area moderate to large in size; umbilical area may be covered, at least partially, by large flaps from the ultimate and penultimate chambers that fuse along a slightly depressed line forming a cover-plate; primary aperture an interiomarginal arch, umbilical-extraumbilical extending toward the periphery; may have one to two small, weakly developed umbilical accessory (infralaminal) apertures in the last chambers.

Paraticinella rohri (Bolli, 1959)
(Figure 5 D)

1959 *Praeglobotruncana rohri* Bolli, p. 267-268, pl. 22, figs. 6 (holotype), 7 (paratype) (non pl. 22, fig. 5).
1966 *Ticinella roberti* var. *bejaouaensis* Sigal, p. 207–208, pl. 5, figs. 8, 9 (non pl. 5, figs. 5-7).
1966 *Ticinella bejaouaensis* Sigal; Moullade, p. 103, pl. 9, figs. 4–5.
1971 *Ticinella bejaouaensis* Sigal; Risch, p. 50–51, pl. 5, figs. 1–9.
1974 *Ticinella bejaouaensis* Sigal; Longoria, p. 94, pl. 18, figs. 1–2; pl. 19, figs. 9–16; pl. 21, figs. 12–13.
1979 "*Hedbergella*" aff. *Ticinella bejaouaensis* Sigal; Sigal, pl. 3, figs.14–15.
1984 *Ticinella roberti* s.l. (Gandolfi); Leckie, p. 600–601, pl. 5, figs. 5–12 (non pl. 5, figs. 1–4).
1984 *Ticinella bejaouaensis* Sigal; Premoli-Silva and McNulty, pl. 2, figs. 1–3.
1985 *Ticinella bejaouaensis* (Sigal); Caron, p. 76–77, figs. 36.1–3, 10, 12, 15.
1985 *Ticinella roberti* (Gandolfi); Bellier, p. 10, pl. 1, figs. 1–3.
1986 *Ticinella bejaouaensis* Sigal; Premoli-Silva and Sliter, pl. 1, figs. 3–5.
1992 *Ticinella bejaouaensis* Sigal; Sliter, figs. 7.8–7.11.
1993 *Ticinella* (?) *bejaouaensis* Sigal; Sliter and Leckie, pl. 5, figs. 1–2.
1998 *Ticinella eubejaouaensis* Randrianasolo and Anglada, p. 28.
1999 *Ticinella bejaouaensis* Sigal; Aguado, Castro, Guillén, figs. 10.24–10.27.
2000 *Ticinella bejaouaensis* Sigal; Lipson-Benitah and Almogi-Labin, p. 12, pl. 1, figs. 1–5.
2002 *Ticinella eubejaouaensis* Randrianasolo and Anglada; Bellier and Moullade, p. 19–20, pl. 1, figs. 13–15.
2009 *Paraticinella eubejaouaensis* (Randrianasolo and Anglada); Premoli-Silva, Caron, Leckie, Petrizzo, Soldan and Verga, p. 131–132, 135, pl. 1, figs. 5a–b, 6a–b; pl. 2, figs. 1a–d, 2–6.
2009 *Ticinella bejaouaensis* (Sigal); Longoria and Monreal, p. 281, pl. 1, figs. 1, 2.
2010 *Paraticinella rohri* (Bolli); Georgescu, text-figs. 1.1–1.3.
2011 *Paraticinella eubejaouaensis* (Randrianasolo and Anglada); Huber and Leckie, p. 85, figs. 10.4, 10.6.
2012 *Paraticinella eubejaouaensis* (Randrianasolo and Anglada); Petrizzo, Huber, Gale, Barchetta, and Jenkyns, pl. 4, figs. 2–3.
2013 *Paraticinella rohri* (Bolli); Ando, Huber, Premoli-Silva, p. 282, figs. 2A, 2B.

Description. Test low, almost flat trochospire; globular chambers; wall calcareous, surface rugose; umbilicus deep.

Ocurrence. Sample PSJ-243, the La Peña Formation, Los Mimbres locality.

Stratigraphic range. Late Aptian (Premoli-Silva *et al*., 2009; BouDagher-Fadel, 2015; Huber and Petrizzo, 2016).

Subphylum Sarcodina Hertwig and Lesser, 1874
Clase Rhizopoda von Siebold, 1845
Orden Foraminiferida Eichwal, 1830
Incerta seadis

Genus *Bishopella* Trejo, 1983

Type species. *Bishopella alata* Trejo, 1983.

Diagnosis. Test monothalamic and micritical, hallow or filled with spatic calcite. Shape of test is sphaerical to lenticular, with a conical face of rounded apex and other slightly convexo or flat. Wall thick, crossed by regular pores with radial orientation.

Bishopella alata Trejo, 1983

(Figures 5 C2, 5 E)

1983 *Bishopella alata* Trejo, p. 12, pl. 26, figs. 2–12; pl. 27, figs. 1, 2, 5, 8; text-fig. 1.

Description. Test monothalamic, filled with spatic calcite; 140 to 200 in diameter. These specimens have an edge formed by the union between oral face slightly convex and aboral face conical redounded. Wall thick and micritical.

Ocurrence. Sample PSJ-239, PSJ-240, the Cuesta del Cura Limestone, Los Mimbres locality.

Stratigraphic range. Middle Albian to late Albian (Trejo, 1983).

Bishopella ornelasae Trejo, 1983

(Figures 5 C3, 5 F)

1983 *Bishopella ornalasae* Trejo, p. 13, pl. 21–34.

Description. Test sphaerical; 150 to 200 μm in diameter. Wall micritical and thick.

Ocurrence. Sample PSJ-239, PSJ-240, the Cuesta del Cura Limestone, Los Mimbres locality.

Stratigraphic range. Middle Albian to late Albian (Trejo, 1983).

Phyllum Protozoa Goldfuss, 1818 emend. Von Siebold, 1845
Class Ciliatea Perty, 1852
Order Tintinnida Corliss, 1955
Superfamily Tintinnidea Bonet, 1956
Family Colomiellidae Bonet, 1956

Genus *Colomiella* Bonet, 1956

Type species. *Colomiella mexicana* Bonet, 1956.

Diagnosis. Colomiellidae with a cylindrical collar and with one or more cylindrical anular rings.

Colomiella recta Bonet, 1956

(Figure 6 A)

1956 *Colomiella recta* Bonet, p. 431, pl. 21.
1989 *Colomiella recta* Bonet; Rosales-Domínguez, fig. 7A.
2009 *Colomiella recta* Bonet; Longoria and Monreal, p. 273, pl. 1, figs. 3, 4, 7, 8.
2012 *Colomiella recta* Bonet; Núñez-Useche and Barragán, fig. 6d.
2017 *Colomiella recta* Bonet; Caetano-Filho, Dias-Brito, Rodrígues and Acevedo, figs. 7C–D, 8B–C, F.

Description. Test thin and hemisphaerical, large necklace. The necklace is separated from test body; thick wall at the necklace base.

Ocurrence. Sample PSJ-244, the La Peña Formation, Los Mimbres locality.

Stratigraphic range. Barremian to uppermost Aptian (Bonet, 1956); Barremian to early Albian (Longoria, 1973).

Phyllum Arthropoda Latreille, 1829
Subphyllum Mandibulata Clairville, 1798
Class Crustacea Pennant, 1777
Subclass Ostracoda Latreille, 1806

Genus *Microcalamoides* Bonet, 1956

Type species. *Microcalamoides diversus* Bonet, 1956.

Diagnosis. Calcitic remains of cylindrical shape, about ¼ to 1 mm in diameter, length unknown. Outer surface with longitudinal furrows. It is ignored if both ends are closed or open, as well as the length of the cylinders. The conserved parts look like fragments of a calcitic skeleton.

Microcalamoides diversus Bonet, 1956

(Figures 5 B2, 6 B)

1956 *Microcalamoides diversus* Bonet, p. 433–436, pls. 27, 29, 30.
1960 *Microcalamoides diversus* Bonet; Trejo, p. 264, 267, 268.
1971 *Microcalamoides diversus* Bonet; Ramírez del Pozo, p. 309–310, pls. 38–2, 45–2, 49–2.

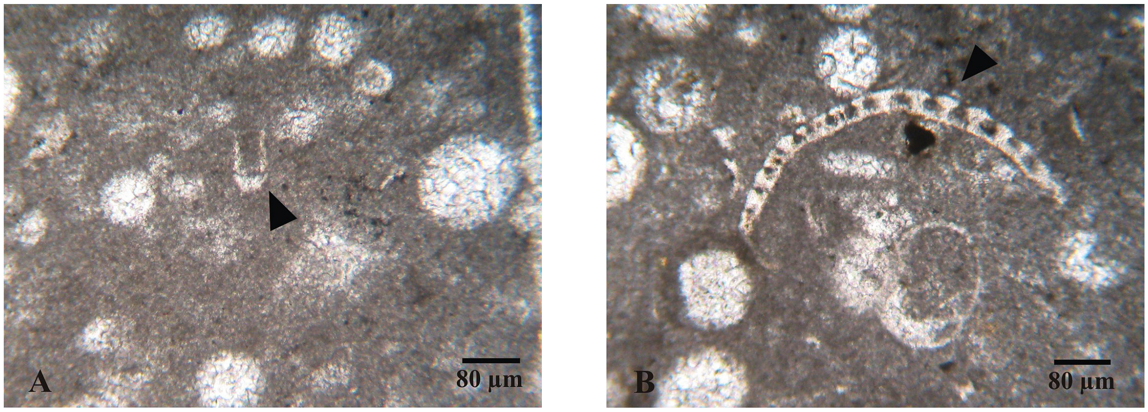

Figure 6. A) *Colomiella recta* Bonet; B) *Microcalamoides diversus* Bonet.

1974 *Microcalamoides diversus* Bonet; O'Neil and Waite, p. 39, pl. 23, figs a–c.
1974 *Microcalamoides diversus* Bonet; Prestat, p.3, pl. 7, figs. 6–8.
1975 *Microcalamoides diversus* Bonet; Trejo, p. 15, 16.
1983 *Microcalamoides diversus* Bonet; Trejo, p. 15, pl. 18, figs. 1–2.
1989 *Microcalamoides diversus* Bonet; Rosales-Domínguez, fig. 8.
2017 *Microcalamoides diversus* Bonet; Caetano-Filho, Dias-Brito, Rodrígues and Acevedo, figs. 8B–C, H.

Description. Calcitic skeletal remains similar to a keg with large dimensions. Probably these remains correspond to globose shells of ostracods. Generally they have arch shape in thin section. Wall thin; external surface has longitudinal grooves.

Ocurrence. Sample PSJ-241, the Cuesta del Cura Limestone, Sample PSJ-242, La Peña Formation, Los Mimbres locality.

Stratigraphic range. Late Valanginian to middle Albian (Bonet, 1956).

4.3. Biostratigraphic results and paleoenviroment considerations

The microfauna analyzed is mostly represented by planktonic and benthic foraminifers, calcisphaerulids, bioclasts of mollusks, echinoid spines, among other unidentified planktonic and benthic microfossils.

4.3.1. The Cupido Formation

At the base of the Cupido Formation, two microfossil associations were found. The first, characterized by poorly preserved chambers of globigerinids, *Hedbergella* sp., co-occurring with some small textulariid benthic foraminifers, indicating a Barremian-middle Albian age. The second association is distinguished by spicules of sponges replaced by calcite, together with scarce and recrystallized planktonic foraminifers as *Hedbergella similis* Longoria, which testifies an early Barremian-Aptian age (Sliter, 1989; Omaña *et al*., 2005); as well as *Hedbergella* sp. Both associations indicate an age from Barremian to Maastrichtian (Caron, 1985; Sliter, 1989). For the middle-upper part of the Cupido Formation, microfauna is represented by *Globigerinelloides blowi* (Bolli), which indicates a late Barremian-Aptian age, *Hedbergella sigali* Moullade, from Barremian to middle Aptian, and *Hedbergella roblesae* (Obregón de la Parra), Barremian-late Aptian (see Range Chart 2 presented by Premoli-Silva and Verga, 2004). The latter is considered by Sliter (1989) from Aptian age. Textulariid benthic foraminifers and bioclasts of mollusks also were recognized. For this studied section, a Barremian-middle Aptian age is suggested based on the first appearance of *Hedbergella similis* Longoria and the last presence of *Globigerinelloides blowi* (Bolli). All this microfaunal assemblage and the sedimentological features in this formation document the presence of a low energy and slightly oxygenated marine setting (shelf).

4.3.2. The La Peña Formation

This unit contains abundant planktonic foraminifers as *Globigerinelloides ferreolensis* (Moullade), *Paraticinella rohri* (Bolli) (=*Ticinella bejaouaensis*) and *Hedbergella* sp., co-occurring with *Microcalamoides diversus* Bonet, roveacrinids, crinoid fragments, scarce benthic foraminifers and undetermined microfossils. A second association for the La Peña Formation is represented by *Hedbergella* sp., *Muricohedbergella delrioensis* (Carsey), and undetermined globigerinids. In the uppermost part of the La Peña Formation, *Hedbergella sigali* is co-occurring with *Colomiella recta* Bonet, whose stratigraphic range in Mexico has been considered from the uppermost late Aptian to early Albian. Also spumellarids and nassellarids radiolarians, and scarce roveacrinids were found. Considering the fossil association identified, a late Aptian age is assigned to this unit at Los Mimbres. The micropaleontological data reveal a low energy, oxygenated deep-sea environment, from the outer shelf to bathyal zones.

4.3.3. The Cuesta del Cura Limestone

At the base of this unit, planktonic foraminiferal assemblage consists of *Muricohedbergella delrioensis*, *Favusella washitensis* (Carsey), unidentified globigerinids, associated with *Microcalamoides diversus* Bonet, crinoidal fragments, mollusks, and undetermined small benthic foraminifers. A middle Albian age was given to this section on the basis of the first occurrence *Favusella washitensis* Carsey (Premoli-Silva and Verga, 2004) and the last appearance of *Microcalamoides diversus* Bonet. For the middle part of this unit, two microfaunistic associations were identified. The first one consists mostly of *Bishopella ornelasae* Trejo and in lower proportion of *Bishopella alata* Trejo, both of middle-late Albian; *Ticinella* sp., undetermined poorly preserved planktonic foraminifers, and calcified spumellarid radiolarian. The second one is characterized by *Bishopella ornelasae* Trejo, *B. alata* Trejo, poorly preserved calcisphaerulids together with bioclasts of mollusks and unidentified textulariid foraminifers. According to the aforementioned micropaleontological association, the deposition of this unit took place in a shallow marine environment of the neritic region.

5. Conclusions

The carbonated rocks of the Cupido, La Peña, and Cuesta del Cura formations are well exposed at Los Mimbres locality. The micropaleontological study allowed to identify an assemblage composed of seven species of planktonic foraminifers, four species of pelagic microfossils, as well as bishopelids, and bioclasts of echinoderms and mollusks.

This microfauna indicates an age from early Barremian to late Albian for the rocks studied. The analyzed microfauna and the lithology suggest a depositional environment characterized by oxygenated, low energy deep-water, belonging to pelagic marine setting (from outer platform to bathyal zone). The present finds shed more light on the Early Cretaceous micropaleontological associations from Nuevo León State and provide valuable information that could be used in future biostratigraphic works from this area and elsewhere in northeastern Mexico.

Acknowledgments

This research was supported by the SGM. We are very grateful to Dr. Ana Luisa Carreño (Instituto de Geología, UNAM), one anonymous reviewer, and to the editor Dr. Josep A. Moreno-Bedmar (Instituto de Geología, UNAM) for their useful comments on the manuscript. Warm thanks to Dr. Ma. del Carmen Rosales-Domínguez and Dr. José Fernández-Carmona (both Independent Consultants) for the discussion on the systematics of foraminifers. The authors thank Dr. Victor M. Bravo-Cuevas (Museo de Paleontología, UAEH) for his kind suggestions that improved the final version of this paper. Special thanks to Ing. Victor M. León-Ayala (SGM Staff) who prepared the Figure 2. Last but not least, thanks to Ing. Blenda Flores-Cadenas (SGM Staff) for her comments on the systematic descriptions.

References

Aguado, R., Castro, J.M., Guillén, G.A., 1999, Aptian bio-events and integrated biostratigraphic analysis of the Almadich Formation, Inner Prebetic Domain, SE Spain: Cretaceous Research, 20(6), 663–683.

Ando, A., Huber, B.T., Premoli-Silva, I., 2013, *Paraticinella rohri* (Bolli, 1959) as the valid name for the latest Aptian zonal marker species of planktonic foraminifera traditionally called *bejaouaensis* or *eubejaouaensis*: Cretaceous Research, 45, 257–287.

Ángeles-Villeda, M.A., Hinojosa-Espinosa, J.J., López-Oliva, J.G., Valdés-González, A., Livas-Vera, M., 2005, Estratigrafía y microfacies de la parte sur del Cañón La Boca, Santiago, Nuevo León, México: Revista Mexicana de Ciencias Geológicas, 22(2), 272–281.

Arvizu-Gutiérrez, I.R., 2006, Paleomagnetismo de rocas jurásicas y cretácicas del Valle San Marcos, Coahuila, México: Juriquilla, Querétaro, México, Universidad Nacional Autónoma de México, Centro de Geociencias, Master's thesis, 121 pp.

Bacon, R.W., 1978, Geology of the northern Sierra de Catorce, San Luis Potosí, México: Arlington, Texas, University of Texas at Arlington, Master's thesis, 124 pp.

Banner, F.T., Desai, D., 1988, A review and revision of the Jurassic-Early Cretaceous *Globigerinina*, with especial reference to the Aptian assemblages of Speeton (North Yorkshire, England): Journal of Micropalaeontology, 7(2), 143–185.

Barboza-Gudiño, J.R., Hoppe, M., Gómez-Anguiano, M., Martínez-Macías, P.R., 2004, Aportaciones para la interpretación estratigráfica y estructural de la porción noroccidental de la Sierra de Catorce, San Luis Potosí, México: Revista Mexicana de Ciencias Geológicas, 21(3), 299–319.

Barchetta, A., 2013–2014, The Tethys (Cismon core) and Pacific (DSDP Site 463) Ocean record of OAE1a: A taxonomic and quantitative analyses of planktonic foraminifera and their biological response across the Selli Level equivalent: Milano, Italia, Università Degli Studi Di Milano, PhD dissertation, 197 pp.

Barr, F.T., 1972, Cretaceous biostratigraphy and planktonic foraminifera of Libya: Micropaleontology, 18(1) 1–46.

Barragán-Manzo, R., Díaz-Otero, C., 2004, Análisis de microfacies y datos micropaleontológicos de la transición Barremiano-Aptiano en la Sierra del Rosario, Durango, México: Revista Mexicana de Ciencias Geológicas, 21(2), 247–259.

Barragán-Manzo, R., Méndez-Franco, L., 2005, Towards a standard ammonite zonation for the Aptian (Lower Cretaceous) of northern Mexico: Revista Mexicana de Ciencias Geológicas, 22(1), 39–47.

Belford, D.J., 1983, A probably Coniacian (Late Cretaceous) foraminiferal fauna, Carnarvon Basin, Western Australia, in Palaeontological papers 1983: Bureau of Mineral Resources, Bulletin 217, 11–27.

Bellier, J.-P., 1985, Foraminifères planctoniques du Crétacé de Tunisie septentrionale: utilisation stratigraphique des formes trochospiralées de l'Albien au Maastrichtien: Mémoires de la Société Géologique de France, Mémoires 146, 67 pp.

Bellier, J.-P., Moullade, M., 2002, Lower Cretaceous planktonic foraminiferal biostratigraphy of the western North Atlantic (ODP Leg 171B), and taxonomic clarification of key index species: Revue de Micropaléontologie, 45, 9–26.

Bellier, J.-P., Tronchetti, G., 2002, Hierarchy of criteria, evolutionary processes and taxonomic simplification in the classification of Lower Cretaceous planktonic foraminifera: Cretaceous Research, 23(1), 111–148.

Bolli, H.M., 1959, Planktonic foraminifera from the Cretaceous of Trinidad, B. W. I.: Bulletins of American Paleontology, 39, 257–277.

Bolli, H.M., Saunders, J.B., Perch-Nielsen, K. (eds.), 1985, Plankton Stratigraphy: Geological Magazine, 123(5), 592–593.

Bonet, F., 1956, Zonificación Microfaunística de las Calizas Cretácicas del este de México: Boletín de la Asociación Mexicana de Geólogos Petroleros, 8(7–8), 389–488.

Boudagher-Fadel, M.K., 2015, Biostratigraphic and geological significance of Planktonic Foraminifera, updated second edition: London, England, Office of the Vice Provost Research, University College, London, 287 pp.

Boudagher-Fadel, M.K., Banner, F.T., Whittaker, J.E., Simmons, M.D., 1997, Early Evolutionary History of Planktonic Foraminifera: British Micropalaeontological Society Publications Series, Chapman & Hall, 269 pp.

Brovina, E., 2017, Planktonic foraminiferal biostratigraphy of the Upper Barremian and Aptian of Crimea: Stratigraphy and Geological Correlation, 25(5), 515–531.

Butt, A., 1966, Foraminifera of the Type Turonian: Micropaleontology, 12(2), 168–182.

Butt, A., 1979, Lower Cretaceous foraminiferal biostratigraphy, paleoecology, and depositional environment at Deep Sea Drilling Project site 397, Leg 47th: Initial Reports of the Deep Sea Drilling Project, 47(1), 251–271.

Caetano-Filho, S., Dias-Brito, D., Rodrígues, R., Azevedo, R.L.M., 2017, Carbonate microfacies and chemostratigraphy of a late Aptian-early Albian marine distal section from the primitive South Atlantic (SE Brazilian continental margin): Record of global ocean-climate changes?: Cretaceous Research, 74(1), 23–44.

Caron, M., 1978, Cretaceous planktonic foraminifers from Deep Sea Drilling Project Leg 40. Southeastern Atlantic Ocean: Initial Reports of the Deep Sea Drilling Project, 40, 651–678.

Caron, M., 1985, Cretaceous planktic foraminifera, *in* Bolli, H.M., Saunders, J.B., Perch-Nielsen, K. (eds.), Plankton Stratigraphy Volume 1, Planktic foraminifera, calcareous nannofossils and calpionellids: New York, Cambridge University Press, 17–86.

Carsey, D.O., 1926, Foraminifera of the Cretaceous of central Texas: University of Texas Bulletin, 2612, 56 pp.

Dailey, D.H., 1973, Early Cretaceous foraminifera from the Budden Canyon Formation, northwestern Sacramento Valley, California: University of California Publications in Geological Sciences, 106, 1–11.

Egger, H., Mohamed, O., Rögl, F., 2013, Plankton stratigraphy of the Santonian at Morzg, Salzburg (Gosau Group, Northern Calcareous Alps, Austria): Austrian Journal of Earth Sciences, 106(2), 89–114.

Eicher, D.L., Worstell, P., 1970, Cenomanian and Turonian foraminifera from the Great Plains, United States: Micropaleontology, 16(3), 269–324.

El-Naggar, Z.R., 1971, On the classification, evolution and stratigraphical distribution of the globigerinacea *in* Farinacci (ed.), Proceedings of the 2nd International Conference on planktonic Microfossils: Rome, Italia, part 1, Edizioni Tecnoscienza, Rome, 421–476.

Flores-Cadenas, B.E., 2017, Bioestratigrafía de la Formación Eagle Ford (Cretácico Superior) en la localidad La Bolita, Municipio de Castaños del estado de Coahuila: Ciudad de México, Instituto Politécnico Nacional, Escuela Superior de Ingeniería y Arquitectura, Bachelor's thesis, 136 pp.

Frederick, C., 1976, A revised classification of Gymnamoebia (Protozoa: Sarcodina): Zoological Journal of the Linnean Society, 58, 61–78.

Georgescu, M.D., 2010, On the status of *Paraticinella rohri* (Bolli 1959): Micropaleontology, 56, 598–599.

Glaessner, M.F., 1937, Studien über Foraminiferen aus der Kreide und dem Tertiär des Kaukasus; I. Die Foraminiferen der ältesten Tertiärschichten des Nordwest-Kaukasus: Problems of Paleontology, Paleontologicheskay Laboratoriya Moskovskogo Gosudarstvennogo Universiteta, 2–3, 349–410.

Huber, B.T., Mesozoic Planktonic Foraminiferal Working Group, 2006, CHRONOS PORTAL: Mesozoic Planktonic Foraminiferal Taxonomic Dictionary, *available at* <http://www.chronos.org>, *consulted on* January 2017.

Heller, L., 1975, Mikrobiostratygrafia osadów kredowych poludniowej czesci synklinorium lodzkiego (Microbiostratigraphy of the Cretaceous deposits in the southern part of Lodz Synklinorium, Central Poland): Annales Societatis Geologorum Poloniae, 45, 233–254.

Herb, R., 1974, Cretaceous planktonic foraminifera from the eastern Indian Ocean, Leg 26 of the Deep Sea Drilling Project, *in* Davis, T.A., Luyendyk, B.P. (eds.), Initial Reports of the DSDP, 26, 745–769.

Huber, B.T., Leckie, R.M., 2011, Planktic Foraminiferal species turnover across deep-sea Aptian/Albian boundary sections: Journal of Foraminiferal Research, 41(1), 53–95.

Huber, B.T., Petrizzo, M.R., 2016, Mesozoic Planktonic Foraminifera, The Micropalaeontological Society supports the project, *consulted on* January 2018.

Humphrey, W.E., 1949, Geology of the Sierra de Los Muertos Area, Mexico (with descriptions of Aptian cephalopods from the La Peña Formation): Bulletin of the Geological Society of America, 60(1), 89–176.

Humphrey, W.E., Díaz, T., 2003, Jurassic and Lower Cretaceous Stratigraphic and Tectonics of Northeast of Mexico: Bureau of Economic Geology, report of investigations no. 267, 152 pp.

Imlay, R.W., 1936, Part IV. Geology of the Western part of the Sierra de Parras in Evolution of the Coahuila Peninsula, Mexico: Geological Society of America Bulletin, 47(7), 1091–1152.

Imlay, R.W., 1937, Geology of the middle part of the Sierra de Parras, Coahuila, Mexico: Geological Society of America Bulletin 48(5), 606–607.

Leckie, R.M., 1984, Mid-Cretaceous planktonic foraminiferal biostratigraphy off Central Morocco, Deep Sea Drilling Project Leg 79, Sites 545 and 547, *in* Hinz, K., Winterer, E.L., Baumgartner, P.O., Bradshaw, M.J., Channell, J.E.T, Jaffrezo, M., Jansa, L.F., Leckie, R.M., Moore, J.N., Jürgen, R., Schaftenaar, C.H., Steiger, T.H., Vuchev, T., Wiegand, G.E., Blakeslee, J.H. (eds.), Initial Reports of the Deep Sea Drilling Project, 79: United States Government Printing Office, 579–620.

Lipson-Benitah, S., Almogi-Labin, A., 2000, Albian planktonic foraminifera from Israel: Geological Survey of Israel Bulletin, 86, 1–50.

Loeblich, A.R., Tappan, H., 1961, Remarks on the Systematics of the Sarkodina (Protozoa), renamed Homonyms and new and validated Genera: Proceedings of the Biological Society of Washington, 213–234.

Loeblich, A.R., Tappan, H., 1988, Foraminiferal Genera and their Classification: New York, Van Nostrand Reinhold Company, 2045 pp.

Longoria, J.F., 1974, Stratigraphic, morphologic and taxonomic studies of Aptian planktonic Foraminifera: Revista Española de Micropaleontología, No. extraordinario, 107 pp.

Longoria, J.F., 1975, Estratigrafía de la Serie Comancheana del noroeste de México: Boletín de la Sociedad Geológica Mexicana, 36(1), 31–59.

Longoria, J.F., Monreal, R., 2009, The use of Planktonic microfossils to resolve chronostratigraphic, tectonic, and paleogeographic uncentainties in the Lower Cretaceous of Eastern Sonora, NW Mexico, *in* Demchuk, T.D., Gary, A.C. (eds.), Geologic problem solving with microfossils: A volumen in honor of Garry D. Jones: SEPM Special Publication no. 93, 269–285.

Luterbacher, H., 1975, Early Cretaceous foraminifera from the north western Pacific. Leg 32 of the Deep Sea Drilling Project Ill, *in* Larson, R.L., Moberly, R. (eds.), Initial Reports of the Deep Sea Drilling Project 32: United States Government Printing Office, 703–718.

Masters, B.A., 1976, Planktic foraminifera from the Upper Cretaceous Selma Group, Alabama: Journal of Paleontology, 50(2), 318–330.

Mayer-Pérez, R.F., 1967, Hoja Viesca 13R-1(5), Resumen de la Geología de la Hoja Viesca, Estados de Coahuila y Durango: México, D.F., Universidad Nacional Autónoma de México, Instituto de Geología, Cartas Geológicas de México serie: 1:100000, 1 mapa con texto.

Méndez-Franco, A.L., 2003, Bioestratigrafía de ammonites y variaciones de litofacies en una secuencia estratigráfica del Barremiano-Aptiano (Cretácico Inferior) del área del Cañón de la Huasteca, estado de Nuevo León: México, D.F., Universidad Nacional Autónoma de México, Facultad de Ciencias, Bachelor's thesis, 179 pp.

Michael, F.Y., 1972, Planktonic foraminifera from the Comanchean series (Cretaceous) of Texas: Journal of Foraminiferal Research, 2(4), 200–220.

Michalík, J., Reháková, D., Lintnerová, O., Boorová, D., Halásová, E., Kotulová, J., Soták, J., Peterèáková, M., Hladíková, J., Skupien, P., 1999, Sedimentary, biological and isotopic record of Early Aptian paleoclimatic event in the pieniny klippen belt, slovak western carpathians: Geologica Carpathica, 50(2), 169–191.

Moullade, M., 1961, Quelques Foraminifères et Ostracodes nouveaux du Crétacé inférieur des Baronnies (Drộme): Revue de Micropaléontologie, Paris, 3e Année, 4, 213–216.

Moullade, M., 1966, Étude stratigraphique et micropaléontologique du Crétacé inférieur de la "fosse vocontienne": Documents des Laboratoires de Géologie de la Faculté des Sciences de Lyon, 15, 369 pp.

Moullade, M., Tronchetti, G., Kuhnt, W., Masse, J.P., 1998, Les Foraminiféres benthiques et planctoniques de la série du Stratotype Historique de l'Aptien inférieur dans la région de Cassis-La Bédoule (SE France): Géologie Méditerranéenne, 25, 187–225.

Moullade, M., Bellier, J-P., Tronchetti, G., 2002, Hierarchy of criteria, evolutionary processes and taxonomic simplification in the classification of Lower Cretaceous planktonic foraminifera: Cretaceous Research, 23(1), 111–148.

Mweneinda, A.K., 2014, Mid-Cretaceous Stratigraphy and Micropalaeontology of the Coastal Basins of Tanzania: Cardiff, United Kingdom, Cardiff University, School of Earth and Ocean SciencesPhD dissertation, 404 pp.

North, B.R., Caldwell, W.G.E., 1975, Ilustrations of Canadian fossil, Cretaceous foraminifera from Saskatchewan and Manitoba: Geological Survey Canada, Paper, 74(38), 1–35.

Núñez-Useche, F., Barragán, R., 2012, Microfacies analysis and paleoenvironmental dynamic of the Barremian-Albian interval in Sierra del Rosario, eastern Durango state, Mexico: Revista Mexicana de Ciencias Geológicas, 29(1), 204–218.

Obregón de la Parra, J., 1959, Consideraciones sobre el Daniano en la cuenca sedimentaria de Tampico-Misantla: Boletín de la Asociación Mexicana de Geólogos Petroleros, 11(1–2), 13–20.

Omaña, L., González-Arreola, C., Ramírez-Garza, B.M., 2005, Barremian planktonic foraminiferal events correlated with the ammonite zones from the San Lucas Formation, Michoacán (SW, México): Revista Mexicana de Ciencias Geológicas, 22(1), 88–96.

Omaña, L., Alencaster, G., Buitrón, B.E., 2016, Mid-early late Albian foraminiferal assemblage from the El Abra Formation in the El Madroño locality, eastern Valles-San Luis Potosí Platform, Mexico: Paleoenvironmental and paleobiogeographical significance: Boletín de la Sociedad Geológica Mexicana, 68(3), 477–496.

Pantoja-Alor, J., 1962, Hoja San Pedro del Gallo 13R-k(3), Resumen de la Geología de la Hoja San Pedro del Gallo: México, D.F., Universidad Nacional Autónoma de México, Instituto de Geología, Cartas Geológicas de México serie 1:100000, 1 mapa con texto.

Patterson, M.G., Warr, P.B., West, M.A., 2004, Organizational climate and company performance: the role of employee affect and employee level: Journal of Occupational and Organizational Psychology, 77, 193–216.

Pérez-Rul, F.A., 1967, Hoja Viesca 13R(5), Resumen de la Geología de la Hoja Viesca: México, D.F., Universidad Nacional Autónoma de México, Instituto de Geología, Cartas Geológicas de México serie 1:100000, 1 mapa con texto.

Peryt, D., 1980, Planktic Foraminifera zonation of the Upper Cretaceous in the Middle Vistula River Valley, Poland: Palaeontologia Polonica, 41, 3–101.

Peryt, D., 1983, Mid-Cretaceous microbiostratigraphy and foraminifers of the NE margins of the Swietokrzyskie (holy cross) Mts., Poland: Acta Palaentologica Polonica, 28(3–4), 417–466.

Pessagno, E.A., 1967, Upper Cretaceous planktonic foraminifera from the Western Gulf Coastal Plain: Palaeontographica Americana, 5(37), 259–441.

Petrizzo, M.R., Huber, B.T., 2006, Biostratigraphy and taxonomy of late Albian planktic foraminifera from ODP Leg 171B (western North Atlantic Ocean): Journal of Foraminiferal Research, 36(2), 166–190.

Petrizzo, M.R., Huber, B.T., Gale, A.S., Barchetta, A., Jenkyns, H.C., 2012, Abrupt planktic foraminiferal turnover across the Niveau Kilian at Col de Pré-Guittard (Vocontian Basin, southeast France): new criteria for defining the Aptian/Albian boundary: Newsletters on Stratigraphy, 45, 55–74.

Petróleos Mexicanos (PEMEX), 1988, Estratigrafía de la República Mexicana: Mesozoico, 216 pp.

Plummer, H.J., Some Cretaceous Foraminifera in Texas: University of Texas Bulletin, 3101, 109–203.

Premoli-Silva, I., McNulty, C.L., 1984, Planktonic foraminifers and calpionellids from Gulf of Mexico sites, Deep Sea Drilling Project Leg 77, *in* Buffler, R.T., Schlager, W., *et al*. (eds.), Initial Reports of the Deep Sea Drilling Project Leg 77: United State Government Printing Office, 547–584.

Premoli-Silva, I., Sliter, W.V., 1986, Late Aptian and CenomanianeTuronian planktonic foraminifers from Deep Sea Drilling Project Site 585, Leg 89, East Mariana Basin, *in* Moberly, R., Schlanger, S.O., *et al*. (eds.), Initial Reports of the Deep Sea Drilling Project 89. United State Government Printing Office, 297–309.

Premoli-Silva, I., Verga, D., 2004, Practical manual of Cretaceous planktonic foraminifera. International School on planktonic foraminifera, *in* Verga D., Rettori, R. (eds.), International School on Planktonic Foraminifera, 3rd Course: Cretaceous. Universities of Perugia and Milan, Tiporafia Pontefelcino, Perugia (Italy), 283 pp.

Premoli-Silva, I., Caron, M., Leckie, R.M., Petrizzo, M.R., Soldan, D., Verga, D., 2009, *Paraticinella* n. gen. and taxonomic revision of *Ticinella bejaouaensis* Sigal, 1966: Journal of Foraminiferal Research, 39(2), 126–137.

Raisz, E., 1964, Landforms of Mexico, escala 1:3000000: Cambridge, Mass, U.S. office of Naval Research, Geography Branch, map and text.

Ramírez del Pozo, J., 1971, Bioestratigrafía y microfacies del Jurásico y Cretácico del Norte de España (Región cantábrica): Memoria del Instituto Geológico y Minero de España, Tomo 78, 361 pp.

Randrianasolo, A., Anglada, R., 1998, About *Ticinella roberti* var. *bejaouaensis* Sigal 1966 and *Ticinella bejaouaensis* Sigal emend Moullade 1966, *in* Joint Regional Meeting of IGCP Projects nos 381 and 362: Geologia y Minería, Memorias 2, 298, 26–28.

Risch, H., 1971, Stratigraphie der höheren Unterkreide der Bayerischen Kalkalpen mit Hilfe von Mikrofossilien: Palaeontographica Abt. A, 138, 80 pp.

Robaszynski, F., Caron, M., El Grupo de Trabajo Europeo de Foraminíferos Planctónicos, 1979, Atlas of mid Cretaceous planktonic foraminifera (Boreal sea and Tethys): Cahiers de Micropaléontologie 1, 1–185.

Romo-Ramírez, J.R., Padilla-Islas, R., 2012, Carta geológico-minera La Soledad G14-C86, estado de Nuevo León, scale 1:50000: Pachuca, Hidalgo, México, Servicio Geológico Mexicano, technical report, 110 pp.

Rosales-Domínguez, M.C., 1989, Micropaleontology and paleogeography of the upper Mural Limestone of southeastern Arizona and northern Sonora: Arizona, EE.UU., The University of Arizona, Faculty of the Department of Geosciences, Master's thesis, 61 pp.

Sigal, J., 1966, Contribution à une monographie des Rosalines 1. Le genre *Ticinella* Reichel, souche des Rotalipores: Eclogae Geologicae Helvetiae, 59, 185–217.

Sigal, J., 1979. Chronostratigraphy and ecostratigraphy of Cretaceous formations recovered on DSDP Leg 47B, Site 398, *in* Sibuet, J.-C., Ryan, W.B.F., *et al*. (eds.), Initial Reports of the Deep Sea Drilling Project 47(2): Unite State Government Printing Office, 287–326.

Sliter, W.V., 1989, Biostratigraphic zonation for Cretaceous planktonic foraminifera examined in thin section: Journal of Foraminiferal Research 19(1), 1–19.

Sliter, W.V., 1992, Cretaceous planktonic foraminiferal biostratigraphy and paleoceanographic events in The Pacific Ocean with emphasis on indurated sediment, *in* Ishizaki, K., Saito, T. (eds.), Centenary of Japanese Micropaleontology, Contributed Papers in honor of Professor Yokichi Takayanagi, 281-299.

Sliter, W.V., 1999, Cretaceous planktic foraminiferal biostratigraphy of the Calera Limestone, northern California, USA: Journal of Foraminiferal Research, 29(4), 318–339.

Sliter, W.V., Leckie, R.M., 1993, Cretaceous planktonic foraminifers and depositional environments from the Ontong Java Plateau with emphasis on Sites 803 and 807, *in* Berger, W.H., Kroenke, L.W., Mayer, L.A., *et al*. (eds.), Proceedings of the Ocean Drilling Program, Scientific Results 130. TX (Ocean Drilling Program): College Station, 63–84.

Soleimani, B., Bahadori, A., Meng, F., 2013, Microbiostratigraphy, microfacies and sequence stratigraphy of Upper Cretaceous and Paleogene sediments, Hendijan oilfield, Northwest of Persian Gulf, Iran: Natural Science, 5(11), 1165–1182.

Stinnesbeck, W., 1983, Sobre una fáunula de amonites de la Formación Cuesta del Cura (Albiano superior-Cenomaniano inferior) de la Sierra de Catorce, San Luis Potosí, México: Actas de la Facultad de Ciencias de la Tierra, Universidad Autónoma de Nuevo León, 8, 129–132.

Tardy, M., Longoria, J.F., Martínez-Reyes, J., Mitre-Salazar, L.M., Patiño, A.M., Padilla, S.R., Ramírez, R.C., 1975, Observaciones generales sobre la estructura de la Sierra Madre Oriental: La aloctonía del conjunto cadena alta-altiplano central, entre Torreón, Coahuila y San Luis Potosí, S.L.P. México: Revista del Instituto de Geología, 1(1), 1–11.

Trejo, M., 1960, "La Familia Nannoconidae y su alcance estratigráfico en América" (Protozoa, *incertae saedis*)": Boletín de la Asociación Mexicana de Geólogos Petroleros, 12(9–10), 259–314.

Trejo, M., 1975, Tintínidos mesozoicos de México (taxonomía y datos paleobiológicos): Boletín de la Asociación Mexicana de Geólogos Petroleros, 27(10-12), 329–449.

Trejo, M., 1980, Distribución Estratigráfica de los tintínidos mesozoicos mexicanos: Revista del Instituto Mexicano del Petróleo, 12(4), 4–13.

Trejo, M., 1983, Paleobiología y Taxonomía de Algunos Fósiles Mesozoicos de México: Boletín de la Sociedad Geológica Mexicana, 44(2), 1–22.

Tronchetti, G., 1981, Les foraminiferes Cretace de Provence (Aptien-Santonien). These, I'Universite de Provence, UER de Sciences Naturelles RCP no. 510; Trav. du Lab. de Gkol. Historique et de Paléontologie, 12, 196 pp.

Manuscript received: November 23, 2017.
Corrected manuscript received: June 6, 2018.
Manuscript accepted: June 8, 2018.